UNIVERSITÀ DEGLI STUDI DI PADOVA

UNIVERSITA' DEGLI STUDI DI PADOVA

Dipartimento di Ingegneria Industriale DII

Corso di Laurea Magistrale in Energy Engineering

Energy flexibility quantification of a typical Danish single-family house

Relatore

Dr. Jacopo Vivian

Università degli Studi di Padova

Candidato

Alessandro Cestone

Matricola 2053094

Correlatore

Prof. Massimo Fiorentini

Aarhus University

Dr. Sara Bordignon

Università degli Studi di Padova

Anno Accademico 2023/2024

Abstract

This thesis focuses on the study of the energy flexibility of buildings, i.e. the ability to adapt their energy demand based on internal and external requirements. The main objectives are to quantify the energy flexibility potential of a typical Danish single-family house and understand how it changes depending on the boundary conditions and on the type of heating system.

The study is performed by simulating some Active Demand Response events, consisting in changing the temperature setpoint of the rooms of the building or forcing the operation of the heat pump compared to normal operating conditions.

The analysis is carried out in different simulation scenarios to understand how the energy flexibility potential varies with different heating systems and different type of ADR events. The possible configuration of the system analyzed are one in which the building is heated through a floor heating system and one in which also a thermal storage tank coupled with a heat pump is considered.

The ADR events are driven by the electricity price and can be upward modulation or downward modulation. The study considers two energy flexibility sources: the building structure and the thermal storage tank.

The analysis is carried out during the heating season, from the beginning of January to the end of May.

The energy flexibility potential is quantified through some energy flexibility indicators, as the available storage capacity and the efficiency of the ADR events compared to a reference operation and other key performance indicators that measure the effect of such events on indoor thermal comfort and operating costs for the end user.

Most of the key performance indicators are grouped on monthly basis to assess how the energy flexibility varies with the seasonality.

The building is modelled using TRNSYS, which allows to reproduce the dynamic behavior of the building and its interaction with the HVAC system, consisting of a radiant floor and an air-source heat pump, with or without a thermal storage tank in between.

The results show that the energy flexibility of the building considered provides a significative shifting capability in the energy consumption towards off-peak hours, reducing peak loads at energy system level, and at the same time saving money for the building owners.

Moreover, the addition of a thermal storage tank contributes to increase the energy flexibility potential of the whole system.

Index

Figure Index

Table Index

1 Introduction

The increasing global energy demand, coupled with the projected decline in available fossil fuels and the mounting evidence of global warming over recent decades, has generated significant interest in renewable energy sources. The penetration of renewable energy sources (RES) is indeed increasing rapidly worldwide, with an increase of installed photovoltaic capacity from 200 GW in 2018 to over 1200 GW expected in 2025 and similar trend observed for installed wind power capacity, with a growing contribution of the off-shore sector. [1]

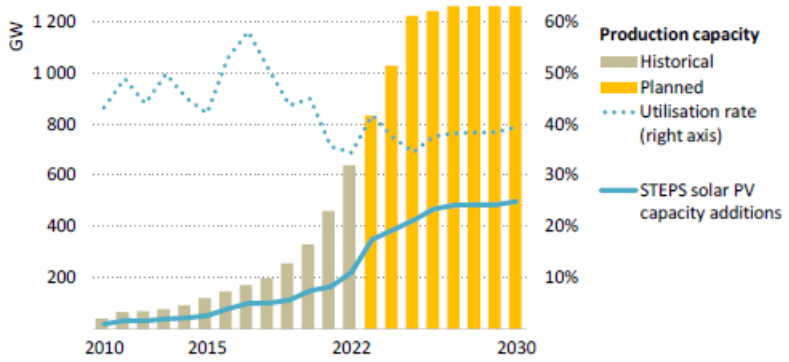

Figure 1-1: Planned expansion of solar PV installed capacity additions to 2030 [1].

This trend is expected to continue as several countries already have highly ambitious targets, as Germany which has a goal of at least 80% of the gross electricity consumption coming from renewable energy by 2050. Some countries have even set RES targets as high as 100% of the total energy mix, including Denmark which plans to cover 100% of the energy demand with renewables by 2050. [2]
However, energy sources, such as wind and solar power, have an intrinsic variability that can seriously affect the stability of the energy system, if they account for a high percentage of the total generation. In order to accommodate a high penetration of variable renewable energy sources in future a transition from generation on demand to consumption on demand is often suggested. In practice, this will mean that the energy consumption needs to become flexible.

This trend ends in the fact that renewable electricity generation is increasingly injected into the electricity grid in a decentralized manner. [3]
In most parts of the world, the basic model of electricity supply has indeed changed since the dawn of the industry in which power is still produced mainly by large, centralised, hydro plants and by thermal

power plants, in which fossil fuels are burned or uranium engaged in nuclear reaction to create steam to turn turbines, and is transmitted over high-tension cables to centres of demand, where it is distributed through local distribution networks at lower voltage to final customers. Nowadays things are changing: technical advances, including the application of information and communication technology, have greatly improved the efficiency of generation, reduced transmission and distribution losses, encouraged distributed generation, facilitated demand-side management and the creation of markets in wholesale and retail power supply. In addition, government incentives have boosted the development and deployment of new generating technologies, based on non-hydro renewable energy sources, opening up the long-term prospect of a decarbonisation of power supply. [4]

Confirming the previous observation, it's notable that the number of traditional controllable power plants is either stagnating or decreasing. [3]

Projections indicate that approximately 2,250 GW, equivalent to 38% of the current global power capacity, will be decommissioned by 2040. Moreover, about 200 GW of capacity, mainly sourced from renewables, commissioned during the projection period, will require replacement by the same year. As a result, the total capacity retirements from 2014 to 2040 are estimated at 2,450 GW, representing roughly one-third of the 7,200 GW of global gross capacity additions during this timeframe. Notably, retirements of oil-fired capacity exceed gross additions by a factor of about three, while retirements of coal-fired capacity make up almost half of the gross additions.

Within OECD countries, a significant share of existing capacity replacement is anticipated, driven partly by the aging infrastructure, with over 40% of fossil fuel-fired capacity and nearly half of installed nuclear capacity being over 30 years old. Consequently, over 45% of existing OECD capacity is expected to be retired by 2040, compared to 16% in China (60% of which is renewables-based capacity) and 40% in other non-OECD countries, on average.

In the OECD region, approximately 60% of gross capacity additions between 2013 and 2040 stem from both the retirement of existing and new capacity, with the remainder attributed to increasing demand and policies aimed at decarbonizing the power sector. Renewables, particularly wind and solar PV, make the most significant contributions to capacity additions, constituting almost two-thirds of all new capacity. Gas accounts for approximately one-quarter of the additions [4].

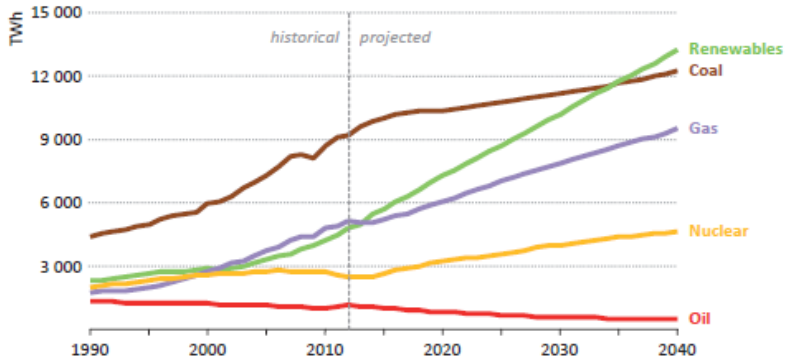

Figure 1-2: World electricity generation by source in the New Policies Scenario [4].

The primary consequence of the above-mentioned dynamics is the anticipated increase in electrical load. This surge in demand is largely attributed to the transition away from fossil-fueled systems towards highly efficient electrical equipment for transportation and heating purposes. As traditional power plants, particularly those reliant on fossil fuels, are retired and replaced with renewable sources, coupled with the electrification of sectors like transportation and heating, the demand for electricity is expected to rise substantially. This shift underscores the critical importance of enhancing flexibility within the energy sector to effectively manage and balance this growing demand. [3]

At the same time, the ambition towards net zero energy buildings (NZEB) imposes new challenges as buildings no longer only consume, but also generate heat and power locally, commonly called prosumers. Consequently, the grid must be designed with respect to the energy demand, both heat and electricity, as well as the local energy generation.

Furthermore, today the distribution grid is often dimensioned based on buildings heated by sources other than electricity, as oil or gas burners. However, the transition to a renewable energy system will in many areas lead to an increase in electrical heating, for example through heat pumps, even if the foreseen reduction in the space heating demand via energy renovation is realized. Also, the expected penetration of electrical vehicles may further increase the loads in the distributed grids, but they may also be used for peak shaving by using their batteries. [2]

The convergence of all the factors discussed necessitates significant upgrades to distribution grids or the adoption of smarter consumption practices to mitigate congestion issues. The concept of SmartGrids (or Smart Energy Networks, when including other energy carriers besides electricity) emerges as a solution where in both demand and local production within distribution networks are actively managed to stabilize energy networks. This approach not only helps alleviate congestion problems but also enhances grid resilience and efficiency.

The primary challenge underlying all the considerations discussed earlier is indeed ensuring the security of the electricity system. Electricity system security includes the ability of the power sector to deliver electricity to all connected users, meeting acceptable standards and desired quantities at any given time [4]. It comprises three distinct, but interconnected, elements:

- Fuel security: maintaining reliable fuel supplies to power stations, enabling them to respond in real time to demand fluctuations.

- System adequacy: the capability of the power system to meet changes in aggregate power requirements both in the present and future, using existing and new resources as required.

- System security: the capability of the power system, using existing resources, to maintain reliable supplies despite unexpected surges in demand or sudden disruptions to supply.

Maintaining system adequacy and security requires efficient, timely and well-located investment. Rapidly increasing deployment of variable renewables-based generation, such as wind and solar power, significantly changes the way electricity systems function from day-to-day, as sudden changes in weather conditions can lead to abrupt swings in the availability of supply from certain types of capacity. This complicates the task of maintaining system adequacy and system security. Consequently, there is a need for other forms of flexible capacity to be readily available to manage these sudden and sometimes unpredictable changes in supply.

Buildings are expected to have an important role in future as the energy flexibility offered by buildings is frequently suggested as a solution to alleviate some of the discussed challenges in the future of the energy systems.

In most developed countries, the energy use in buildings accounts for 35–40% of the total energy consumption and itis used for space heating, heating of domestic hot water, cooling, ventilation, pumps, control and lighting of rooms as well as for appliances used by occupants. [2]

A large part of the energy demand of buildings may be shifted in time, and it may thus significantly contribute to increasing flexibility of the demand in the energy system. In particular, the thermal part of the energy demand, as. space heating/cooling, ventilation, domestic hot water as well as hot water for washing machines, dishwashers and heat for tumble dryers, can be shifted. Care should, however, be taken when obtaining energy flexibility from buildings in order not to jeopardize the thermal comfort of the occupants.

In particular, all buildings incorporate thermal mass within their structures, making possible to store a certain amount of heat. Depending on the amount, distribution, speed of charging and discharging of the thermal mass, it is possible to postpone heating or cooling for a certain period of time without affecting the thermal comfort in the building. Moreover, if a building is excessively pre-heated or cooled within the comfort range of the room temperature, reaching the upper limit of comfort for heating or the lower limit for cooling, prior to discontinuing heating/cooling operations, it becomes feasible to extend the shutdown period. The time constant of buildings varies, depending on the amount and exploitability of the thermal mass together with the heat loss, internal gains, user pattern and the actual climate conditions, typically between a few hours to several days. Many buildings may also contain different kinds of discrete storages as domestic hot water tanks and storage heaters, but also batteries (in connection with PV systems or electric vehicles) that may add to the flexibility of the energy demand of the buildings. One such typical storage is the domestic hot water tank, which might be excess pre-heated before a low energy level situation. In general water tanks are better suited to provide short-term flexibility. The excess heat may be utilized for space heating, but may also be used for white goods such as hot-fill dishwashers, washing machines and tumble dryers in order to decrease and shift their electricity need. [2]

An explanation of the situation described above, in which buildings can provide energy flexibility, is given through the example shown in Figure 1-3.

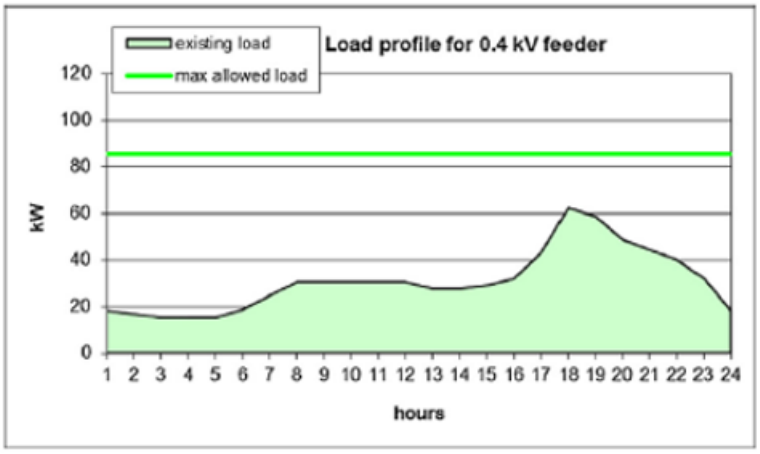

Figure 1-3: Existing situation of a single-family house [2].

Figure 1-3 shows a winter situation for a small Danish feeder oh 0.4 kV with one single-family house, the existing situation is presented, in which there is an existing load (green area) and a maximum allowed load limit (green line). The peak from 17:00 to 20:00 is called the “cooking peak” due to people coming home from work and start cooking. The peak also is due to switching on other appliances.

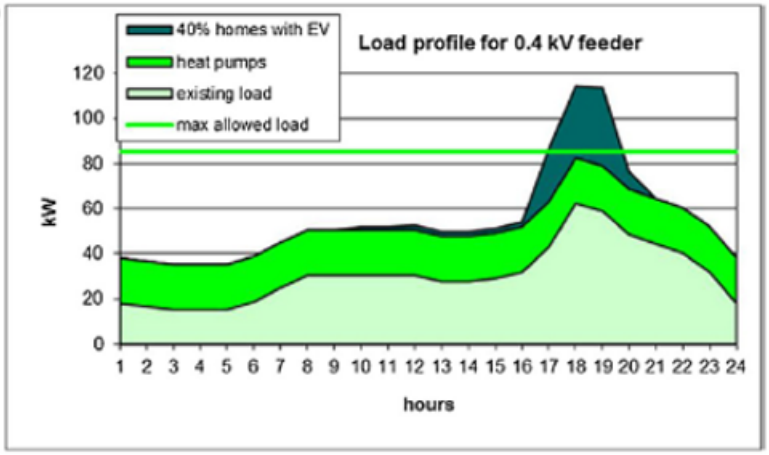

Figure 1-4: Heat pumps and electrical vehicles introduction [2].

Figure 1-4 shows a situation in normal operation where the addition of heat pumps and electrical vehicles (EVs) in the system will demand a reinforcement of the grid as the demand exceeds the max allowed load.

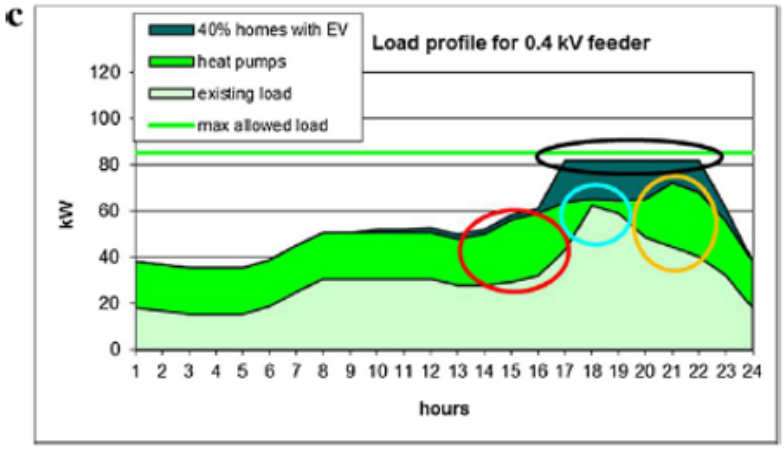

Figure 1-5: Building providing energy flexibility to the grid [2].

Figure 1-5 shows of how the flexibility of houses with heat pumps and "intelligent" appliances may decrease the need for reinforcement of the local 0.4 kV, where the houses are situated.

This is a possible Smart Grid solution where the buildings prior to the cooking peak between 17:00 and 20:00, while gives excess of heat in the hours before the peak, remaining within the comfort band of the room temperature (red circle). The buildings are mainly free floating during the cooking peak (blue circle) and, since the higher amount of energy received in the hours before the peak, it requires less energy respect a normal operation condition during the peak, allowing the building to require less energy from the heat pump during the critical time, but need extra heat after the cooking peak (orange circle).

Concerning the electric vehicles, in this situation they are controlled in an intelligent way to flatter the load request during the charge (black circle). The combinations of these two aspects allow the building to shift his load in not critical hours, shaving the peak of energy required to the gird and help mitigating some of the problems previously discussed. This is an example of how the building can provide energy flexibility.

To gives some general rule assessing the Energy Flexibility in buildings, among most of the existent work concerning this relative new research area, three general properties of energy flexibility emerge:

- the time over which energy and power can be shifted or shaved
- the amount of energy or power that can be shifted or shaved
- the associated cost or efficiency loss at the building level that results from activating this flexibility

The IEA EBC Annex 67 working definition of Energy Flexibility of a building is presented:
"The Energy Flexibility of a building is the ability to manage its demand and generation according to local climate conditions, user needs, and energy network requirements.
Energy Flexibility of buildings will thus allow for demand side management/load control and thereby demand response based on the requirements of the surrounding energy networks." [2]

The energy flexibility of the buildings is exploited from the so called Demand Side Management (DSM) program, which emerges as a frequently recommended solution to cope with the above discussed evolutions and problems.
Demand Side Management (DSM) is the planning and implementation of those electric utility activities designed to influence customer uses of electricity in ways that will produce desired changes in the utility's load shape. [5]
DSM includes all programs designed to influence the customer's energy use, changing consumer energy consumption patterns to achieve more efficient and sustainable use of energy resources. It includes a variety of strategies, like incentives, pricing mechanisms, education and technological interventions, all designed to encourage consumers to adjust their energy usage behaviors. By shifting or reducing electricity demand during peak periods, DSM can help alleviate strain on the grid, lower overall energy costs and mitigate environmental impacts associated with energy production.
In particular, a relevant Demand Side Management strategy is represented by the so called Active Demand Response (ADR) mechanisms, intended to achieve changes in electric usage by end-use

customers from their normal consumption patterns in response to changes in the price of electricity over time. [6]

These intentional changes to the electricity consumption behaviors of end-use customers can be direct or indirect and are implemented to affect the timing, level of instantaneous demand or the overall electricity usage.

A higher degree of energy flexibility of the buildings serves to favor their suitability for participation in Active Demand Response (ADR) programs, which are often orchestrated based on directives from the system operator (SO) or through engagement with external entities known as "aggregators", responsible for acquiring the flexibility from the customers, aggregating it into a portfolio and offering the flexibility service to the grid operator.

These ADR programs typically involve two modes of control: direct and indirect. In direct control scenarios, the SO or the aggregator can directly modify the consumption pattern, whereas indirect control grants users a full autonomy in the control of their appliances, allowing them to feely decide whether or not to participate in the ADR program. [7]

Aggregators and end-users, which are building owners and building managers, are the major stakeholders interested in the energy flexibility potential of a given building. Building owners are primarily interested in energy usage and associated cost savings from activating the flexibility of specific devices.

On the other hand, aggregators exhibit a more comprehensive interest, including both the broader business opportunities presented by active demand response (ADR) program and the technical issues to facilitate grid integration of residential building stock. These technical considerations include assessing the building's capacity for power shifting, its response time to demand signals and the maximum duration for which a response can be sustained. [8]

One of the most promising applications of active demand response (ADR) consists of exploiting the thermal capacitance of the buildings and, where present, utilizing thermal energy storage systems to effectively shift the load of electrically driven HVAC devices, such as heat pumps.

Exploiting the building structure, either independently or in conjunction with existing thermal energy storage systems, presents a disruptive opportunity as it requires minimal additional investment costs, primarily focused on enhancing the "intelligence" and "connectivity" of existing HVAC control devices. [7]

A way to incentivize building owners to engage in ADR programs is through time-varying prices, meaning by offering cheaper prices at off-peak times respect during peak times.

This concept is illustrated in Figure 1-6, that presents the principle of how a building can participate in a price-based Active Demand Response program. [9]

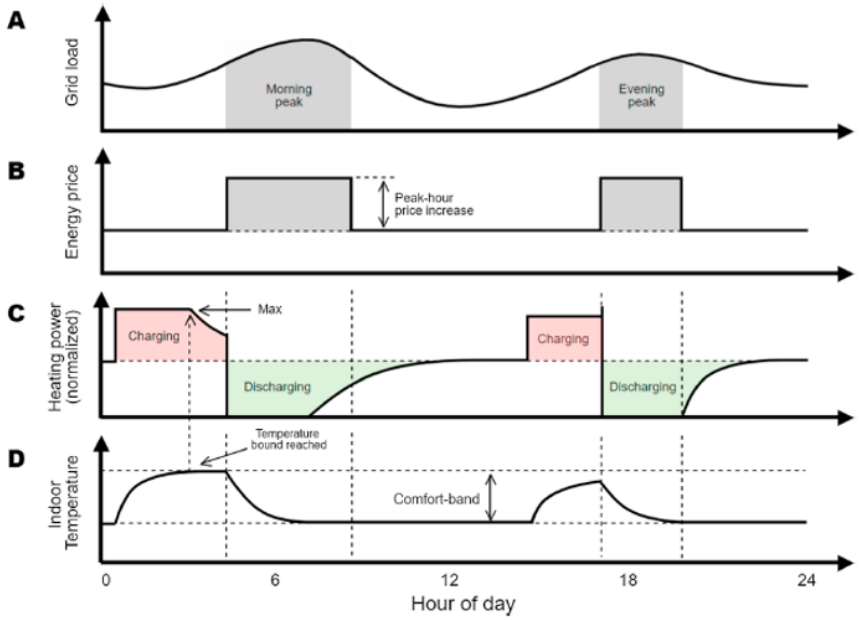

Figure 1-6: Principle of the price-based active demand response program [9].

The profile (A) shows the expected load to the grid, with the typical fluctuation shape of a single day, with two load peaks, one in the morning and one in the evening.

The profile (B) shows the resulting increase in the energy price during the peak period, meaning that the consumption of energy in these period cost more for the building owners and end-use customers in general.

Finally, profile (C) describes the actions taken by the building energy management system in order to minimize the economic expense of the building owner. The thermal mass of the building is charged with a surplus of energy with respect to the instantaneous normal need through an increase in the temperature setpoint of the building, resulting in an increase in the room temperature before the peak, as shown in profile (D).

This energy charge before the peak hours allows the building to be autonomous from the energetic point of view during the peak hours or part of that, eliminating the necessity to consume energy during peak hours when the price of the energy is higher. The charging phase before the peak is typically limited by the guarantee of thermal comfort inside the room.

As shown in profile (D), indeed, the temperature inside the room starts to increase when the heating system is forced to stay switched on because of the charging phase until it reaches the upper comfort limit. At this point the heating system is switched off to avoid jeopardizing the thermal comfort inside the room.

This control strategy allows the energy flexibility of the building to result in a cost saving for the building owners related to the fact that the energy is consumed before the peak at a lower price, instead of consuming energy during peak hours at higher price.

At the same time, the energy consumed by the building during the peak hours is lower, helping to alleviate congestion problems to the grid. Through ADR programs, both the building owners and grid energy systems can take advantages.

The work of this thesis is intended to increase the knowledge on the application of the Active Demand Response program to a typical single-family house.

To do that, the quantification of the energy flexibility potential of the building is performed through some key performance indicators.

Moreover, in order to have a comprehensive knowledge of the behavior of the energy flexibility, the boundary conditions of the analysis are changed. In particular, the energy flexibility potential is analyzed in different configurations of the system, considering the effect of different technological setup and the effect of the seasonality.

2 Case study

In this chapter the building considered for the quantification of the energy flexibility, which is a typical Danish single-family house, is presented.

The first section provides a description of the building characteristic, with the construction layers and the materials composing each of them and their thermal properties. Also the technological setup present in the building is mentioned.

The second section provides a description of the weather conditions of the place in which the building is located, which have a main importance in this type of analysis.

2.1 Building

The building considered for this work is a typical single-family house located in Denmark, in the suburban area of Aarhus. The house was built in 1970 and is currently occupied by a family of four people, composed by two adults and two minor children.

The house has a gross floor area of approximately 185 m^2 distributed on one floor and the room height is 2.3 m. The single-family house presents large windows located mainly in the south and west oriented facades. [10]

The building is located in a large garden with some trees around it which contribute to partially shade the house. Some real picture of the house are provided in Figure 2-1, Figure 2-2 and Figure 2-3.

Figure 2-1: Picture of the single-family house (South-west) [9].

Figure 2-2: Picture of the single-family house (North-west) [9].

Figure 2-3: Picture of the single-family house (South) [9].

The external walls are brick cavity walls with a total width of 0.29 m, in which approximately 0.075 m is mineral wool insulation.

The ground floor is made of a 0.022 m solid wood layer placed on a 0.08 m concrete cast on a layer of sand, within an insulation layer of approximately 0.075 m of mineral wool.

The roof consists of a ceiling cladding of 0.022 m wood mounted on the 0.1 m rafter heads with mineral wool insulation in between. An additional layer of approximately 0.3 m paper wool insulation was added in the year 2012.

The internal partitions walls are made of 0.08 m of concrete block covered with gypsum internal plaster in both side of the internal wall.

The original windows were replaced in 2005 with double-layer glazing in the combined aluminum and wood frames.

The thickness and the main thermal properties, as thermal conductivity, thermal capacity and density of each layer composing the different constructions of the building are summarized in Table 2-1 [11]

Construction types						
	Layers	Thickness	Thermal conductivity	Thermal capacity	Density	U-value
		[m]	[kJ/h m K]	[kJ/kg K]	[kg/m^3]	[W/ m^2 K]
External wall	Gypsum	0.013	0.58	1.83	784.9	0.4
	Brick	0.1	3.20	0.79	1920	
	Mineral wool	0.075	0.13	0.84	91	
	Brick	0.1	3.20	0.79	1920	
Internal wall	Gypsum	0.013	0.58	1.83	784.9	2.468
	Concrete block	0.08	3.96	0.92	800	
	Gypsum	0.013	0.58	1.83	784.9	
Ground floor	Wood	0.022	0.54	1.63	608	0.393
	Concrete block	0.065	3.96	0.92	800	
	Mineral wool	0.075	0.13	0.84	91	
	Sand gravel	0.3	7.74	2.9	2400	
Roof	Wood	0.022	0.54	1.63	608	0.092
	Rafter heads	0.1	0.17	0.84	265	
	Paper wool	0.3	0.13	0.84	91	
	Membrane	0.01	0.58	3.46	3121.3	

Table 2-1: Layers and material properties of each construction type of the building.

The U-value of the external walls is equal to 0.4 W/(m^2 K), while the floor presents a U-value equal to 0.393 W/(m^2 K) and the internal walls between the different rooms a U-value equal to 2.468 W/(m^2 K). The average infiltration rate is equal to 0.5 ACH. There is no mechanical ventilation present in the building and no cooling system, since in Denmark external temperature rarely reach values over 26 °C.

The single family-house is composed of 15 rooms, consisting of two main rooms, the living room and the dining room, both equipped with one facade almost totally covered by glazed surface, three bedrooms, three bathrooms and four rooms dedicated to different uses.

Most of the rooms' surfaces facing South and West orientation are equipped with large glazed surface to capture solar radiation, typical arrangements of the buildings located in colder climate zone.

Each room of the building is considered as a single thermal zone interacting with the others. Each room is equipped with one simple thermostat that control the temperature of the air inside the room. The thermostat is set to 20°C during normal operations during the heating season.

The house is heated up with a radiant floor heating system, described in detail in the next chapter.

A schematic plant of the single-family house is shown in Figure 2-4.

Figure 2-4: Plant of the case study single-family house.

2.2 Weather

The single-family house considered is located in Aarhus, the second biggest city in Denmark, with its own meteorological station, from where the climatic data are collected. The weather data is taken from the from the database [12], starting from TMY data collected from 2004 to 2018 converted in EPW format to be suitable for the analysis performed in this work.

A typical meteorological year (TMY) is a set of meteorological data with data values for every hour in a year for a given geographical location. The data are selected from hourly data in a longer time period (normally 10 years or more). For each month in the year the data have been selected from the year that was considered most "typical" for that month. [13]

The most important parameters included in the dataset are dry bulb temperature, dew point temperature, relative humidity, atmospheric pressure, global horizontal radiation, direct normal radiation, diffuse horizontal radiation, wind direction and wind velocity.

In particular, the external air temperature and the solar radiation are shown in Figure 2-5 and Figure 2-6, respectively.

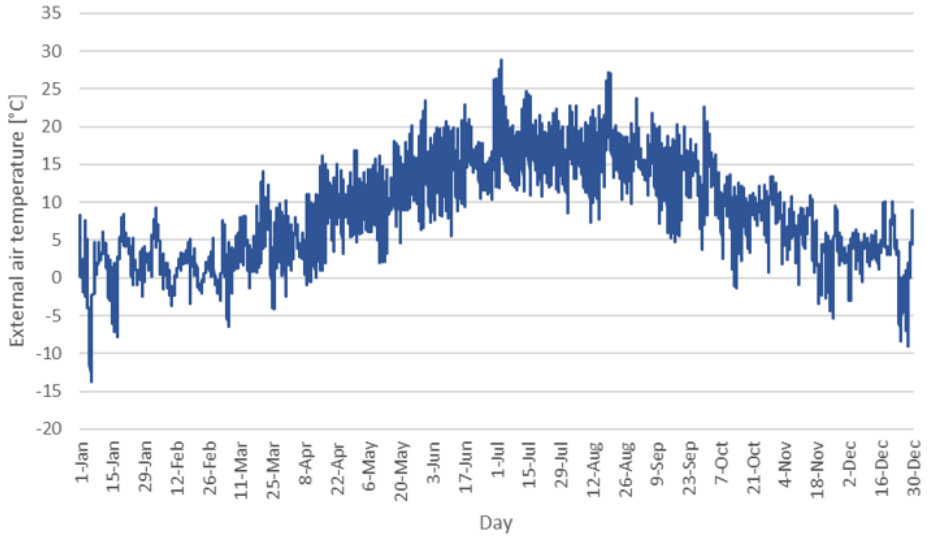

Figure 2-5: External air temperature in Aarhus.

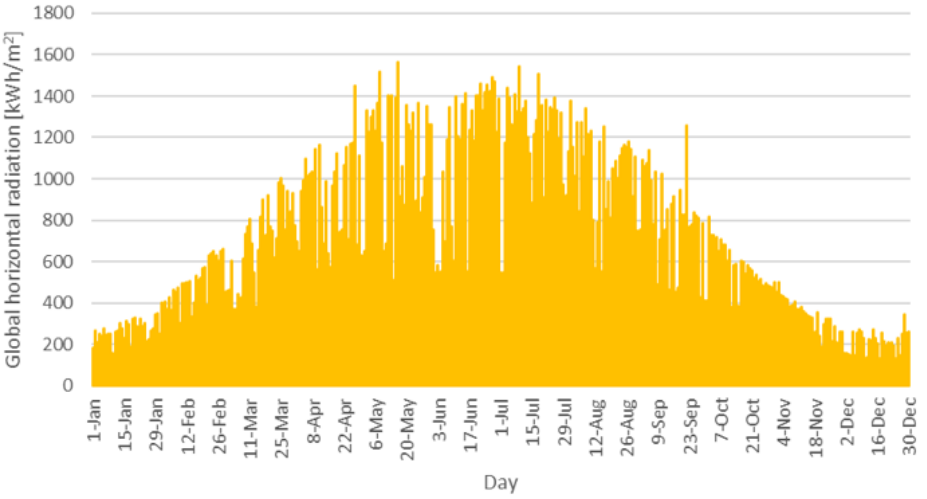

Figure 2-6: Global horizontal radiation in Aarhus.

3 Model

The model of the building considered in this work is created using two different software, Google SketchUp [14] for what concern the geometrical information and TRNSYS [15] for what concern the energy behavior of the building.

TRNSYS is a complete, modular, and expansible simulation environment for the transient simulation of thermal systems including multi-zone buildings. The creation is made in different TRNSYS modules: TRNBuild, TRNFlow and SimulationStudio.

TRNBuild program models the thermal behavior of a building divided into different thermal zones and non-geometric objects, such as materials, constructions, schedules, internal heat gains, regime types, heating, cooling and controls can be added to the project.

TRNFLOW program models the air flow network of a building. With this program the air flows between the different arinodes composing the building, which is known as coupling, from the outside environment into the building, which is known as infiltration, and from the ventilation system can be calculated.

The result of these different programs is the thermal building model of TRNSYS, called Type56, which is used in the simulation environment.

SimulationStudio is the environment in which the numerical energy simulation is performed and the different elements of the building model are controlled and interact with other elements, like technological systems and controllers. TRNSYS simulations are indeed constructed by connecting individual component models, known as Types, together into a complete model. These individual components represent a piece of equipment that can be represented by a system of equations to calculate its performance. These are then connected together in the TRNSYS environment similarly to how they would be connected in real life.

TRNSYS uses a method called successive substitution to solve the system of Types and connections at any point in time.

At the most fundamental level, a component, referred to as a Type, in TRNSYS is merely a black box. The TRNSYS kernel feeds inputs to the black box and in turn, the black box produces outputs. The kernel takes care of solving the system of black boxes.

TRNSYS makes a distinction between inputs that change with time and inputs that do not change with time. Time dependent inputs are referred to as inputs while time independent inputs are referred to as parameters. At each iteration and at each time step, a component turns the current values of the inputs and parameters into outputs. [16]

3.1 Building

In this chapter the description of the building energy model is presented in detail.
The chapter is divided in different sections concerning different topics, starting from the description of the geometry of the building.
Then the energy model is explained, focusing on the constructions composing the building and the respective materials, the air flow network description, the internal mass furniture model and the internal heat gains and schedules description.

3.1.1 Building geometry

The building model contains 3D geometric surface information that is required for the detailed calculations performed in the analysis. To associate the geometric information into the building model, a plug-in called TRNSYS3d for the software SketchUp is used.
To correctly described the thermal behavior of the building, the building model is made of 15 different thermal zones, as shown in Figure 2-4, one for each room.

Starting from the plant of the building, provided by the building owners, knowing the dimensions of each room and the fact that the height of the room is 2.3 m, the building structure is created.
In particular, the different surfaces of the building are created and a surface type describing the function of the respective surface is assigned.
Moreover, to each of them a boundary condition is assigned, describing which is the environment in contact with that surface, choosing between outside environment, internal room environment or ground. This is important for the energy model, which should correctly consider the dynamic flow of energy, the infiltration effects and the heat gains due to solar radiation and internal heat gains.
The other external shading objects, like trees and obstacles, are not modelled in SketchUp but they are directly considered through some components present in Simulation Studio, the simulation software used to carry out the numerical simulation.
The boundary conditions are also assigned to each surface of the building, basically for the floor surface the boundary is the ground floor, for the external walls, roof and glazed surface the boundary condition is the outside environment for the external side and the adjacent room for the internal side. It's indeed

important to assign correctly to each surface also the adjacent surface, in order to take into account the right thermal exchange through the surfaces. [17]

The result of the building geometry model created in SketchUp is shown in Figure 3-1.

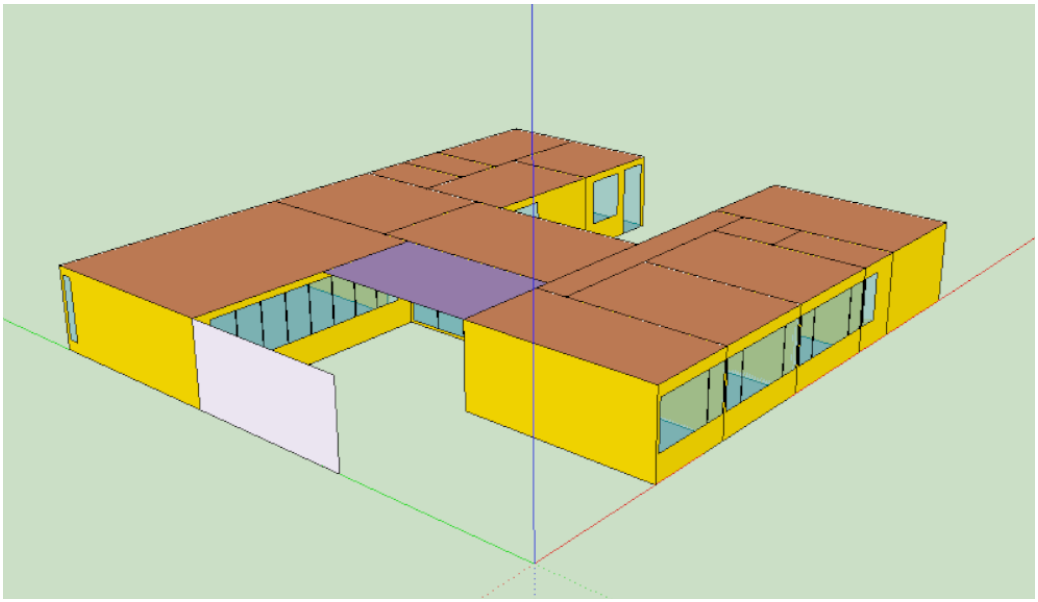

Figure 3-1: SketchUp model of the single-family house.

3.1.2 Construction types and windows

The building is modelled considering the thickness and the material properties of each layer composing the different constructions.

As said, the main construction types are the external walls, the internal walls, the ground floor and the roof. For each of the main thermal properties as the thermal conductivity, the thermal capacity and the density.

A summary of the materials composing the layer of each construction type and their relative thermal properties is shown in Table 2-1.

The windows of the building model are described specifying the glazing and frame properties. The external doors of the building are also defined with the same feature used for the windows, assuming they are completely made of wood.

The window type is chosen from the available TRNBuild library, the window representing a double-glazed window with argon in the cavity between the two glazed surface, is assigned to the window surfaces. This window type is chosen because the U-value and g-value most similar to the real values of the windows present in the building.

The U-value and the g-value of the glazing chosen are equal to 1.34 $\mathrm{W/(m^2\,K)}$ and 0.63, respectively.

The external windows of the building are made with aluminum spacer, while for the external doors of the building no spacer is present and this information are used to account the edge correction.
The c-value, without considering the heat transfer coefficients, is chosen equal to the default value of 8.17 kJ/(h m^2 K). The solar absorptance is used for both sides of the frame and is assumed equal to 0.6, while the emissivity is assumed equal to 0.9, both as default.
The window frame fraction is assumed equal to 0.15 for external windows, so the 15% of the total area of the window is covered by the frame and 75% by the glazed part. For the external door definition this parameter is set equal to 0.99 to simulate the wood door behavior.
The convective heat transfer coefficient defined is used for the whole window, thus accounting for both glazing part and frame. The values used are the most common ones, inside 11 kJ /(h m^2 K) and outside 64 kJ /(h m^2 K). The outside surface heat transfer coefficient is dominated by forced convection due to wind, while for the inside surface the internal calculation of the glass surface temperature varies largely with room conditions.
In Table 3-1 a list of the external windows and external doors present in each room is presented. The windows present in rows in the building facades, when very close each other's, are merged together and considered as a whole unique window called large window.

External windows and external doors			
Room	Type of opening	Heigth	Width
		[m]	[m]
Living room	Large window	1.34	5.76
	Window	1.77	0.3
Dining room	Large window	2	4.5
Bedroom 3	Large window	1.3	3
Bedroom 2	Large window	1.3	3
Bedroom 1	Large window	1.3	1.8
Entrance	Window	2	0.9
	External door	2.1	0.9
Guest room 1	Large window	1.3	1.8
Guest room 2	Large window	1.3	2.4
Kitchen	Window	1.34	1.2
Utility room 1	Window	1.3	1.2
	External door	2.1	0.9
Corridor	Window	1.77	0.6
	External door	2.1	0.9
Toilet 1	Window	0.6	0.6
Bathroom	Window	1.3	0.6

Table 3-1: External windows and external door present in the single-family house.

3.1.3 Air flow network

The infiltrations through the external environment and the exchange of air through the different thermal zones composing the building are modelled using the TRNFlow program of TRNSYS.

TRNFLOW is the integration of the multizone air flow model COMIS (Conjunction of Multizone Infiltration Specialists) into the thermal building module of TRNSYS. COMIS has been developed in an international collaboration in the frame of the IEA Annex 23. [18]

The air flows in a building are calculated with a multizone air flow model that idealizes the building as a network of nodes and air flow links between them as represented in Figure 3-2.

The nodes represent the rooms and the building surrounding. The links represent openings, doors, cracks and window joints.

The wind pressures on the facade and the indoor and outdoor air temperatures are the important boundary conditions, considering also thermal loads as people and electrical equipment. On the other hand, the room temperatures are calculated with a dynamic thermal building model.

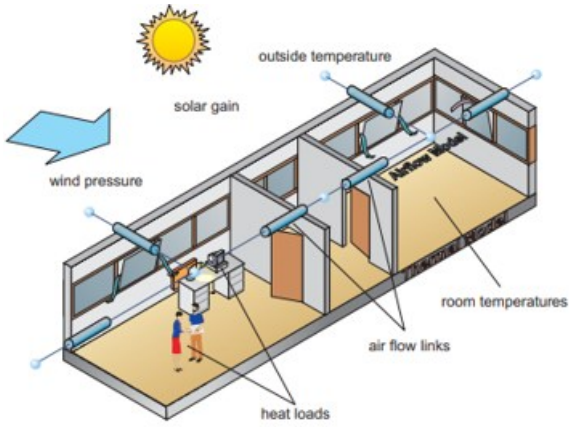

Figure 3-2: Thermal and air flow model of a naturally ventilated building [16].

The thermal model and the air flow model are linked as black boxes. For simplification, in Figure 3-3 the information flow between the two models is represented by one room air temperature node and one variable air flow. In fact, there are at least as many air temperature nodes as there are rooms in the building and each node has at least one air flow. In the solution process, the air flow model starts with the input node temperatures $\vartheta_{in,1}$ and calculates the corresponding air flows $\dot{m}$ of each node. These flows are used in the thermal model, which calculates the output room temperatures $\vartheta_{out,1}$. With an iterative solver algorithm the input temperatures set is found which matches the output temperatures set. [18]

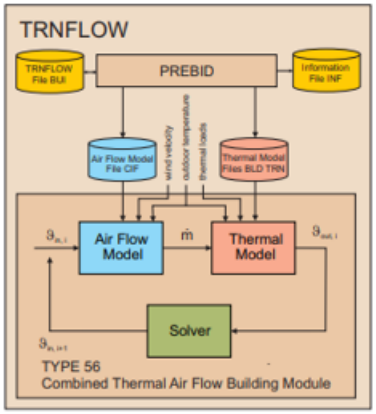

Figure 3-3: Information flow of the combined thermal air flow building module and the user interface for building data input [16].

The description of the air flow network of the building model is presented, starting from the description link and nodes of the TRNFlow network.

The main link type used in the model the building is the crack. Cracks are present in each surface and through them an air flow passes, exchanging heat between the different thermal zones and with the external environment.

To make the flow network reliable, but as simple as possible, only cracks of external walls and cracks related to the large opening, like door and windows, are created. The cracks of the large opening are modelled within the large opening itself, with a specific feature of the software described later.

The crack components use the power law form to express the leakage characteristic:

$$\dot{m} = C_s \cdot (\Delta p)^n \qquad (6)$$

where C_s is the air flow coefficient in kg/s at 1Pa and *n* is the adimensional air flow exponent.

The air flow exponent is in the range of 0.5 for turbulent flow, typical of large opening, and 1.0 for laminar flow, typical of very small cracks. Most cracks have a mixed flow regime with a flow exponent of 0.6 to 0.7.

Values of the air mass flow coefficient for whole buildings or for building components can be found in literature [18].

Component	C [kg/s/m@1Pa]	n
window new weather stripped	≤ $3.33 \cdot 10^{-5}$	0.6
window old weather stripped	$6.67 \cdot 10^{-5} - 2 \cdot 10^{-4}$	0.6
external doors weather stripped	$1.0 \cdot 10^{-4} - 1.0 \cdot 10^{-3}$	0.6
internal doors	$1.3 \cdot 10^{-3} - 2.4 \cdot 10^{-3}$	0.6
brick wall plastered [kg/s/m^2@1Pa]	$2.0 \cdot 10^{-5} - 2.5 \cdot 10^{-5}$	0.85
wall/ceiling joint caulked (masonry/concrete)	$8.0 \cdot 10^{-6} - 1.8 \cdot 10^{-5}$	0.6

Figure 3-4: Examples of mass flow coefficient and air flow exponent in [16].

According to the literature, all the cracks of the external walls of the model present an air flow coefficient assumed equal to $2.5 \cdot 10^{-5}$ kg/s at 1Pa and an air flow exponent equal to 0.85.

Modelling the cracks, also the factor for the mass flow coefficient is requested. A value equal to zero means the crack is totally closed, which has the same effect as there would be no link at all. In the model cracks are assumed to be always full open, so the crack factor is set equal to 1.

Large opening are used to model the behavior of the external windows, external doors and internal doors. The program calculate the air mass flow through these openings in the following way.

As the pressure difference between two airnodes with different air densities is a function of the height z, the flow in a large opening has a vertical velocity profile. A numerical integration of this profile results into an air mass flow for both flow directions:

$$\dot{m}_{12} = C_d \int_0^H \sqrt{2\rho(z) f_{12}(z)} \cdot w(z) \cdot dz \qquad (7)$$

With $f_{12}(z)$=Δp(z) if Δp(z)>0, $f_{12}(z)$=0 if Δp(z)<0

$$\dot{m}_{21} = C_d \int_0^H \sqrt{2\rho(z) f_{12}} \cdot w(z) \cdot dz \qquad (8)$$

With $f_{12}(z)$=0 if Δp(z)>0, $f_{12}(z)$=-Δp(z) if Δp(z)<0

In the previous equations C_d is the discharge coefficient, described later in detail, $w(z)$ is the width of the opening in meters at the height z, H is the height of the opening in meters, ρ is the density, Δp(z) is the pressure difference between two airnodes and $_{12}$ is the flow direction between the two airnodes.

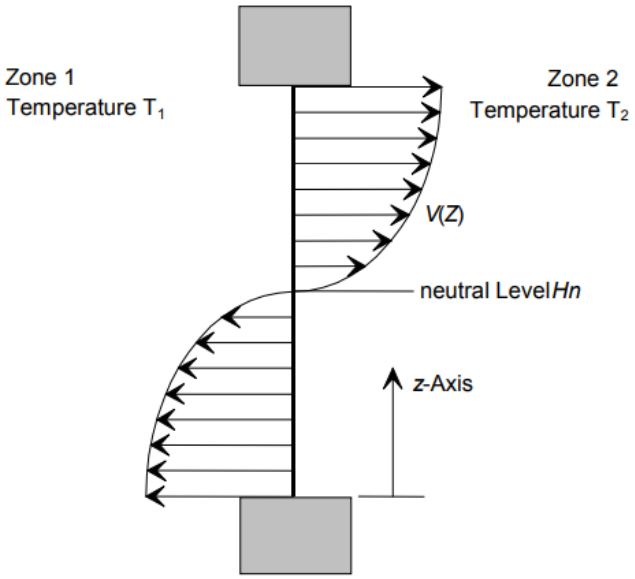

Figure 3-5: Velocity profile in the large vertical opening [16].

The Figure 3-6 shows an example of the TRNFlow setting window for the definition of the large openings characteristic. The category chosen, casement window/door, is divided in four sub categories according the characteristic how the opening area increases with the opening factor. The 'side and for vertical axis' category is chosen to correctly describe the type of windows actually present in the building.

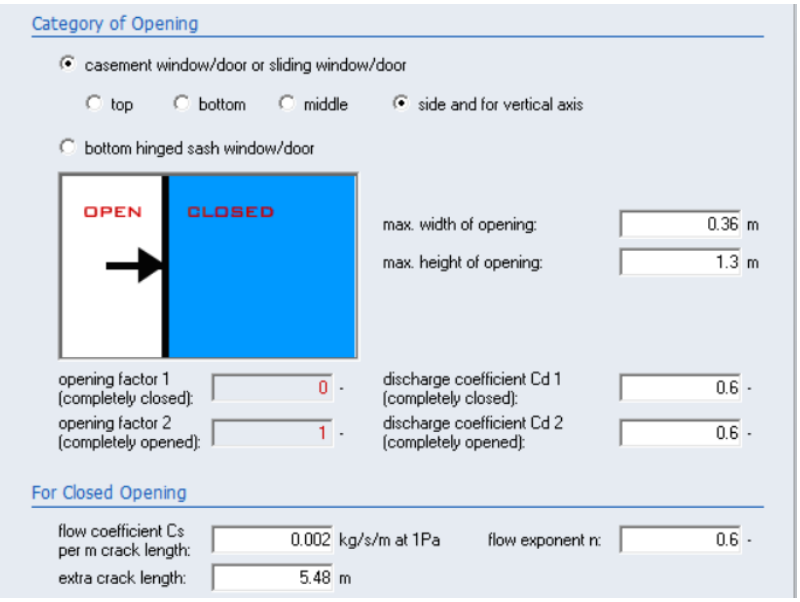

Figure 3-6: Large opening TRNFlow setting window.

The width and the height of the totally opened window, or eventually door, is specified here to model the behavior of the openings present in the building.

In Table 3-2 all the dimensions of each large opening of the building are summarized, grouping them for the corresponding thermal zone.

For the external window, the max width of opening is assumed to be 20% of the total width of the window, while for the door, since they are modelled as always open, the max width of opening is the total width of the door.

Large opening dimensions				
Room	Type of opening	Heigth	Width	Max width opening
		[m]	[m]	[m]
Living room	Large window	1.34	5.76	1.152
	Window	1.77	0.3	0.06
	Door	2.1	0.9	0.9
Dining room	Large window	2	4.5	0.9
	Door	2.1	0.9	0.9
Bedroom 3	Large window	1.3	3	0.6
	Door	2.1	0.9	0.9
Bedroom 2	Large window	1.3	3	0.6
	Door	2.1	0.9	0.9
Bedroom 1	Large window	1.3	1.8	0.36
	Door	2.1	0.9	0.9
	Door	2.1	0.9	0.9
Entrance	Window	2	0.9	0.18
	Door	2.1	0.9	0.9
	External door	2.1	0.9	0.9
Guest room 1	Large window	1.3	1.8	0.36
	Door	2.1	0.9	0.9
Guest room 2	Large window	1.3	2.4	0.48
	Door	2.1	0.9	0.9
Kitchen	Window	1.34	1.2	0.24
	Door	2.1	0.9	0.9
Utility room 1	Window	1.3	1.2	0.34
	Door	2.1	0.9	0.9
	External door	2.1	0.9	0.9
Corridor	Window	1.77	0.6	0.12
	External door	2.1	0.9	0.9
Toilet 1	Window	0.6	0.6	0.12
	Door	2.1	0.9	0.9
Bathroom	Window	1.3	0.6	0.12
	Door	2.1	0.9	0.9
Utility room 2	Door	2.1	0.9	0.9
Toilet 2	Door	2.1	0.9	0.9

Table 3-2: Large opening dimensions for each thermal zone.

The discharge coefficient C_d is used to take into account the physical effects of flow contraction and friction loss and is defined as the ratio between the real flow rate through the opening and the theoretical flow rate calculated with the Bernoulli equation. This value is depending on the shape of the opening edges, the geometry of the opening and on the surrounding conditions on both sides of the opening.

For common situations a value of 0.6 to 0.7 can be found very often in literature. It should be defined for the completely opened and for the completely closed opening and in this work, in both cases, it is assumed to be equal to 0.6. For a partly opened window or door an interpolation between the two given values will be made. In fact, the value for the closed opening is only used for this interpolation, as the closed opening will be modelled with the crack flow characteristic according to the flow coefficient and exponent specified for the closed opening. Here the flow coefficient is given per meters of crack length. The total crack length is calculated from the height and the width of the door or window plus, if necessary, an additional extra crack length. The extra crack length is used to account for all the perimeter of the edges not already considered defining the window dimensions used in the window definitions. Since large window, like in the living room and the dining room, as explained before, are modelled as only one large opening, this parameter is useful to account for the right amount of infiltration through the edges of every window composing the whole large opening.

When the large opening is closed, there is still an air mass flow through the cracks, so similarly to cracks, the flow coefficient and flow exponent are defined for the different type of large opening, as shown in Table 3-3.

Type of opening	flow coefficient Cs	flow exponent n
	[kg/s m at 1Pa]	[-]
Window	0.002	0.6
Internal door	0.0024	0.6
External door	0.0001	0.6

Table 3-3: Flow coefficient and flow exponent for all the large opening type.

Additional parameters should be defined for describing the large openings created, as the opening factor and the own height factor.

If the value of the opening factor is set equal to zero, it means the door or window is closed. It has then a leakage with a crack flow characteristic defined before during the large opening definition. A value equal to 1 means the large opening is totally open. A value in between means the opening is partly opened. The internal doors in the house are assumed to be always open so the opening factor is set equal to 1. The external doors are instead assumed to be always close, so the opening factor is set equal to 0. The opening of the external window is controlled outside TRNFlow, with a dedicated control in the simulation environment of Simulationstudio.

With own height factor slanted windows can be defined. It is the cosine of the angle between the opening plane and the vertical plane. A value of one means the opening is located in a vertical wall and a value of

zero means the opening is located in a horizontal ceiling or floor. In the considered building every window or door is located in a vertical wall, so a vale equal to 1 is set for each large opening.

The driving forces of the air flow network described are mainly wind pressure and buoyancy.

The wind pressure on a facade is defined as the difference between the local pressure on the surface and the static pressure in the undisturbed wind at the same height. The relation factor of this pressure difference to the dynamic pressure of the reference wind velocity v_0 is known as wind pressure coefficient or Cp-value. The wind pressure can be calculated with the Cp-value according to equation (9):

$$\Delta p_w = C_p \frac{\rho}{2} \cdot (v_0)^2 \qquad (9)$$

Where Δp_w is the wind pressure difference between the pressure on the facade and the static pressure in the undisturbed wind of the same height, C_p the wind pressure coefficient, v_0 the reference wind velocity at the building location and reference height and ρ the air density.

For all external nodes the same reference wind velocity v_0 at the building reference height is used.

The wind velocity profile exponent depends on the roughness of the terrain, values for four roughness classes are given in Figure 3-7. Since the single-family house is located in the suburbs area of Aarhus, a coefficient equal to 0.3 is assumed for all wind directions.

class	terrain description	α
1	sea, flat terrain without obstacles	0.1 - 0.15
2	open terrain with isolated obstacles	0.15 - 0.25
3	wood, small city, suburb	0.25 - 0.35
4	city centre	0.35 - 0.45

Figure 3-7: Roughness classes and coefficient.

Not only wind effect, but also buoyancy resulting from temperature and air composition differences, is taken into account. Therefore the vertical position of the nodes and links must be defined. In Figure 3-8 a general link between an external node and a thermal airnode is shown to have a better understanding of how the buoyancy effect is taken into account in the model.

The pressure difference between the two sides of the link is defined as:

$$\Delta p = p_{L1} - p_{L2} \qquad (10)$$

where p_{L1} and p_{L2} are the pressure in the two sides of the link.

In Figure 3-8:

$$p_{L1} = p_{ref} - g \cdot \int_0^{z_{L1}} \rho_1(z) \cdot dz \qquad (11)$$

$$p_{L2} = p_2 - g \cdot \int_{z_2}^{z_{L1}} \rho_2(z) \cdot dz \qquad (12)$$

where p_{ref} and p_2 are the pressure at the building reference level and at the airnode, g is the gravity acceleration, ρ_1 and ρ_2 are the density in the external and internal airnodes and z_{L1} is the height of the link.

And with the assumption of a uniform air density in the airnode and at the outside:

$$p_{L1} = p_{ref} - \rho_1 g h_{L1} \qquad (13)$$

$$p_{L2} = p_2 - \rho_2 g h_{L2} \qquad (14)$$

where h_{L1} and h_{L2} are the height of the two sides of the link respect the reference level of the respective airnode.

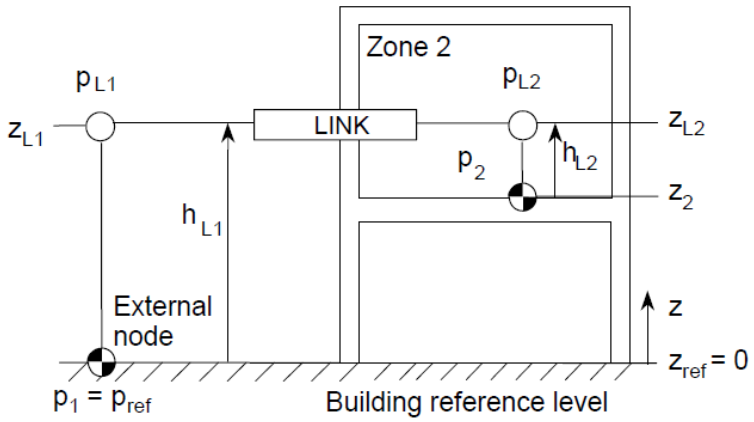

Figure 3-8: Links height and pressure in the airnode [16].

This is the reason why it's important also defining the height of the links connecting the different thermal zones with others rooms or with the outside environment. For the crack of the walls, the height of the link is assumed to be equal half of the height of the room, so 1.35 m. For what concern the external windows, the height of the link is assumed to be the height of the bottom edge of the window itself.

3.1.4 Internal mass furniture

Many numerical models for building energy simulation assume empty rooms and do not account for the indoor content of occupied buildings. Furnishing elements and indoor items have complicated shapes and are made of various materials. Therefore, most of the people prefer to ignore them. However, this simplification can be problematic for accurate calculation of the transient indoor temperature. [19]
The performance of the heat storage capacity of a building, indeed, strongly depends on the amount of thermal mass which can be activated in the indoor environment. Since the focus of this work is to assess the energy flexibility of the considered building, the thermal mass of the furniture, contents and internal structural walls is considered when modeling thermal zones. This should be also done to avoid unrealistic quickly variations of temperature and consequently heat exchange in the building.

The approach chosen to model the internal mass is the one adopted by Johra et al. in [20].
The additional indoor thermal mass/furniture is modelled as an equivalent fictitious planar element which aggregates all indoor items into an homogenous representative material.
The equivalent homogeneous material of the element is assumed to be with a density of 715 kg/m^3, a thermal conductivity of 0.3 W/(m K) and a specific heat capacity of 1400 J/(kg K). It is assumed that 50% of the internal radiative heating gains and solar radiation are absorbed by the surfaces of the planar elements.
The additional indoor content is concentrated in an equivalent slab which is 4.7 cm thick.
The surface area of one side of the element is equal to 1.8 times the surface area of the floor in the thermal zone. The equivalent planar element does not have any real geometrical representation or position in the room. The element is coupled to the rest of the thermal zone in the same way as if it was an internal wall only connected to the air node. The mixed convection/radiation surface thermal resistance coefficient is assumed constant and equal to 0.13 (m^2 K)/W.

3.1.5 Internal gains and schedules

Internal gains as people, lights and other electrical devices are defined and assigned to each thermal zone of the building.
In this work all the electrical equipments, considering also lights and appliances, are merged together to simplify the model and their impact is considered to be proportional to the floor area of the room in which they are assigned.
The radiative power is assumed equal to 11.274 kJ/(h m^2) and the convective power is assumed equal to 7.516 kJ/(h m^2). The electrical power fraction of this type of gain is set equal to 1 since all the lights and appliances are powered by electricity.

To correctly evaluate the impact of the people living in the house, two different type of internal heat gains are defined: one describing a general person in relaxed conditions and one describing an active behavior of the person. In this case the internal gains are chosen from the available library present in TRNBuild based of standards EN13379: 80W person, with both convective and radiative power emitted equal to 99 kJ/h and absolute humidity equal to 0.037 kg/h, and 170W person, with both convective and radiative power emitted equal to 153 kJ/h and absolute humidity equal to 0.125 kg/h.

Different schedules are assigned to the different internal loads to better quantify their impact on the thermal zones in which they are assigned.
A different schedule for people activity, electric equipment and people occupancy is created, defining them daily and weekly. The weekly schedule is composed assigning the different daily schedule to each day of the week.
The schedule used are built based on occupants' behavior of the building analyzed.
Different schedules are created for passive zone and active zone, meaning that in passive zone people usually stay for long time, while in the active zone, as living room, dining room and kitchen, people usually stay for short time event like lunch and dinner. Also, the behavior of the people in passive and active zone is different, indeed, in passive zones like bedrooms, people usually stay relaxed or sleep, while in kitchen or dining room people move more and do some activities. This is the reason why also an activity schedule is created.
The subdivision of the different thermal zones of the building in passive zones and active zones is shown in Figure 3-9.

Figure 3-9: Passive zones (light blue) and active zones (yellow).

People occupancy schedules are created assuming a different behavior during the weekdays and the weekend, distinguishing between active and passive zone. It's difficult to perfectly track the behavior of the occupants of different ages in the different rooms of the house, consequently some assumptions are made to generalize as much as possible the people behavior, keeping it as correct as possible.

The active zone occupancy schedules are created based on the following assumptions.

During weekdays is assumed that all the 4 people meet and stay together from 7 am to 8 am in the kitchen and dining room for breakfast and from 5pm to 9 pm remain in the kitchen preparing the dinner, while in the dining room eating and cleaning and some hour stay also in the living room. During the weekend is assumed that, in general, 2 people stay in the active zones during daily time, from 8 am to 10 pm.

To create the weekly schedule that are assigned to the different rooms of the building, a daily schedule is created based on the previous assumptions, one for each available day of the week.

Figure 3-10 and Figure 3-11 shows the weekdays and weekend days occupancy schedule related to the active zones, respectively.

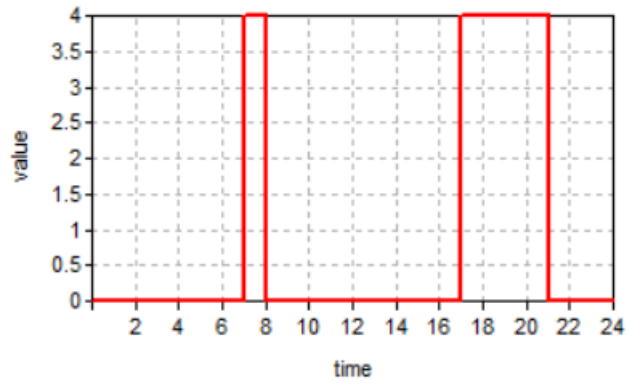

Figure 3-10: Active zone weekdays occupancy schedule.

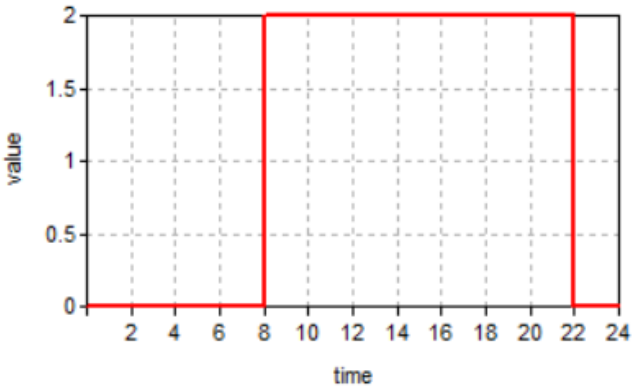

Figure 3-11: Active zone weekend days occupancy schedule.

The passive zone occupancy schedules are created based on the following assumptions.

During the days of the week is assumed that all the 4 people stay in the sleeping rooms during the night from 9 pm to 7 am of the day after. During the weekend is assumed that 4 people spend the night in the same way of the weekdays but, in general, 2 people also stay in the passive zones during day hours, from 8 am to 10 pm.

As before, to create the weekly schedule that are assigned to the different rooms of the building, a daily schedule is created based on the previous assumptions, one for each available day of the week.

Figure 3-12 and Figure 3-13 show the weekdays and weekend days occupancy schedule related to the passive zones, respectively.

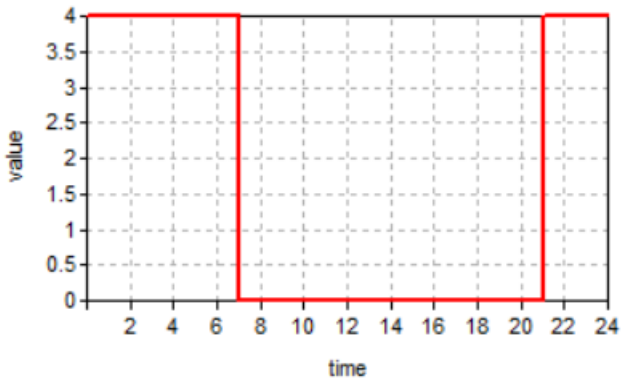

Figure 3-12: Passive zone weekdays occupancy schedule.

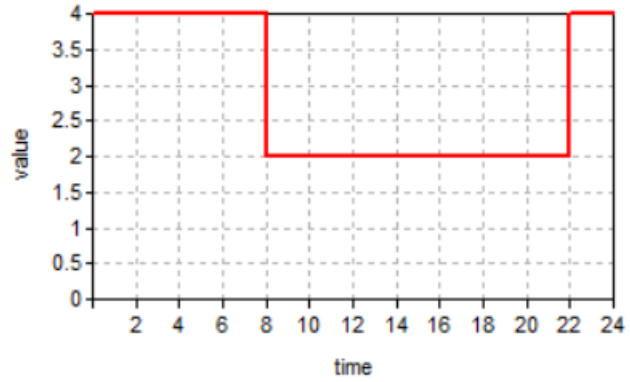

Figure 3-13: Passive zone weekend days occupancy schedule.

To assess in a more precise way the internal heat gains given by the people inside the rooms, different activity schedules are defined, for weekdays, Saturday and Sunday.

As said before, two type of activity schedule are created, one for the relaxed people behavior and one for active people behavior. The logic within these schedules is created is that in each room of the building both active and relaxed people are added as internal gains, so two different type of internal gains together, but only one of them will be “activated” depending on the room. These activity schedules are indeed added as multiplier for the occupancy schedule. This means that when this schedule presents a value of 1, the people that are in relaxed mode are “activated”, so are effectively present in the room with their behavior, while when the value is set to 0, it’s like there are no people with that behavior in the room, but it is possible that the other behavior is activated.

The relaxed behavior is activated during sleeping hours from 10 pm to 7 am of the day after, except for Saturday in which one hour less of relaxed behavior is assumed during night.

As before, to create the weekly schedule that are assigned to the different rooms of the building, a daily schedule is created based on the previous assumptions, one for each available day of the week.

The active behavior is instead activated during the day time, starting from 7 am in the weekdays and 8 am in the days of the weekend, while the end of the activation period is 10pm for each day except for Saturday in which is 11pm.

A schedule for the lights, appliances and all electrical equipment is created.

As explained before, all the equipment that use electrical energy are merged together and account as only one internal heat gain, but the heat gain is weighted with the floor area of each room in which the schedule is added.

In this case the value set in the schedule vary from 0.2 to 1, since the whole system is not always switched on. During the night the value is set to 0.2, which is the minimum amount of energy used, in general, for the electrical equipment, there is an increase until 0.5 from 7 am to 8 am after the weaking of the people and the schedule is set to 1 from 4 pm to 7 pm, during the dinner time.

In the weekend the consumption pattern is similar, but it is reasonable think there is a little higher consumption in the middle of the day because people can stay inside the house.

Figure 3-14 and Figure 3-15 show the weekdays and weekend days electric equipment, respectively.

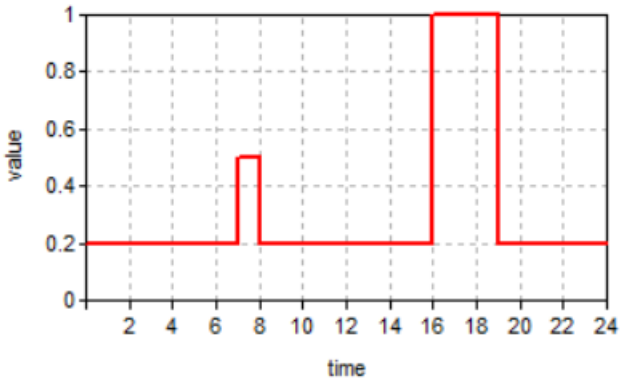

Figure 3-14: Electric equipment weekdays schedule.

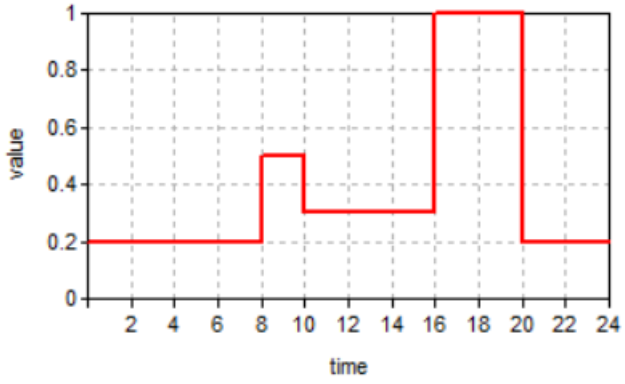

Figure 3-15: Electric equipment weekend days schedule.

3.2 Energy systems

In this chapter the models describing the energy systems present in the single-family house are presented. Depending on the different simulation scenarios simulated, the energy systems can vary. The building is always heated through a radiant floor heating system in all the simulation scenarios, while in some of them, a thermal energy storage coupled with a heat pump is added.

3.2.1 Floor heating system

The single-family house is heated through a radiant floor heating system and every room is a heated space. The floor heating system is controlled through one simple thermostat for each room. The system is controlled in different way depending on the simulation scenario and it will be explained in the next chapter.

To model the radiant floor heating system in TRNBuild, an "active layer" is added to the floor construction. The layer is called "active" because it contains fluid filled pipes that either add or remove heat from the surface. The active layer is basically described by 5 parameters as shown in Table 3-4.

Pipe spacing	0.15	[m]
Pipe outside diameter	0.02	[m]
Pipe wall thickness	0.002	[m]
Pipe wall conductivity	1.26	[kJ/(h m K)]
Specific heat coefficient of water	4.18	[kJ/(kg K)]

Table 3-4: Floor heating system model parameters.

For surfaces containing an active layer, the convective heat transfer coefficient between the surface and zone air depends on the temperature of the active layer.

The inlet mass flow rate and the inlet temperature are inserted outside the program as input through some components in the simulation environment of Simulation Studio.

The radiant floor heating system is composed by the following layers shown in Figure 3-16 and is added to the floor construction of each room of the building.

No.	Layer	Thickness	Type
1	Wood	0.022	massive
2	Concrete_block	0.045	massive
3	Active_layer		active layer
4	Concrete_block	0.020	massive
5	Mineral_wool	0.075	massive
6	Sand_gravel	0.300	massive

Figure 3-16: Floor heating system construction layers.

To control the floor heating system, a simple thermostat for each room of the building is used. The simple thermostat is modeled using the Type 166. The Type 166 present as parameter a dead band, which is set equal to 0.5 °C, and as inputs the monitoring temperature and the heating setpoint temperatures. The monitoring temperature is the temperature of the air inside each room in which the thermostat is placed, while the heating setpoint temperature is set to be constant and equal to 20°C.

The output of the thermostat is an on/off signal that is used to control the mass flow rate sent through the floor heating system.

Thus, Type 166 monitor the temperature in the room and when it reaches 20°C gives as output 0, while when the room air temperature is below 20°C gives as output 1.

These two numbers are taken from Type 166 and sent to a “calculator”. Calculators are used in Simulation Studio to create new inputs, that can be connected with the outputs of other components or manually inserted, perform mathematical and logic calculation and give back new outputs.

The control, one in each room, of the floor heating system is shown in Figure 3-17. In the calculator named “m_and_Tin_input” the design mass flow rate and the inlet temperature of the floor heating system are collected. In the calculator named “Control”, a product between the signal from the thermostat and the mass flow rate input is performed.

In this way, when the thermostat signal is equal to 0, so when the temperature is higher than 20°C, the result of the product is 0, meaning that the flow rate to be sent through the radiant floor heating system is null. Otherwise, when the thermostat signal is equal to 1, the product leave as results the number quantifying the mass flow rate to be sent in the floor heating system. This output is thus sent to the floor heating system model of the building.

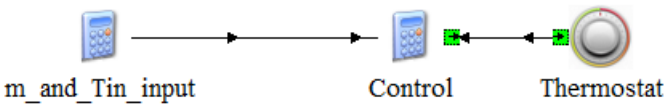

Figure 3-17: Floor heating system control present in each room.

The inlet temperature is set equal to 39°C when the external air temperature is below 2°C, equal to 29°C when the outside temperature is above 12°C and between these values a linear interpolation is performed, as shown in Figure 3-18.

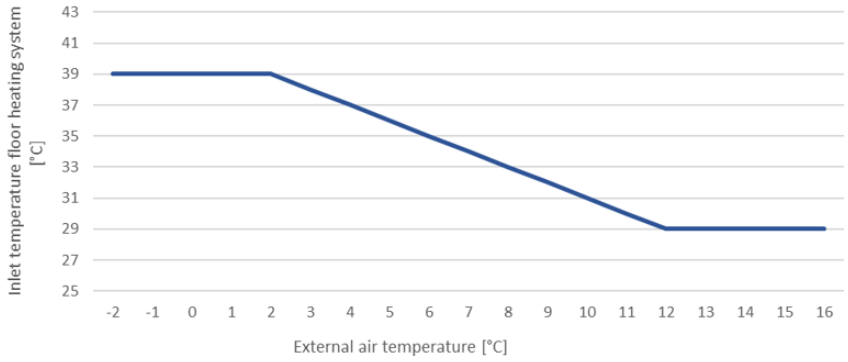

Figure 3-18: Inlet temperature decision depending on external temperature.

The resulting whole control system of the floor heating system is thus composed by one simple thermostat dedicated at each of the rooms of the buildings, resulting in 15 different thermostats.
The thermal zones of the building, one for each room, exchange air and thermal flow each other's influencing the internal temperature of the single room controlling the thermostat, but the 15 thermostats act independently for each room. The final mass flow rate circulating in the floor heating system will be the sum of the requirement for each of the rooms of the building.

3.2.2 Heat pump coupled with thermal storage tank

The thermal storage tank is modeled through the Type 158. This model consists of a constant volume storage tank with a vertical configuration filled with water.
The fluid in the storage tank interacts with the external environment through thermal losses from the top, the bottom and the edges of the tank and with up to two flow streams that pass into and out of the storage tank.
The tank is divided into isothermal temperature nodes to model the stratification phenomena typical of the storage tanks. Each constant-volume node is assumed to be isothermal and interacts thermally with the nodes above and below through several mechanisms such as fluid convection between nodes and through fluid movement, either forced movement from inlet flow streams or natural destratification mixing due to temperature inversions in the tank.

The Type 158 allows to define as parameter different characteristic of the tank. In particular, a tank of 400 liters is chosen, with a height of 1.5 m. The tank is modeled with 10 isothermal nodes and the fluid inside the tank is water, with the corresponding fluid density, thermal conductivity. The top, bottom and edge and loss coefficient are equal to 3.325 kJ/(h m^2 K) and the thermal losses depends on the room temperature in which the tank is placed, in this case assumed to be the utility room. The thermostat monitoring the tank temperature is placed at 70% of the total height of the tank.

As said, the thermal storage tank has four different ports, two of them to interact with the heat pump and two to interact with the building floor radiant system. In particular, one stream is sent to the tank from the outlet of a mixer, modelled through Type 649, collecting all the streams coming from the outlet of the floor heating system present in each room. The water is mixed in the tank with the stream coming from the heat pump and is sent back to the floor heating system. The outputs of the Type 158 are thus the two mass flow rates exiting the tank and their corresponding temperatures

The whole technological system scheme comprehensive of thermal storage tank (Type158) and floor heating system (present in the building in Type56) with information flows, represented through a black line, and the water flow, represented through a blue line, is presented in Figure 3-19.

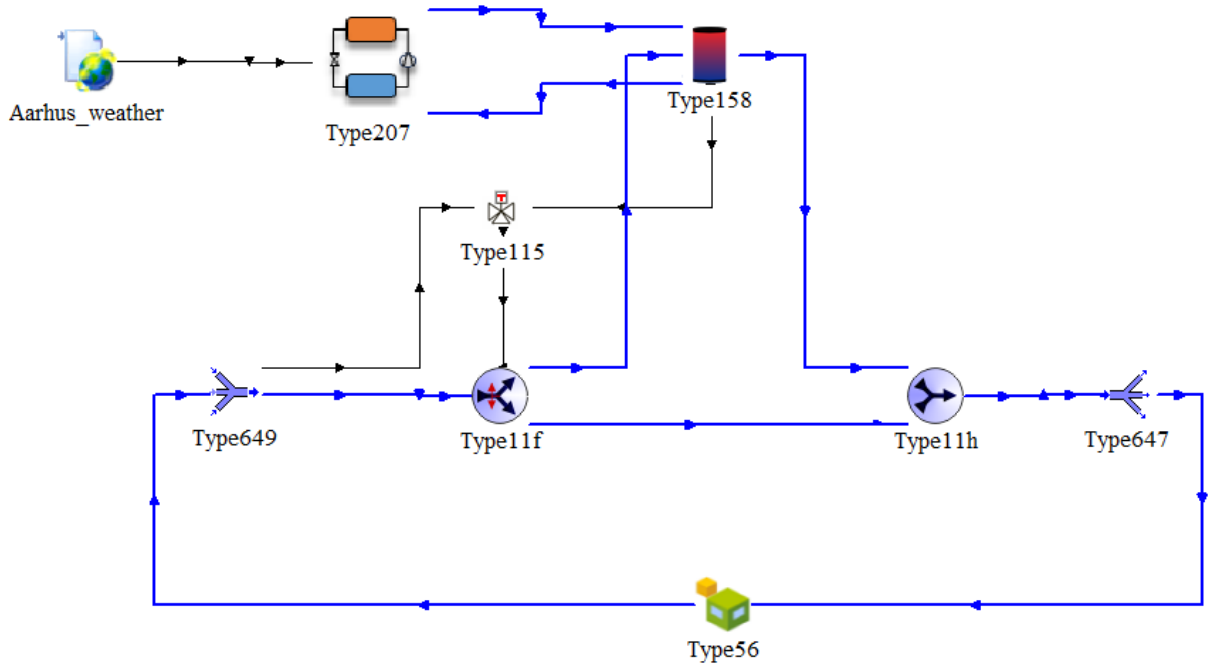

Figure 3-19: Technological system scheme comprehensive of thermal storage tank (Type158) and floor heating system (present in the building in Type56) with information flow (black line) and water flow (blue line).

The temperature of the flow rate to be sent to the inlet of the floor heating system is controlled through a tempering valve, of which the control is modeled with the Type 115.

This component calculates the fraction of fluid that should be sent to the source for a standard tempering valve, while one minus the fraction sent to the source is sent directly to the mixing valve. The controller calculates the amount of fluid that should be sent through the source and the amount of fluid bypassing the source that, when mixed together, provide the setpoint temperature chosen. [21]
In this case the source is the thermal storage tank, while the setpoint temperature is the desired inlet temperature of the floor heating system. Thus, one input of the Type 115 is the tempering temperature of the stream that should be divided, a part sent to the tank and a part that should by-pass the tank.
The part that by-pass the tank is then to be mixed with the hot stream coming from the thermal storage tank to regulate the final temperature, this is the reason why is called tempering temperature. One other input is the temperature of the source, meaning the temperature of the flow rate exiting the storage tank and mixing the by-pass flow rate.
As said, the Type 115 only controls the different temperatures of the fluid entering and exiting the tempering valve. The outputs of this component are indeed only the two fractions to be sent to the tank and the by-pass the tank. These two outputs are sent to another component, the Type 11f.

Type 11f modeled a flow diverter externally controlled by external signal, in which a single liquid stream is split according to the information given by Type 115 previously described.
The inputs of this type are the temperature of the fluid entering the valve and the mass flow rate, both the information are taken from the mixer already cited.
This mixer merges the streams coming from the return of the floor heating system of each room, giving back the total temperature and the total amount of water circulating in the system.
Type11f gives back as outputs the mass flow rate and corresponding temperature desired to be sent to the tank and to a new mixer, modeled through Type 11h, that has the objective to materially merge the hot stream coming from the thermal storage tank and the by-pass stream, to obtain the desired temperature at the inlet of the floor heating system.
The mixer cited are modeled through Type649, which simply allows to receive as inputs the temperature and the mass flow rate of a defined amount of stream, mixing them and calculating the temperature and mass flow rate of the exiting stream.
The heat pump coupled with the thermal storage tank is an on/off air to water heat pump.
This means that the heat pump can only operate in two different states, switched on, at full load, or switched off, with no load. The heat pump is only used in heating mode and the heat source is the external air.
The heat pump model is described through Type207. [22] The information about the compressor presents in the heat pump and the refrigerant used are inserted in the model through the polynomial coefficients of the compressor. These coefficients are provided from the Select 8 Copeland Emerson

selection software. The refrigerant chosen is the R454C, presenting a global-warming potential equal to 148 (GWP 148) with a security classification ASHRAE A2L, less flammable than others refrigerant. [23]
Global-warming potential, abbreviated as GWP, is a term used to describe the relative potency, molecule for molecule, of a greenhouse gas, taking account of how long it remains active in the atmosphere. [24]
The compressor is chosen starting from the refrigerant and knowing the operating conditions, selecting -15°C as evaporation temperature and 40°C as minimum condensation temperature, while the superheating desired is equal to 10°C and the subcooling equal to 0°C. The compressor model 3DA-75 is chosen from the selection software, presenting a heating capacity of 16.25 kW, power of 5.16 kW and a COP equal to 2.20 in standard condition.
Type 207 modeling the heat pump receive as main input the information about the external temperature of the air, while the amount of air taken is assumed constant and equal to 6000 kg/h.
The external temperature, as already explained, is taken as input from the Energy Plus weather data file (epw) and so varies over time. This causes a variation over time also of the COP and so the power released by the heat pump to the fluid.
The other inputs are the temperature of the fluid taken from the thermal storage tank and its amount, chosen equal to 2200 kg/h.
The heat pump is controlled externally in different ways depending on the simulation scenario considered and it will be explained in detail in the next chapters.

In the Simulation Studio environment is also possible to model external shading objects different from the one considered in the geometry of the building and this is done through the combination of the use of Type 34 and Type 67.
Type 34 give the possibility to model the shading effect of overhangs and wingwalls.
The geometry of the receiving surface is modeled through the parameters present in Type 34, as the height and the width of the receiver and the length of the overhang. The overhangs are created for the south and west facade to cut some of the incident solar radiation as it happens in the real-life conditions. The overhang length is of 0.2 m in the west facade and 0.5 m in the south facade, while the distance from the window below the overhangs is set equal to 0.1 m.
The information about position of the sun and intensity of solar radiation are taken from the weather data file and sent to Type 34 as inputs, in particular solar zenith angle, solar azimuth angle, total horizontal radiation, horizontal diffuse adiation, beam radiation on surface and the incidence angle. What is generated as output from the Type 34 is a new orientation to be used in the building model in TRNBuild accounting for the shading operated by the overhangs, both for west and south orientation. In Figure

3-20 is shown the interaction between the different components modelling the shading for the west orientation.

Figure 3-20: Overhang model and information flow for West orientation.

Regarding the south orientation, also the shading contribution due to the trees present in the garden of the single-family house is considered.

The flow of information is similar to the one applied for the west orientation, but in this case Type67 is used to model the presence of the trees and their impact on the solar radiation, as shown in Figure 3-21.

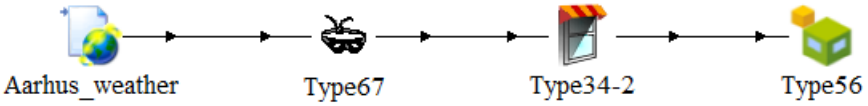

Figure 3-21: Overhang model and information flow for South orientation.

Type 67 reads a data file containing the angular heights of obstruction objects seen from an arbitrary opening and outputs two numbers which describe the time dependent shading of the opening.

The first value is equal to 0 or equal to 1, corresponding to whether beam radiation is blocked or visible. The second is a number with a value between 0 and 1, which gives the fraction of diffuse radiation visible from the opening. A value equal to 0 indicates that no diffuse radiation is visible and a value equal to 1 indicates that all the diffuse radiation normally visible by the window is indeed visible.

The beam radiation calculation is made simply by deciding whether the sun is obstructed by an object at any given time. The diffuse fraction calculation is made by integrating the shading effects seen by the window and dividing by the view from the opening were there no shading objects present. With these dimensionless numbers, the radiation normally incident on the opening can be adjusted to account for shading. [25]

The openings are defined as having a 360 degrees view angle and that the plane containing the opening would be considered an obstruction shading the opening.

Obstructions are defined by an angular height as viewed from the opening. Surface angles (α) are defined in an absolute co-ordinate system, so as opposed to relative to the opening, and for each one, an angular

obstruction height ϑ is required as shown in Figure 3-22. An obstruction height angle around 60 degrees is chosen for most of the surface angles.

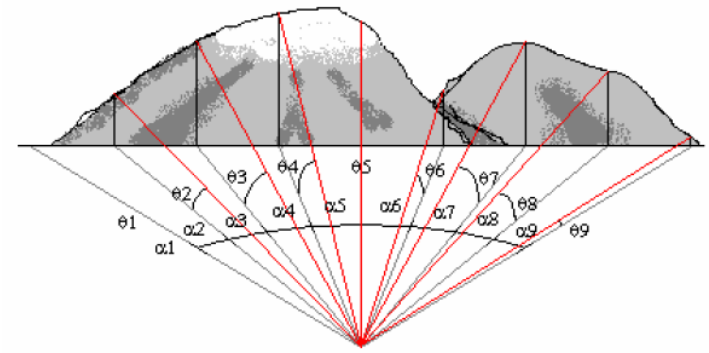

Figure 3-22: Definition of surface angles (α) and obstruction height angles (ϑ) [23].

4 Method

The quantification of the energy flexibility of the Danish single-family house analyzed is carried out using the Active Demand Response (ADR) method, consisting in generating some events that force to change the normal operation of the systems in the building to create some advantages during the period of effect of the ADR events. There are different types of ADR events that can be generated, in this chapter an explanation of in which the different events consist of is provided.
In this study also the building technological setup is changed in different scenarios to understand how the energy flexibility change in different configurations. The energy flexibility is quantified through different key performance indicators, described in detail in the next chapter.

The logic under the use of the Active Demand Response event in this analysis is strictly related to the new SG Ready standard for the heat pump. SG Ready (short for smart grid ready) is a label certifying that a heat pump or a complimentary management technology can respond to defined external control signals. The label was introduced in 2012 by the German heat pump association (Bundesverband Wärmepumpe, BWP) together with 17 heat pump manufacturers. The label aims to promote the external control of heat pumps so that they can be operated in response to price signals and the state of the grid. This allows heat pumps to support the power grid, have a lower carbon footprint and be more cost-effective to operate.
SG Ready supports different mode: blocked operation, in which the operation of the heat pump is blocked for a maximum of two hours per day, normal operation, in which heat pump runs in energy efficient normal mode and encouraged operation, in which the operation of the heat pump is forced to increase electricity consumption for heating and warm water. [26]
When combined with dynamic electricity prices, heat pumps can be scheduled to operate during low price periods to reduce energy costs.

According to these directives, in this work the ADR events are designed to change the normal operation of the system for 2 hours, making the heat pump working in blocked operation or encouraged operation. The schedule of the ADR events is designed starting from the electricity price signal in the central region of Denmark, the area in which Aarhus is located.
According to the electricity price, when a low-price period is identified in the chosen day, the operation of the heat pump is forced to stay on for 2 hours (upward event), while in the high price period, the operation of the heat pump is blocked for 2 hours (downward event). The schedule is designed with only one event each 4 days, alternating upward and downward events, this because the goal of this work is to have independent events, meaning that the change in consumption due to one event should not affect

the thermal behavior of the building during the time period of the successive event. This allows to study the impact of the ADR events on the energy flexibility that they can make available in a clearer way.
The simulation is carried out during the heating season, from the month of January to May. This decision is made because in this way is possible to analysis both the colder months and the warmer months, maintaining the computational time required for the simulation as low as possible but having a comprehensive analysis.

4.1 Type of Active Demand Response event

The energy flexibility is studied through two different configurations of the system, one in which only the floor heating system is used to heat up the building, one in which also the thermal storage tank coupled with the heat pump is present.
The Active Demand Response events are realized in two different ways: in one case the events are generated changing the heating setpoint temperature of the thermostats of the rooms composing the building, while in the other case the events are generated forcing the operation of the heat pump coupled with the thermal storage tank in the desired operation state.

The change in the heating setpoint temperature of the thermostats of the rooms consists in the increase of the setpoint from 20°C, set during normal operations, to 22°C during upward events and 18°C during downward events.
During the upward events the heating setpoint is increased for 2 hours, from 20°C to 22°C, resulting in higher heating energy required to bring the room temperature to 2°C more compared to normal operation, requiring the floor heating system to be activated for more time, resulting in higher energy consumptions. The energy released to the room environment is used to increase the temperature of the air inside the room, but is also stored in the building structure of the room, as internal and external walls, floor and internal furniture.
This energy stored is released back to the room environment with a delay in time, resulting in a sort of free internal heating gain in the period after the finish of the ADR event. This results in a decrease in the energy consumption after the ADR event respect the consumption that would be necessary if the event is not happened.
Similarly, in case of a downward event, the heating setpoint is decreased for 2 hours, from 20°C set during normal operation to 18°C . This results in a decrease in the energy consumption during the 2 hours of the ADR event because the floor heating system is activated for less time, since there is less energy required to reach the target temperature of 18°C compared to 20°C. After the event, since the room temperature

is decreased, there is more energy need compared to a situation without ADR event, because the system has to bring back the temperature to 20°C starting from lower values, instead only keeping it to around 20°C.

In these type of ADR events, thus, the energy flexibility is given from the building structure, because this is the element of the building that is charged of energy and from which the energy comes back to the room environment during the ADR events.

A schematic representation of a general upward ADR event is provided in Figure 4-1. [27]

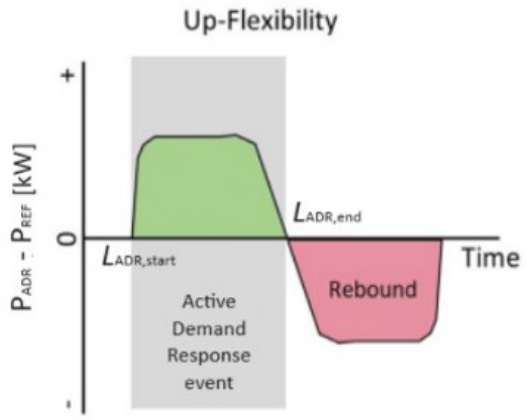

Figure 4-1: Schematic representation of an upward ADR event [27].

The figure represents the difference between the power consumption of the building during the ADR event and the power consumption of the building during normal operation, without the ADR event. The increase in the heating setpoint temperature results in a higher consumption of the ADR profile, resulting in an energy surplus stored in the building structure, represented by the green area. The grey area represents the duration of the ADR event, during which the heating setpoint is increased. After the event, the surplus of energy stored in the building structure is released to the environment, resulting in a decrease in the consumption of the ADR profile respect the normal operation. This effect is called "rebound effect" and is represented by the red area.

Similarly, a schematic representation of a generic down-ward event is provided in Figure 4-2. [27]

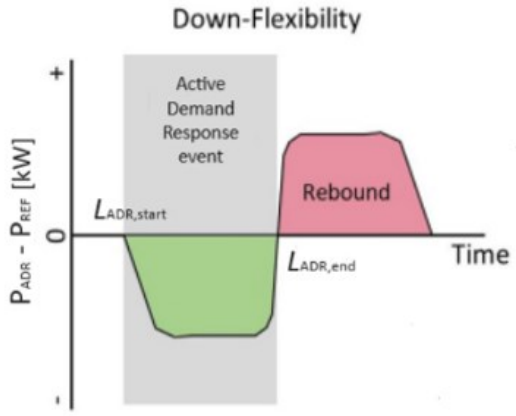

Figure 4-2: Schematic representation of a downward ADR event [27].

In this case the decrease in the heating setpoint results in a lower consumption of the ADR profile, resulting in a sort of save of energy during the e duration of the ADR event, represented by the green area. After the event, since the building is previously charged with a lower amount of energy, it requires more energy after the event to reach again the heating setpoint temperature, represented by the red area.

The other possibility considered in this analysis is to generate the Active Demand Response events forcing the heat pump coupled with the thermal storage to stay in the desired operation state.
During the upward events, the operation of the heat pump is forced to stay switched on for 2 hours.
This means that, since the heat pump is forced to stay always switched on, the energy consumption of the heat pump during this period is higher respect the one required during normal operation, in which the heat pump switches off when the temperature inside the thermal storage tank goes above the setpoint temperature of the heat pump control. In this case, during the ADR events, the operation of the heat pump become independent from the heating setpoint of the storage tank.
The energy released to the thermal storage is used to increase the temperature of the thermal storage tank, storing more energy compared to the one that is required in the same moment during normal operation.
The surplus of energy stored in the thermal storage tank is used after the ADR events from the control of the system to provide the desired temperature at the inlet of the floor heating system. This results in a decrease in the energy consumption after the ADR event respect the consumption that would be necessary if the event is not happened.
During the downward events, the operation of the heat pump is forced to stay off for 2 hours. This means that the energy consumption of the heat pump during this period is lower respect the one required during

normal operation, in which the heat pump switches on when the temperature inside the thermal storage tank goes below the heating setpoint of the tank. Also in this case, during the ADR events, the operation of the heat pump becomes independent from the heating setpoint of the storage tank.

Since the heat pump is switched off during the ADR events, the energy released to the thermal storage is null and, in any case, lower compared to the one asked in normal operation. This results in a decrease of the temperature of the thermal storage tank because of the thermal losses with the environment and because the building's floor heating system is asking thermal energy from the tank to keep the indoor room temperature above the heating setpoint.

When the heat pump switches on again, after the end of the ADR event, it remains on for more time compared to the time needed in the normal operation, to cover the decrease in temperature due to the forced shutdown of the heat pump during the event. This results in a decrease in the energy consumption during the ADR event compared to the consumption that would be necessary if the event is not happened and an increase in the energy consumption right after the event.

In these type of ADR events, thus, the source of the energy flexibility is the thermal storage tank, because this is the element of the building that is charged with a surplus of energy and from which the energy comes back to the room environment during the ADR events.

Table 4-1 provided a summary of the different type of ADR events performed in this analysis, highlighting in what change the events consist and which is the source of energy flexibility exploited.

Type of ADR event	Change applied	Source of energy flexibility
upward event	+2°C on room heating setpoint temperature	building strucutre
	Forcing heat pump to stay on	thermal storage tank
downward event	-2°C on room heating setpoint temperature	building strucutre
	Forcing heat pump to stay off	thermal storage tank

Table 4-1: Type of ADR event performed in the analysis.

The schedule of the Active Demand Response events present in the study is created starting from the hourly electricity price in each day of the year 2022 for the central region of Denmark.

To generate the schedule of the ADR events, a MATLAB script is used. The script automatically takes the electricity price data of each hour of each day during the period in which the simulation is performed, so from the beginning of January to the end of May.

One ADR event is created each 4 days, the scope of this decision is to try to have the different events as independent as possible each other. Having independent events means that the increase or decrease in the energy consumption due to one event does not affect the energy consumption during the consequent event, as if the first event has not occurred.

The goal of this analysis is to create the upward ADR events in a time period of the day when the electricity price is the lowest possible, so increasing the energy consumption when the energy cost less.

To achieve this target, the MATLAB script sums up all the price in a time window of 20 timestep of the simulation, resulting in a 2 hours period.

Once the time windows with the lowest price are identified, the script generates a schedule in which the ADR events are planned to happen in the time windows chosen.

Similarly, the goal is to create the downward ADR events in a time of the day when the electricity price is the highest possible, so decreasing the energy consumption when the energy cost more.

In this case the MATLAB script calculates the total energy cost in a time window of 2 hours and once the time windows with the highest price are identified, the script generates a schedule in which the ADR events are planned to happen in the chosen time window.

The upward and downward ADR events are alternated. The type of schedule and the type of ADR events depend on the way in which the ADR events are applied to the system and, thus, from the simulation scenario chosen, as explained in the next chapter.

4.2 Simulation scenarios

To have a comprehensive study of the energy flexibility behavior, it is decided to perform the analysis in different simulation scenarios. The different scenarios can change for the type of ADR events performed and for the technological setup of the building.

In this chapter an explanation of what type of Active Demand Response events are created in each of the possible simulation scenarios is provided, discussing in which way the ADR events are activated and how the technological systems are controlled to correctly apply the events.

There are 4 main simulation scenarios:

- Configuration without the heat pump coupled with the thermal storage tank, Active Demand Response events which act on the building structure (scenario A)
- Configuration with the heat pump coupled with thermal storage tank, Active Demand Response events which act on the building structure (scenario B)
- Configuration with the heat pump coupled with thermal storage tank, Active Demand Response events which act on the thermal storage tank (scenario C)
- Configuration with heat pump coupled with the thermal storage tank, Active Demand Response events which act on both the building structure and the thermal storage tank (scenario D)

Scenario	Technological setup	Source of energy flexibility
A	floor heating system	building structure
B	floor heating system + heat pump coupled with thermal storage tank	building strucutre
C	floor heating system + heat pump coupled with thermal storage tank	thermal storage tank
D	floor heating system + heat pump coupled with thermal storage tank	building structure + thermal storage tank

Figure 4-3: Simulation scenarios with their corresponding technological setup and source of energy flexibility.

Scenario A:

In this scenario the building is heated up with only the use of the radiant floor heating system, without the use of the thermal storage tank. It is possible to consider the building connected to the district heating system, which provide the thermal energy needed to the floor heating system.The ADR events are created changing the heating setpoint temperature of each room composing the building, in this way the source of the energy flexibility is the building structure.

During the normal operation the heating setpoint of the thermostat of each room is set equal to 20°C. During the upward ADR events the heating setpoint is increased of 2 °C for 2 hours, resulting in a heating setpoint equal to 22°C, while during the downward events the heating setpoint is decreased of 2°C for 2 hours, resulting in a heating setpoint equal to 18°C.

The schedule of the ADR events is created starting from the electricity price, alternating one upward event and one downward event each 4 days, as shown in Figure 4-4, representing as example the heating setpoint temperature for the month of January.

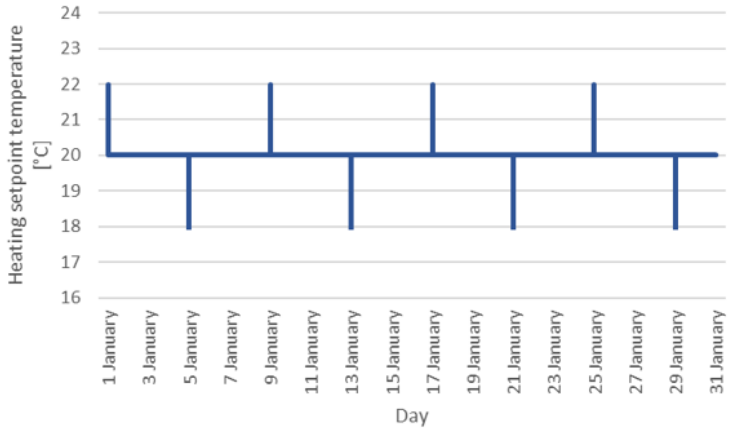

Figure 4-4: Heating setpoint temperature for the month of January.

The schedule is written in an external text file based on the previous considerations and insert in the simulation program through Type 9. This schedule is used as input for the Type 166 previously described, which models the behavior of a simple thermostat. In particular, the schedule is connected to the heating setpoint temperature of each of the thermostats of the building, meaning that at the same time, when an ADR event occurs, the same event happens in all the 15 rooms, so the event is applied to the whole building.

Scenario B:

In this scenario the building is always heated up with the use of the radiant floor heating system, but also a thermal storage tank coupled with a heat pump is added to the whole system.
The meaning of this choice is to study and analyze how the energy flexibility vary changing the technological setup of the building.
Similarly to Scenario A, the ADR events are created changing the heating setpoint temperature of each room composing the building. Thus, also in this case the source of the energy flexibility is expected to be the building structure.
During the normal operation the heating setpoint of the thermostat of each room is set equal to 20°C. During the upward ADR events the heating setpoint is increased of 2 °C for 2 hours, resulting in a heating setpoint equal to 22°C, while during the downward events the heating setpoint is decreased of 2°C for 2 hours, resulting in a heating setpoint equal to 18°C.
The schedule of the ADR events is created starting from the electricity price, alternating one upward event and one downward event each 4 days, as made for Scenario A.

In Scenario B also the thermal storage tank coupled with a heat pump is present.
The heat pump is modeled through Type 207 and interact with the thermal storage tank, modelled through Type 158, as already explained in the previous chapter.
The heat pump operation is controlled through Type 165, a component which models a differential hysteresis controller.
The on/off differential controller generates a control function γ which can have a value equal to 1 or equal to 0. The value of the control signal is chosen as a function of the difference between upper and lower temperatures T_H and T_L, compared with two dead band temperature differences ΔT_H and ΔT_L. The new value of the control function γ_i depends on the value of the input control function at the previous timestep.
A high limit cut-out temperature is included with this controller. Regardless of the dead band conditions, the control function will be set to zero if the high limit condition is exceeded. [21]
The controller behavior is explained in detail.

If the control function γ was previously “off”:

If $\gamma_{i-1} = 1$ and $\Delta T_L \leq (T_H - T_L)$, $\gamma_i = 1$

If $\gamma_{i-1} = 1$ and $\Delta T_L > (T_H - T_L)$, $\gamma_i = 0$

If the control function γ was previously “on”:

If $\gamma_{i-1} = 0$ and $\Delta T_H \leq (T_H - T_L)$, $\gamma_i = 1$

If $\gamma_{i-1} = 0$ and $\Delta T_H > (T_H - T_L)$, $\gamma_i = 0$

Where:

- ΔT_H [°C] upper temperature difference dead band
- ΔT_L [°C] lower temperature difference dead band
- T_H [°C] upper input temperature
- T_L [°C] lower input temperature
- γ_{i-1} [0;1] input control function at the previous timestep
- γ_i [0;1] output control function at the current timestep

The control function is graphically illustrated in Figure 4-5. [28]

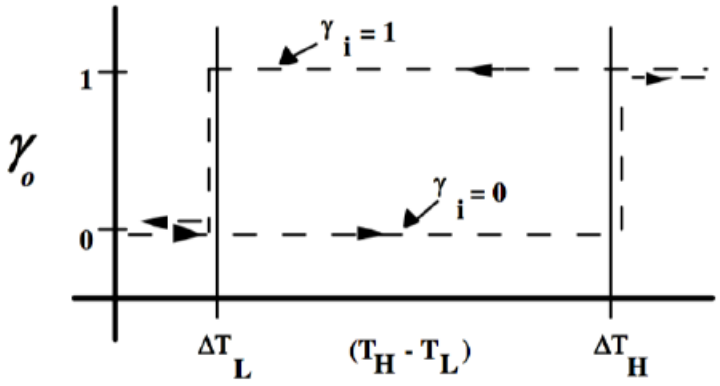

Figure 4-5: Control function [26].

Since Type 156 model a controller component, also the monitoring temperature is provided as input.
In normal conditions the operation of the heat pump is controlled based on the temperature at the thermostat present in the thermal storage tank.
The heat pump is controlled with a linear temperature setpoint plus two different temperature difference dead band. In order to correctly model this behavior, the information of the temperature of the thermal storage tank provided by the thermostat present inside the tank is connected as input to the monitoring temperature of Type 156 and also to the lower input temperature T_L.

The upper input temperature T_H is function of the external temperature. For this reason, it is provided through an external "calculator", receiving as input the information about the external temperature from the weather data file and performing the following conversion, represented in Figure 4-6.

The upper input temperature is constant and equal to 39 °C when the external air temperature is above 12°C, constant and equal to 49 °C when the external air temperature is below 2 °C and vary linearly between these two values.

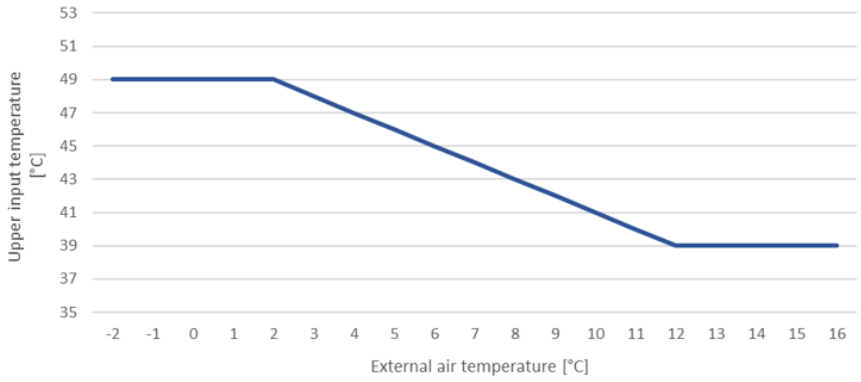

Figure 4-6: Upper input temperature function of external air temperature.

The upper temperature difference dead band ΔT_H is set equal to 2°C, resulting in a minimum allowed temperature of the thermal storage tank equal to 37°C.

The lower temperature difference dead band ΔT_L is set equal to -5°C, resulting in a maximum allowed temperature of the thermal storage tank equal to 54°C.

The high limit cut-out temperature is set equal to 100°C.

When the heat pump is previously switched on and temperature in the thermal storage, stored as T_L, reaches the value of the setpoint temperature, stored as T_H, plus the lower dead band ΔT_L, with a value equal to -5°C, the controller performs the following calculations.

Since the heat pump is already switched on ($\gamma_{i-1} = 1$), when the setpoint temperature is the maximum possible and equal to 49°C, only when the temperature in the tank reaches a value above 54°C the rule $\Delta T_L > (T_H - T_L)$ becomes true and the heat pump switches off, $\gamma_i = 0$.

Until this logic rule does not become true, the heat pump remains in his previous state of operation.

Similarly, when the heat pump is previously switched off and temperature in the thermal storage, stored as T_L, reaches the value of the setpoint temperature, stored as T_H, plus the upper dead band ΔT_H, equal to 2°C, the controller performs the following calculations.

Since the heat pump is already switched off ($\gamma_{i-1} = 0$), when the setpoint temperature is the lowest possible and equal to 39°C, only when the temperature in the tank reaches a value below 37°C the rule $\Delta T_H > (T_H - T_L)$ becomes true and the heat pump switches on, $\gamma_i = 1$.

The decision behind this setpoint temperatures is taken to guarantee that the thermal storage tank is able to provide the necessary amount of thermal energy to heat up the water stream and to reach the desired inlet temperature of the floor heating system. At the same time, a higher allowed temperature difference near the maximum value is chosen to better exploit the usage of the thermal storage tank.

A simplified representation of the element composing the whole system present in Scenario B is presented in Figure 4-7. The system consists mainly in the building model (Type 56), the floor heating system, controlled externally through the thermostats, the heat pump (Type 207), controlled based on the temperature in the tank and the thermal storage tank (Type 158).

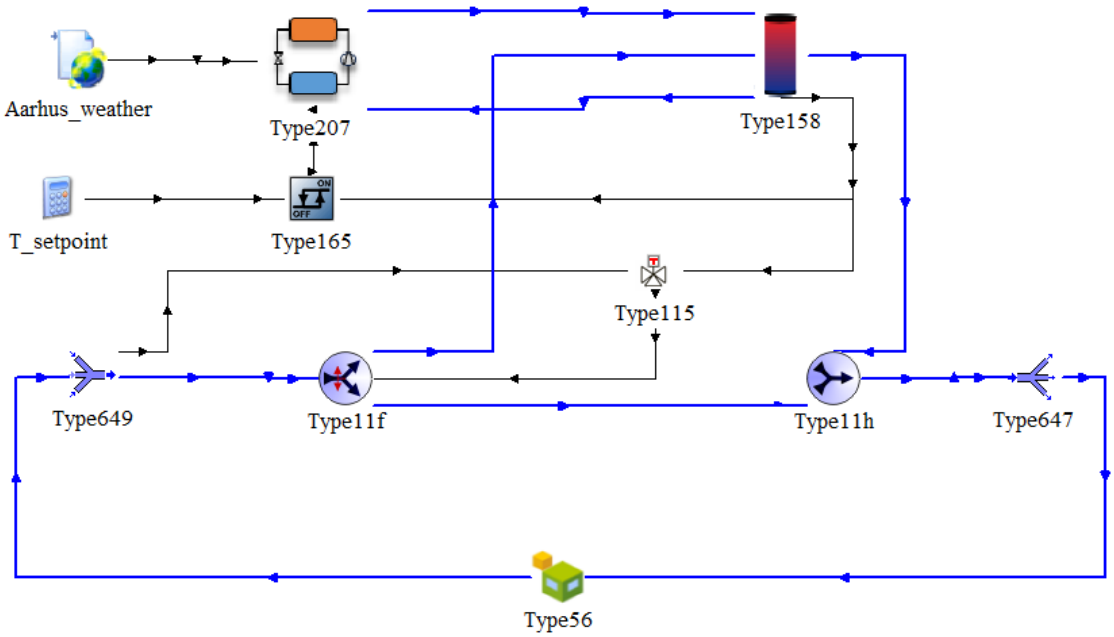

Figure 4-7: Scenario B simplified representation.

Scenario C:

In this scenario the configuration of the whole system is the same of Scenario B, with the building heated up with the use of the radiant floor heating system and the presence of the thermal storage tank coupled with the heat pump.

In this case the Active Demand Response events are created forcing the state of operation of the heat pump coupled with the thermal storage tank. The heating setpoint of the rooms of the building is maintained constant and equal to 20°C.

The meaning of this choice is to study and analyze how the energy flexibility vary changing the type of ADR events and the source of the energy flexibility.
In this case, indeed, is expected that the source of energy flexibility is the thermal storage tank and not the building structure as in the previous case, since the ADR events directly act on the heat pump which, in consequence, acts on the temperature inside the thermal storage tank.

During the normal operation the heat pump is controlled by the temperature at the thermostat present in the thermal storage tank, trough the Type 165, as already explained for Scenario B.
During the upward ADR events the heat pump is forced to stay switched on for 2 hours, independently of other conditions.
Instead, during the downward events the heat pump is forced to stay switched off. In order to force the operation of the heat pump, an external schedule is created.
Since is expected that the temperature in the thermal storage tank rise during forcing operation, the high limit cut-out temperature is set equal to 70°C.

The schedule of the ADR events is created starting from the electricity price, alternating one upward event and one downward event each 4 days, as done in the previous case.
In this case the difference is that the ADR events are created directly changing the state of operation of the heat pump, resulting in a different control of the heat pump itself.
The whole control of the heat pump is the combination of three different control logic.
As said, during the ADR events, the heat pump should remain in the desired state of operation for 2 hours. In order to do this, an external schedule is created, in which three different values are present.
An input value equal to 1 means the heat pump is switched on, a value equal to -1 means the heat pump is switched off and an input value equal to 0 means the heat pump is controlled as when there are no ADR events, so through the temperature in the thermal storage tank, as in Scenario B.
The schedule of the ADR events forcing the heat pump operation in the month of January is shown in Figure 4-8.

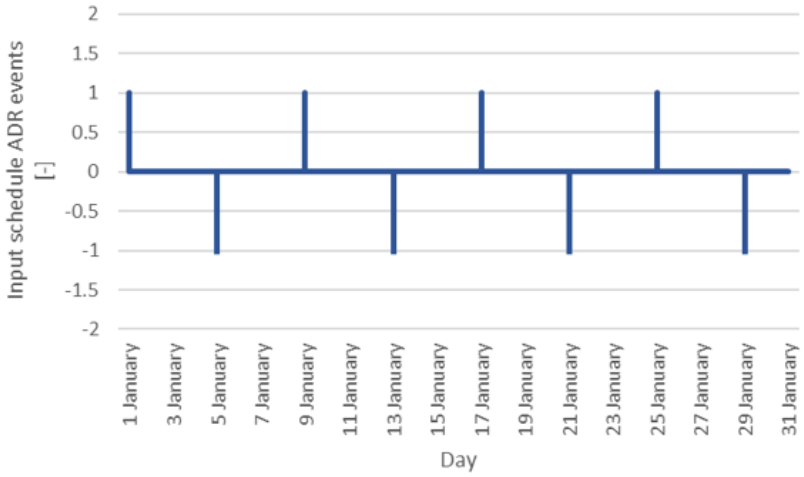

Figure 4-8: Input schedule of the ADR events in Scenario C.

This schedule, named "ADR_based_control", is used as input in a "calculator" in order to be combined with the other control logics.

The second logic that controls the heat pump, named "Seasonal_control", is simply an external schedule that stop the operation of the heat pump when the heating season is ended, from July to September.

When the heat pump should operate in normal conditions, the input value written in the schedule is equal to 1, while when the heat pump is switched off, the input value is equal to 0.

The third control logic, named "Tank_based_control", is the one based on the temperature in the thermal storage tank, as already explained in Scenario B.

The whole control logic implemented in the "calculator" controlling the operation of the heat pump is the following.

If 'Seasonal_control' = 0, output = 0

If 'Seasonal_control' = 1 and 'ADR_based_control'=1 and 'T_tank' < 70, output = 1

If 'Seasonal_control' = 1 and 'ADR_based_control'=1 and 'T_tank' > 70, output = 'Tank_based_control'

If 'Seasonal_control' = 1 and 'ADR_based_control'=0, output = 'Tank_based_control'

In this way, when the heating season is ended, the heat pump is switched off, while during the heating season, if there are no ADR events happening, the heat pump is controlled based on the thermal storage tank temperature as in Scenario B. When an ADR event occurs, if the temperature of the tank is lower than 70 °C the heat pump is switched on, when the temperature reaches 70°C the heat pump is automatically switched off and comes back in the operation controlled by the temperature of the thermal storage.

A simplified representation of the element composing the whole system present in Scenario C is presented in Figure 4-9. The system consists mainly in the building model (Type 56), the floor heating system, controlled externally through the thermostats, the heat pump (Type 207), controlled based on the temperature in the tank and the thermal storage tank (Type 158).

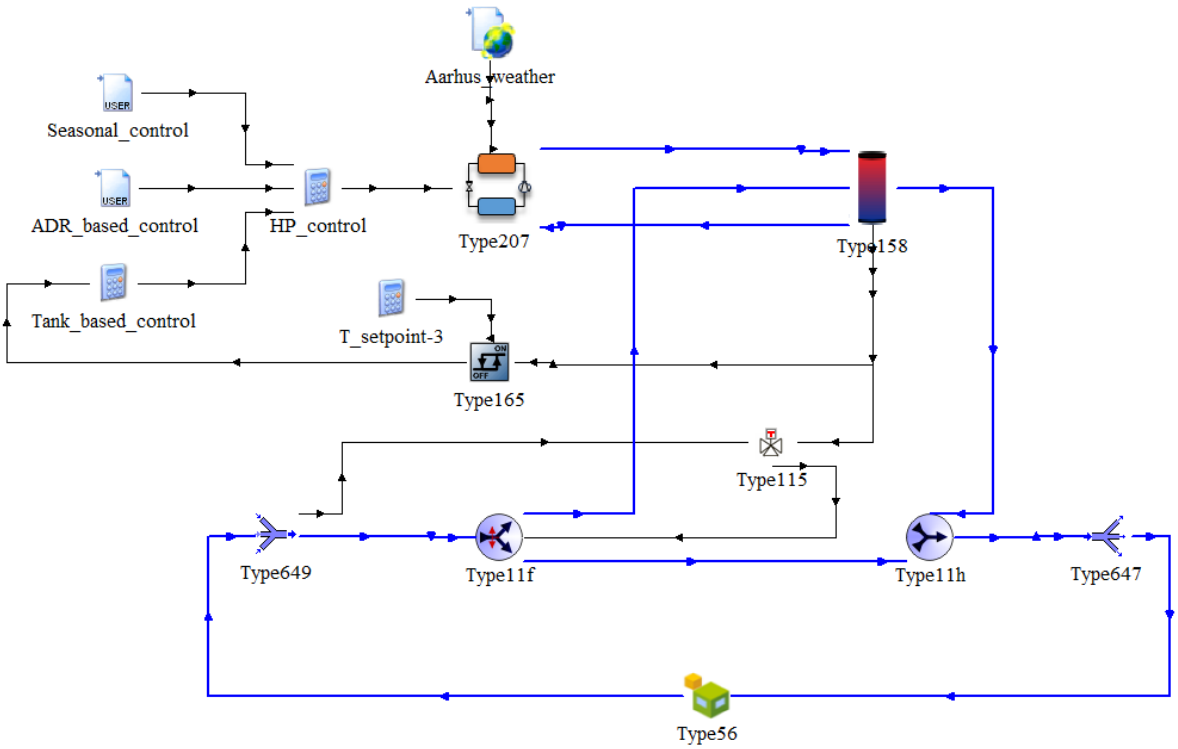

Figure 4-9: Simplified representation of the whole system in Scenario C.

Scenario D:

In this scenario the configuration of the whole system is the same of Scenario B and Scenario C, with the building heated up with the use of the radiant floor heating system and the presence of the thermal storage tank coupled with the heat pump.

In this case the Active Demand Response events are still created forcing the state of operation of the heat pump coupled with the thermal storage tank, but the heating setpoint of the rooms of the building is also changed during the ADR events and not maintained constant and equal to 20°C.

When an upward event occurs, the heat pump is forced to stay switched on as Scenario C, but the ADR event is also created increasing the heating setpoint of the thermostats of each room of the building of 2°C for 2 hours as Scenario B, resulting in both the heat pump switched on and the heating setpoint equal to 22°C at the same time.

Similarly, when a downward event occurs, the heat pump is forced to stay switched off as Scenario C, but the ADR event is also created decreasing the heating setpoint of the thermostats of each room of the building of 2°C for 2 hours as Scenario B, resulting in both the heat pump switched off and the heating setpoint equal to 18°C at the same time.

The schedule of the ADR events also in this case is created starting from the electricity price, alternating one upward event and one downward event each 4 days, but with both the changing in the heating setpoint of the thermostats in the room and forcing the state of operation of the heat pump at the same time, as shown in Figure 4-10 for the month of January.

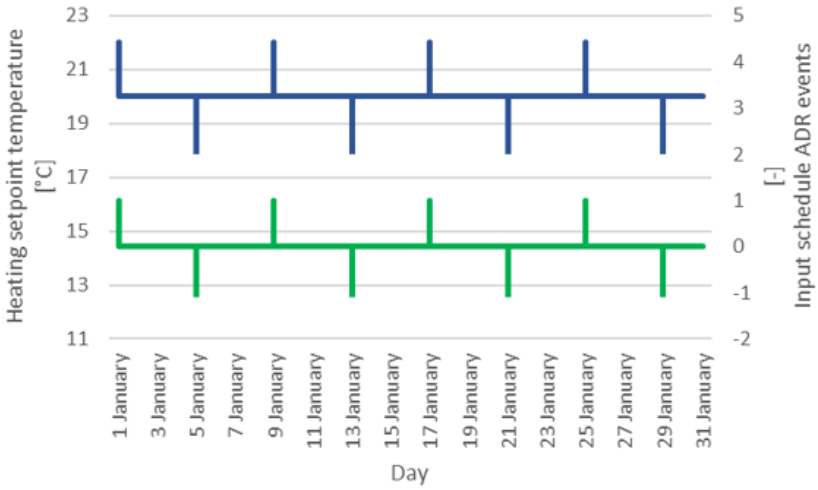

Figure 4-10: ADR events input in Scenario D.

The meaning of this choice is to study and analyze how the energy flexibility vary changing the type of ADR events and the source of the energy flexibility at the same time.

In this case, indeed, is expected that the sources of energy flexibility are both the thermal storage tank, as in Scenario C, and the building structure, as in Scenario B, since the heat pump directly acts on the temperature inside the thermal storage but also the heating setpoint of the thermostat in the rooms composing the building is changed.

4.3 Key Performance Indicators

The main objective of this work is to quantify the energy flexibility potential of a typical Danish single-family house. This is done through the use of some Key Performance Indicators (KPI).
The indicators are evaluated in different conditions, changing the technological setup of the building and varying the boundary conditions, basically the external temperature, in this way both the impact of the configuration and the seasonality on the energy flexibility are taken into account.
The whole set of Key Performance Indicators for each of the simulation scenarios explained before is compared with the others and at the same time they are also compared month by month in the same scenario.

In order to quantify the energy flexibility potential of the single-family house, the method proposed by Reynders et al. is chosen because the easy interpretation of the related KPIs and its reduced computational effort. [29]
The method is based on the comparison between two different simulations.
The first simulation is called reference simulation, in this case every control logic of the technological systems is left as in normal conditions, without any ADR event occurs. The second simulation is called ADR simulation, in this case the control logic of the technological systems is changed when the ADR events occur, as explained in the previous chapter.
Both the simulations performed results in a heating or electricity consumption profiles, depending on the simulation scenario analyzed. The thermal and electrical load profiles obtained with the simulations are then used to calculate the first two energy flexibility indicators.

The firs indicator presented is the available storage capacity (C_{ADR}), which represents the energy that can be shifted during an Active Demand Response event.
The available storage capacity is the amount of energy that can be added or removed, during a specific ADR event, to the building structure or the thermal storage tank, depending on the type of ADR event.
In this way, the energy that can be stored within the building structure not only depends on the thermal properties of the building fabric, but also on the properties and actual use of the heating and other technological systems.
Moreover, this performance indicator is not constant but vary with the climatic conditions and occupants behavior. The definition explicitly takes into account the time-dependent aspect. [29]
The C_{ADR} is defined by Reynders at al. as “the amount of energy that can be added to the storage system, without jeopardizing comfort, in the time-frame of an ADR event and given the dynamic boundary conditions”. [29]

As said, to quantify the available storage capacity the energy consumption profiles of the ADR simulation and the reference simulation are analyzed and compared.

A conceptual representation of a generic ADR event is provided in Figure 4-11. [30]

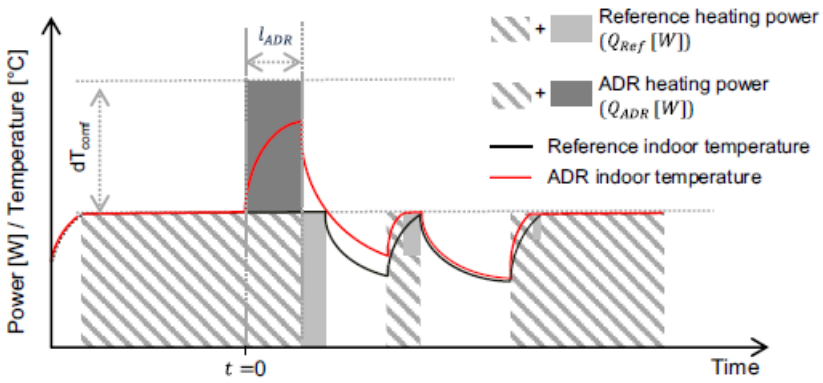

Figure 4-11: Conceptual representation of a generic ADR event used to quantify the available storage capacity and the storage efficiency [28].

During the ADR event the heating setpoint temperature is increased by dT_{comf} [°C] for the duration l_{ADR} [h]. The available storage capacity C_{ADR} [kWh] is given by equation (15), representing the integral of the difference between the heating power consumption during the ADR event Q_{ADR} [kW] and the reference heating power consumption in normal operation Q_{REF} [kW], represented by the dark-gray area.

$$C_{ADR} = \int_0^{l_{ADR}} (Q_{ADR} - Q_{REF})\, dt \qquad (15)$$

where Q_{REF} is the heat load profile of the building in the reference simulation, Q_{ADR} is the energy demand in the ADR simulation and l_{ADR} is the duration of the event.

C_{ADR} indicator measures the surplus or deficit of energy stored in the building structure during the ADR event, which can be considered as the capacitance of a virtual thermal storage.

Since the number of events in a specific month can vary based on the schedule, it is decided to process this indicator to obtain average values of thermal power shifted on a monthly/seasonal basis, dividing it for the total number of hours in which the events occur, as shown in equation (16).

$$\bar{C}_{ADR} = \frac{\sum_i^N C_{ADR}}{N \cdot l_{ADR}} \qquad (16)$$

Where N is the number of ADR events during the considered period, in this case a specific month, while l_{ADR} is the duration of the event, equal to 2 hours .

In the case of upward ADR events, the heating setpoint temperature is increased and this results in higher indoor temperature, thus, the transmission, ventilation and infiltration losses increase. Consequently, only a part of the energy surplus stored can be used effectively to maintain the desired indoor temperature and reduce the energy consumption in the period following the ADR event.
Similarly, in the case of downward ADR events, the heating setpoint is decreased and the energy spent after the ADR event is higher than the energy saved due to the forced shut down during the ADR event.
Therefore, the second indicator presented measures the "efficiency" of the virtual thermal storage.
The storage efficiency (η_{ADR}) is defined as the fraction of the heat that is stored during the ADR event that can be used subsequently to reduce the heating power needed to maintain thermal comfort. [29]
The storage efficiency is calculated comparing the same two profiles used before, the reference profile and the ADR profile, to calculate the available storage capacity. The efficiency is calculated through equation (17) as follows:

$$\eta_{ADR} = 1 - \frac{\int_0^t (Q_{ADR} - Q_{REF})\, dt}{\left|\int_0^{l_{ADR}} (Q_{ADR} - Q_{REF})\, dt\right|} \qquad (17)$$

The integral at the denominator is equal to the energy stored during the ADR event, thus the available storage capacity C_{ADR}, represented by the dark-gray area in Figure 4-11.
A part of this energy can be used after the ADR event to reduce the heating power needed to guarantee the heating need of the building. This reduction in power is represented by the light-gray area in Figure 4-11.

The storage losses induced by activating the thermal mass, equal to the numerator of equation (17), thus correspond to the fraction of the energy stored during the ADR event that is not recovered after a long period. This long period, represented as the integration from 0 to *t*, is evaluated in a time window of 72 hours. This choice is made because it is noted that the rebound effect due to the ADR events is almost stopped after 3 days.
The ADR efficiency of the virtual storage can be interpreted as the ratio between the "rebound effect" and the "ADR event", meaning the difference between the energy needs of the building after and during the ADR event respectively. As consequence of this definition, it can be concluded that any ADR events involves a certain loss of energy. [7] Also in this case, the indicator is averaged on monthly basis.
It is noted that both available storage capacity C_{ADR} and storage efficiency η_{ADR} of the ADR events are not constant, but vary in time depending on the boundary conditions.

The participation of the buildings to Active Demand Response programs brings benefits to the whole energy system and to the user in economic terms. However, forced start-ups and shut-downs of HVAC plants during the ADR events unavoidably change the indoors thermal comfort conditions.
Therefore, it is important to assess the thermal discomfort eventually caused by different ADR events.
In order to do this, the third indicator is introduced, called thermal discomfort index (TDI_{ADR}), calculated in the following way.
First, the number of degree-hours of thermal discomfort, known as TDDH, is calculated through to equation (18).

$$TDDH = \int_0^{l_{ADR}} \left| T_{op} - T_{op,lim} \right| dt \qquad (18)$$

where T_{op} is the operative temperature of the indoor environment of the different room of the building and $T_{op,lim}$ indicates, in case of downward events, the minimum operative temperature suggested by Annex A of Standard EN 15251 (European Committee for Standardization, 2007), equal to 20 °C. Since the maximum operative temperature suggested by the Annex, equal to 25°C, is never reached in all the cases studied, to have an indicator describing the impact of the upward ADR events on the building comfort in different conditions, the $T_{op,lim}$, in case of upward events, is set equal to 22°C.
Since in case of upward events the index does not take into account for a real discomfort, but consider simply the number of degree-hours in which the operative temperature of the room rise above 22°C, the index is named degree-hours of overheating, OHDH, calculated through the same equation (19).

$$OHDH = \int_0^{l_{ADR}} \left| T_{op} - T_{op,lim} \right| dt \qquad (19)$$

Note that the degree-hours are summed up only during the period l_{ADR}, in this case considered equal to 72 hours for the upward events and equal to 6 hours for the downward events. This choice is made because, to study the impact of an upward event on the thermal comfort, should be taken into account that when there is an increase in indoor temperature in the building due to the ADR event, this increase is maintained for more time after the ADR event itself, meaning that the impact of the event is not stopped with the end of the event, but cause a change in the thermal comfort also in the period after the event. Similarly, when a downward event occurs, the decrease in the indoor temperature causes a change

in the thermal comfort which is maintained also after the end of the ADR event itself, this because the system requires some time to bring back the indoor temperature at the desired value.

The time window in which the effect of the upward ADR events is considered is longer due to the fact that the system requires more time to goes back to the desired temperature, since the temperature decreases only because thermal losses. In the downward events, instead, the heating system of the building provide energy to increase the temperature and goes back to the desired one, requiring less time respect the upward events.

The thermal discomfort index TDI_{ADR} of any ADR events is calculated as the variation of degree-hours of thermal discomfort in the ADR simulation and the reference simulation, through equation (20).

$$TDI_{ADR} = TDDH_{ADR} - TDDH_{REF} \qquad (20)$$

In case of upward events, similarly as before, the index is named overheating index OHI_{ADR}, since it does not take into account for a real thermal discomfort but only for the degree-hours above 22°C through equation (21).

$$OHI_{ADR} = OHDH_{ADR} - OHDH_{REF} \qquad (21)$$

A graphic representation of how the index is calculated is provided in Figure 4-12. The overheating index calculates the difference between the area under the temperature profile of the ADR simulation (red line), equal to $OHDH_{ADR}$, and the area under the temperature profile of the reference simulation (blue line), equal to $OHDH_{REF}$, only when the temperature is above 22°C, resulting in the yellow area.

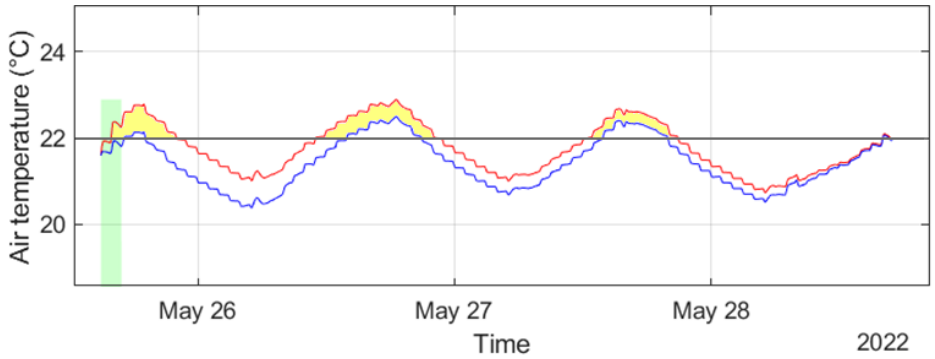

Figure 4-12: Overheating index representation.

Comparing the ADR simulation and the reference simulation is possible to have a description of only the effect of the ADR event on the thermal comfort of the building, excluding other external contributions

such as external temperature variation, solar radiation and internal heat gains, because they are present also in the reference simulation and bring the same contribution in both the simulations.

In the simulation scenario where the heat pump is used, the available storage capacity C_{ADR} can be defined both in terms of thermal energy and electrical energy.
To have a comprehensive analysis of the behavior of the energy flexibility when a heat pump is used, also the COP of the heat pump in the ADR simulation and the reference simulation is calculated through equation (22) and (23) respectively.

$$COP_{ADR} = \frac{\int_0^{l_{ADR}} \left(P_{ADR,th}\right) dt}{\int_0^{l_{ADR}} \left(P_{ADR,el}\right) dt} \qquad (22)$$

$$COP_{REF} = \frac{\int_0^{l_{ADR}} \left(P_{REF,th}\right) dt}{\int_0^{l_{ADR}} \left(P_{REF,el}\right) dt} \qquad (23)$$

The COP of the ADR simulation COP_{ADR} is calculated as the ratio of the integrals of the energy consumption profiles of the heat pump on thermal basis and electrical basis in the ADR simulation, while COP_{REF} is calculated in the same way, but considering the reference simulation. It is expected that the COP indicator is the scaling factor between the available storage capacity calculated in terms of thermal energy $C_{ADR,th}$ and the one calculate in terms of electrical energy $C_{ADR,el}$.

In the simulation scenario where the heat pump is used, also a rough economic analysis in performed.
This is made through a cost saving indicator, calculated through equation (24).

$$cost\ saving = \int_0^{l_{ADR}} \left(P_{ADR,el}(t) - P_{REF,el}(t)\right) p_{el}(t)\ dt \qquad (24)$$

The cost saving is calculated multiplying the integral of the difference of the electricity consumption in the ADR simulation and the reference simulation at a certain time for the cost of the electricity in that time.
In fact, since the cost saving is chosen to be evaluated in the time period of 72 hours required for the end of the effect of the ADR event, the electricity price varies over time and is necessary to correctly weight the amount of energy saved with the related cost.

5 Results

In this chapter the results obtained from the different analysis performed are presented and discussed. The analysis is performed during the heating season, from the beginning of January to the end of May. Most of the results are collected on monthly basis in order to understand the impact of the boundary conditions depending on the seasonality on the behaviors of energy flexibility indicators.

Firstly, a generic upward ADR event impact on the energy consumption of the building in Scenario A is presented in Figure 5-1.

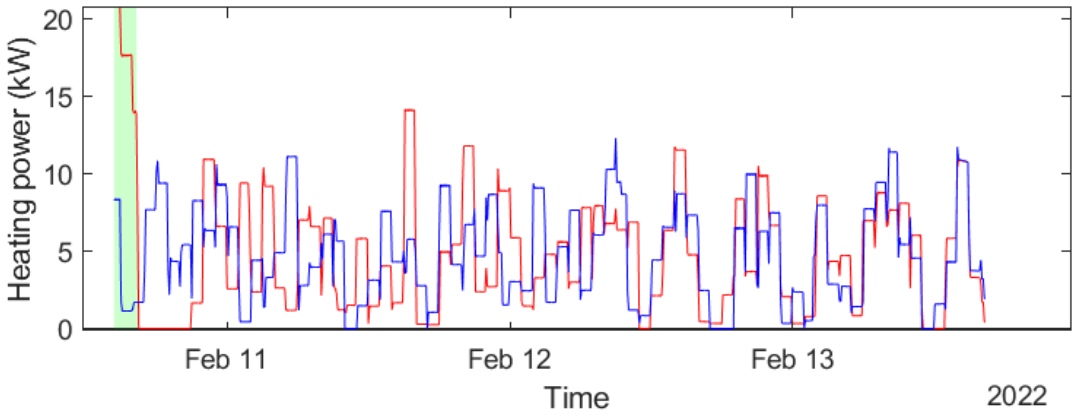

Figure 5-1: Generic upward ADR event impact on the energy consumption of the building.

The figure represents the heating profile of the building in the reference simulation (blue line) and the heating profile in the ADR simulation (red line) during a generic upward ADR event, in this case the second of February. The duration of the upward ADR event is highlighted with the green area.
As expected, the increase in the heating setpoint temperature, which passes from 20°C to 22°C, results in an increase in the heating consumption in the ADR simulation compared to the reference simulation during the ADR event. Part of the surplus of energy given to the indoor environment is stored in the building structure. Part of the energy stored in the building structure is used in the hours after the ADR event to decrease the energy consumption. This behavior is well shown in Figure 5-1, indeed, in the hours after the ADR event the ADR simulation present null value of heating consumption, while the reference simulation presents the heating profile demand as the ADR event never happen. This rebound effect continues until a compensation is reached. Figure 5-2 shown the difference in the heating profile between the ADR simulation and the reference simulation.

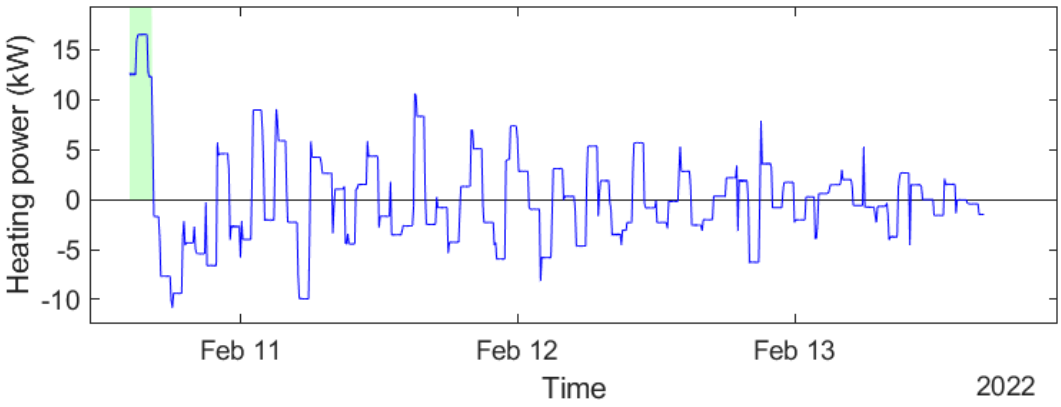

Figure 5-2: Heating profile difference between the ADR and reference simulations.

It is noted that the amplitude of the oscillation due to the rebound effect caused by the ADR event decreases over time, until almost no difference between the heating profile of the two simulations is reached.

The impact of the increase in the heating setpoint temperature in the different rooms of the building results in the consequent increase in the indoor temperature. The indoor temperature profiles of the ADR simulation and the reference simulation of a generic room are presented in Figure 5-3, in this case the room considered is the Bedroom 2.

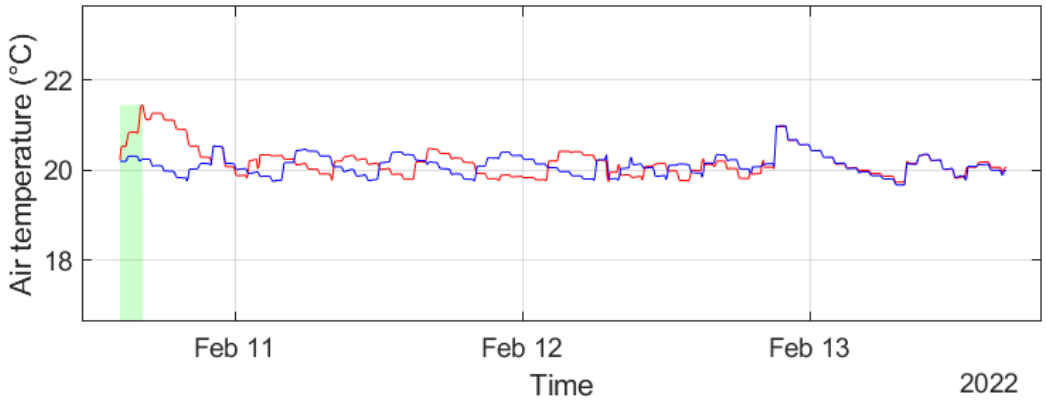

Figure 5-3: Indoor temperature profiles of the ADR and reference simulation in Bedroom 2.

As expected, the increase in the heating setpoint temperature results in an increase in the heating consumption and thus in an increase in the indoor temperature during the upward ADR event. The temperature profile of the ADR simulation is represented in the figure with a red line, while the reference simulation, with a constant heating setpoint temperature of 20°C is represented with a blue line. The oscillation of the two temperature profiles is due to the combination of both the presence of a dead band

of 0.5 °C on the thermostat controlling the radiant floor heating system and the fact that the heating system is an on/off heating system, thus react to the control of the thermostat with discrete release of heat in the room environment. This release of heat can be not aligned in time in the two simulations. In any case, after a certain period, the two temperature profiles came back aligned when the effect of the ADR event ends.

The impact of each upward ADR events is merged and considered together in the analysis of the results. Most of the results are indeed collected on monthly basis in order to understand the impact of the boundary conditions depending on the seasonality on the behaviors of energy flexibility indicators.

One of the main objectives of this work is to quantify the energy flexibility potential of a typical Danish single-family house. This is mainly described by the available storage capacity C_{ADR}.

The first simulation scenario analyzed is the Scenario A, in which the building is heat up through the radiant floor heating system, and there is not the thermal storage tank coupled with the heat pump. It is possible to consider the building connected to the district heating system, which provide the thermal energy needed to the floor heating system. Consequently, the ADR events are created changing the heating setpoint of the thermostats in the rooms of the building and the source of energy flexibility is the building structure.

The results quantifying the average available storage capacity C_{ADR} of the upward ADR events are presented in Figure 5-4.

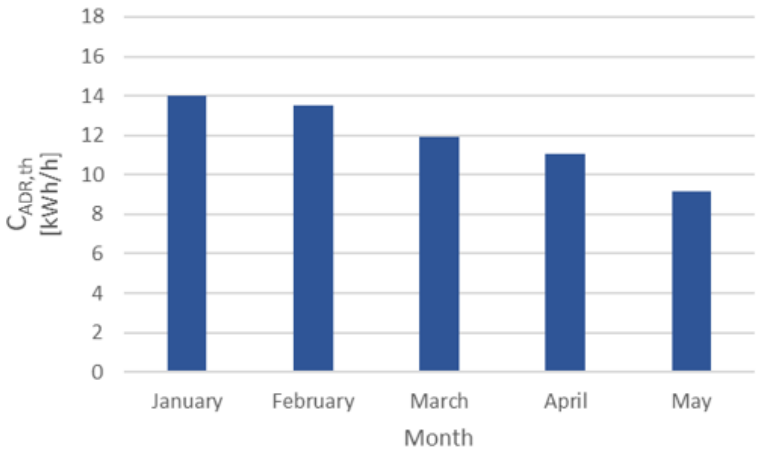

Figure 5-4: Available storage capacity C_{ADR} of upward events on monthly basis.

The results are presented in kWh/h, since the available storage capacity of each upward ADR event is summed up for each month of the heating season and divided for the total number of hours of duration of the events. In this way the results give a more uniform evaluation of the energy flexibility behavior,

since in some month the total number of events is different from the others and this aspect can influence the evaluation.

The results of C_{ADR} on monthly basis, as said, are due to the contributions of the different ADR events happening during the different months. In order to understand how the previously graph is created, the available storage capacity of each upward ADR event, measured in kWh, is presented in Figure 5-5.

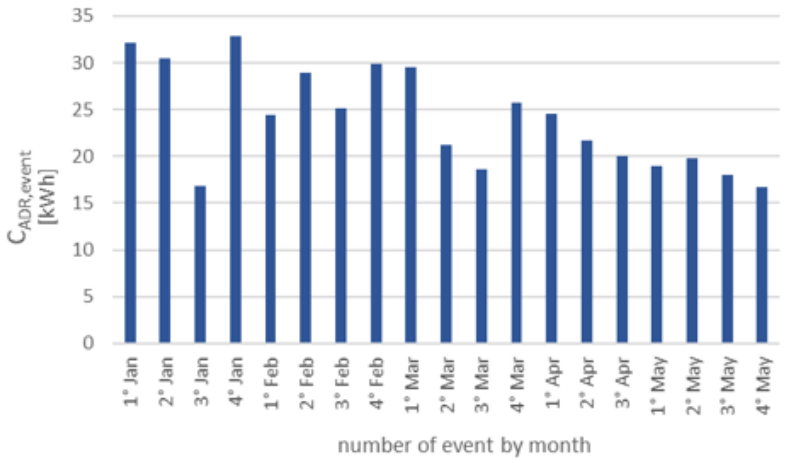

Figure 5-5: Available storage capacity C_{ADR} of each single ADR event in Scenario A.

In Figure 5-5 some strange values are present. In particular the third event of January presents lower values compared to the other of January, this because the event occurs when a low peak is reached in the external temperature, with almost 8°C less than other cases, resulting in lower energy difference between the ADR and reference simulation. In the third event of March, instead, are observed lower values because the event occurs during a high peak in the external temperature, which is similar to the one observed in April, resulting in similar values of April.

In any case, from the previous two graphs a trend is observed: the available storage capacity C_{ADR} decrease over time with the progression of the months. This trend is mainly caused by the external temperature which, on average, increases over time with the progression of the months. With higher external temperature, indeed, the energy consumptions needed to heat up the building until the indoor temperature reaches the desired value is lower. This means that the energy consumption, on average, decreases over time with the progression of the months, accordingly with the increase in external temperature. Since the heating consumption is lower, the energy provided to the building from the heating system is lower and lower is also the thermal energy which can be stored in the building structure during the ADR events. This is the reason why in colder month the available storage capacity is higher and in warmer month is lower.

Similarly, also the results of the storage efficiency η_{ADR} of the upwards ADR events are calculated on monthly basis as done for the available storage capacity C_{ADR}. The results are shown in Figure 5-6.

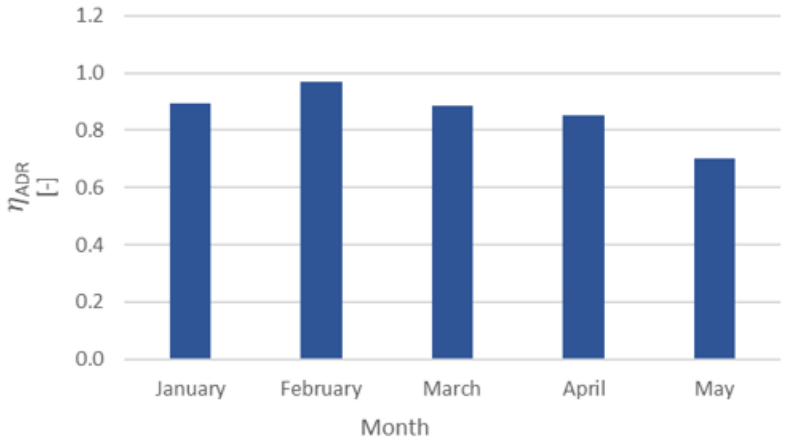

Figure 5-6: Storage efficiency η_{ADR} of the upward ADR events on monthly basis in Scenario A.

Similarly, as before, these results come from the average of the storage efficiency of each one of the different events happened during each month. Generally, the efficiency of the different events can vary depending on the time of the day in which the ADR event is started, which is the amount of energy released from the heating system during normal operations in the hours before the event and the consequently amount of energy stored in the building structure. Also the external temperature, which varies not always gradually during the month, has an impact on the thermal behavior of the building and consequently on the storage efficiency, since this indicator is evaluated in the 72 hours after the ADR event. For these reasons the values of the storage efficiency can be affected by some oscillations.
In general, it is noted that the storage efficiency η_{ADR} present values between 0.97 and 0.7 and decrease in the warmer month. This trend is explained by the increase in the external temperature, which results in a lower heating consumption of the building. This means that, when the heating setpoint is increased and some energy is stored in the building structure during the ADR event, the surplus of energy is not used properly to decrease the heating consumptions in the hours after the ADR event itself since the energy consumption is already low.

The overheating index OHI_{ADR} is presented in Figure 5-7 , remembering that in the case of the upward ADR events this index not properly define a real discomfort, but simply takes into account how much and for how long time the indoor temperature of the rooms composing the building rise above the heating setpoint of 22°C.

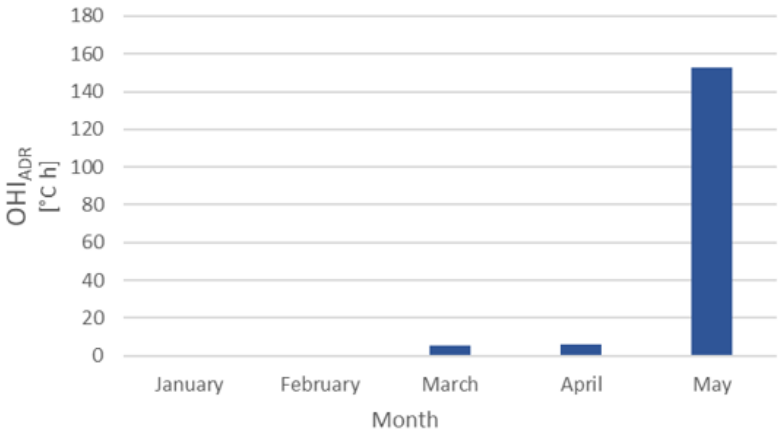

Figure 5-7: Overheating index of the upward ADR events in Scenario A.

The results of OHI_{ADR}, as said, are calculated from the difference between the overheating degree-hours in the ADR simulation $OHDH_{ADR}$ and the overheating degree-hours in the reference simulation $OHDH_{REF}$, only when the temperature is above 22°C, both represented in Figure 5-8 on monthly basis.

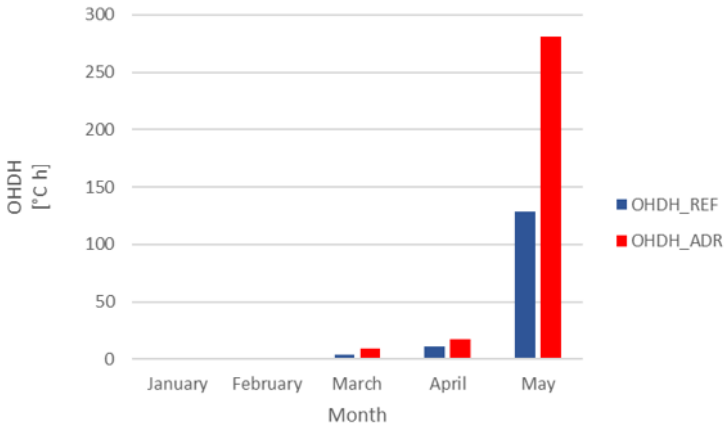

Figure 5-8: Overheating degree-hours OHDH in the ADR simulation and reference simulation during upward ADR events.

From the first graph is observed that the overheating index OHI_{ADR} increases from the coldest month to the warmest month. In particular it presents null values for January and February, since the external temperature is very low and during the ADR events, when the setpoint temperature is increased at 22°C, in general, in 2 hours the heating system bring the indoor temperature near 22°C but never passing them. When the ADR events ends, indeed, the heating system switched off for a while since the heating setpoint is back to 20°C and there is no need of heat. In this situation the indoor temperature starts quickly to decrease naturally because the thermal losses.

In the case of warmer month, when the external temperature is higher, it is possible that the heating system brings the indoor temperature at 22°C or more, remembering the presence of a dead band of

0.5°C in the room's thermostats. After the ADR events, since the external temperature is higher, the thermal losses are low respect colder month and the indoor temperature remains naturally above 22°C for more time. In the month of May this behavior is extremized because during the last ADR event the external temperature is relatively very high, above 20°C. This means that, when the heating system switched on because the increase in the heating setpoint during the ADR event, a part of the energy released increases the indoor temperature, while a part is stored in the building structure. When the ADR event ends, the temperature is above 22°C but also the external temperature presents similar values, resulting in a very slow decrease of the indoor temperature which remain above 22°C for a long period respect the other months, resulting in higher values of the index. Also, during the event is present also the contribution of the heat gain due to the solar radiation that normally increases the indoor temperature. This contribution facilitates the fact that the temperature profile in the ADR simulation reaches higher values, increasing the degree-hours of duration above the limit of 22°C used to calculate the thermal index OHI_{ADR}. These considerations described are shown in Figure 5-9, which represents the indoor temperature profiles of the last ADR event of May in a generic room, in this case the Bedroom 2.

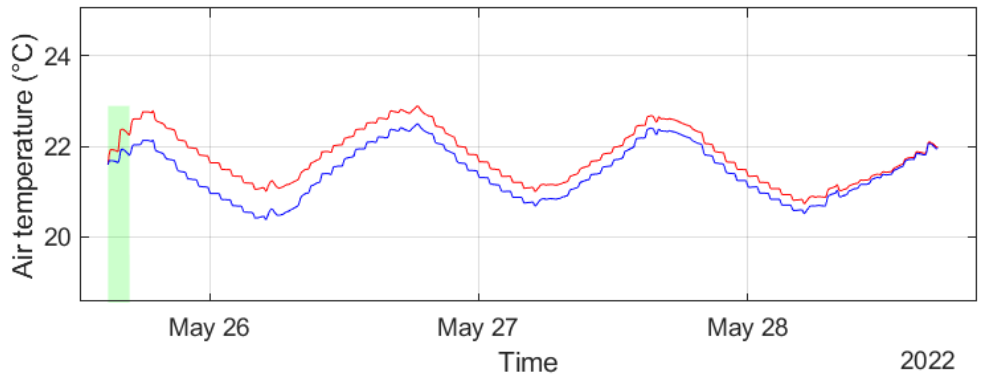

Figure 5-9: Indoor temperature profiles during an upward ADR event in Bedroom 2.

A similar analysis is performed for the downward ADR events created in the simulation, calculating the same key performance indicators.

Firstly, a generic downward ADR event impact of the energy consumption of the building is presented in Figure 5-10.

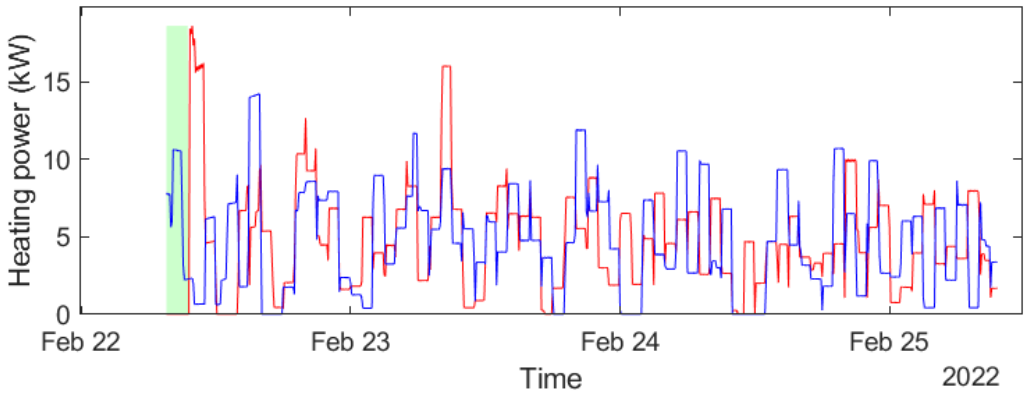

Figure 5-10: Generic downward ADR event impact on the energy consumption of the building.

The figure represents the heating profile of the building in the reference simulation (blue line) and the heating profile in the ADR simulation (red line) during a generic downward ADR event, in this case the third of February.

As expected, the decrease in the heating setpoint temperature, which passes from 20°C to 18°C, results in a decrease in the heating consumption in the ADR simulation respect the reference simulation during the ADR event. Since the energy provided to the building is lower during the ADR event, the indoor temperature starts to decrease. When the downward ADR event ends, the temperature of the room is below the restored heating setpoint of 20°C and the heating system reacts increasing a lot the energy consumption to quickly restore the setpoint temperature, resulting in an increase of the energy consumption in the hours after the ADR event respect the reference simulation. This behavior is well shown in figure, indeed, in the hours of the ADR event the ADR simulation present null value of heating consumption, while the reference simulation presents the heating profile require as the ADR event never happen. The ADR simulation present null values because the heating setpoint temperature is set equal to 18°C but the indoor temperature does not reach this value in only two hours of event, resulting in no consumption from the floor heating system. After the events the energy consumption of the ADR simulation is higher respect the reference simulation because this energy is used to restore the requested temperature in the rooms of the building.

Similarly to the upward events, the results quantifying the average available storage capacity C_{ADR} of the downward ADR events in Scenario A are presented in Figure 5-11.

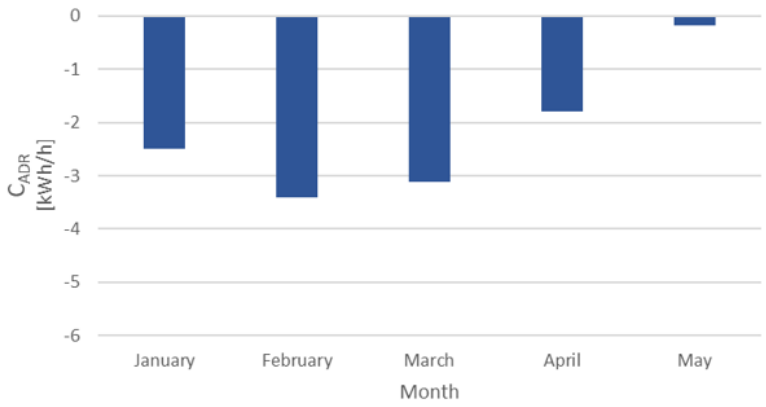

Figure 5-11: Available storage capacity C_{ADR} of downward events on monthly basis.

As done for the upward ADR events, the results are presented in kWh/h, since the available storage capacity of each downward ADR event is summed up for each month of the heating season and divided for the total number of hours of duration of the events. In this way the results give a more uniform evaluation of the energy flexibility behavior, since in some month the total number of events is different from the others and can influence the evaluation.

The results of C_{ADR} on monthly basis, as said before, are due to the contributions of the different ADR events happening during the different months.

In the case of downward events the available storage capacity presents negative values. This happen because when the heating setpoint is changed to 18°C, the energy consumption profile in the ADR simulation presents lower values compared to the reference simulation during the ADR event, resulting in negative values. The meaning of negative values of available storage capacity is that this amount of energy is saved and not used compared to the reference simulation.

From the previous a graph a trend is observed: the available storage capacity C_{ADR} decrease in absolute value over time with the progression of the months.

This trend is mainly caused by the external temperature which, on average, increases over time with the progression of the months. With higher external temperature indeed the energy consumptions needed to heat up the building until the indoor temperature reaches the desired value is lower. This means that the energy consumption, on average, decreases over time with progression of the month, accordingly with the increase in external temperature. Since the heating consumption is lower, the energy saved during the ADR events compared to the reference simulation from the heating system is lower. This is the reason why in colder month the available storage capacity is higher in absolute value and in warmer month is lower.

Similarly, also the results of the storage efficiency η_{ADR} of the downwards ADR events are calculated on monthly basis. The results are shown in Figure 5-12.

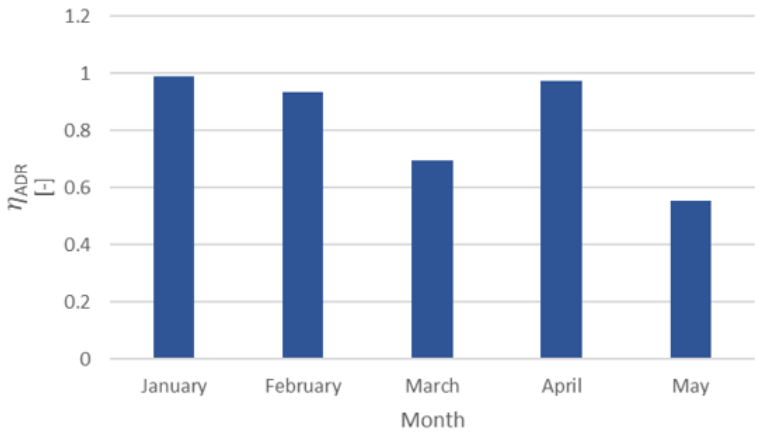

Figure 5-12: Storage efficiency η_{ADR} of the downward ADR events on monthly basis.

Similarly, as before, these results come from the average of the storage efficiency of each one of the different events happened during each month. Generally, indeed, the efficiency of the different events can vary depending on the time of the day in which the ADR event is started, which is the amount of energy released from the heating system during normal operations in the hours before the event and the consequently amount of energy already stored in the building structure. Also, the external temperature, which varies not always gradually during the month, has an impact on the thermal behavior of the building and consequently on the storage efficiency, since this indicator is evaluated in the 72 hours after the ADR event. For these reasons the values of the storage efficiency can be affected by some oscillations and, in general, there is not a general trend observed for the efficiency of the downward ADR events. It is noted that the storage efficiency η_{ADR} present values between 0.99 and 0.7, with a lower value of 0.55 in the warmer month of May. Values lower than 1 means that the surplus of energy consumption after the ADR event is higher than the energy saved during the ADR event, as expected.

The thermal discomfort index TDI_{ADR} is presented in Figure 5-13. In the case of the downward ADR events this index takes into account how much and for how long time the operative temperature of the rooms composing the building fall below the thermal discomfort limit of 20°C.

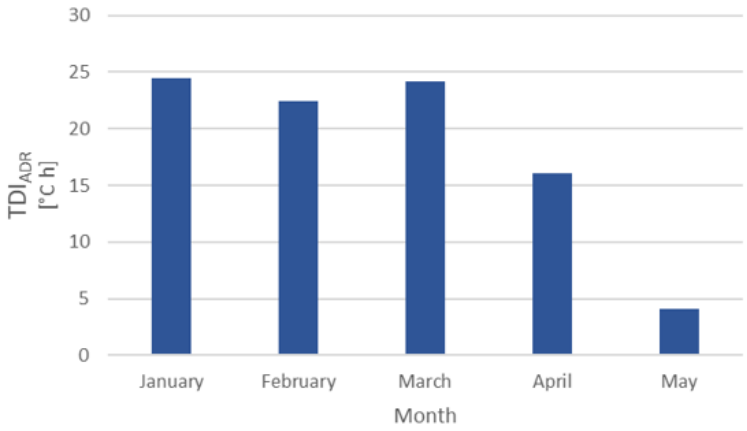

Figure 5-13: Thermal discomfort index of the downward ADR events in Scenario A.

The results of TDI_{ADR}, as said, are calculated from the difference between the thermal discomfort degree-hours in the ADR simulation $TDDH_{ADR}$ and the thermal discomfort degree-hours in the reference simulation $TDDH_{REF}$, only when the temperature is below 20°C, both represented in Figure 5-14 on monthly basis.

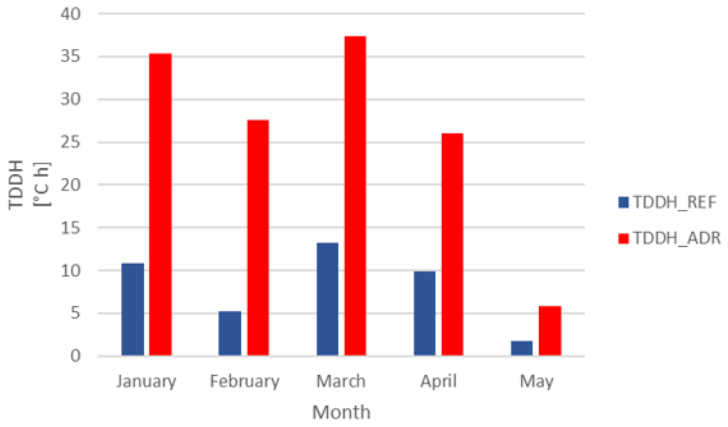

Figure 5-14: Thermal discomfort degree-hours TDDH in the ADR simulation and reference simulation during downward ADR events.

From the first graph is observed that the thermal discomfort index TDI_{ADR} decreases from the coldest months to the warmest months. In particular it presents higher values for January, February and March, since the external temperature when the ADR events occurs is in general enough similar in these months. During these months, when the downward ADR events occur, the heating setpoint is decrease to 18°C and the indoor temperature starts naturally decrease because thermal losses, since there is no more heating energy provided from the radiant floor system to the building. In the warmer months this behavior is still similar, but since the external temperature is generally higher, the thermal losses are

lower and the indoor temperature decrease slowly compared to the coldest months, resulting in lower degree-hours of thermal discomfort due to the forced shout-down of the heating system during the ADR events.

The aspects described are shown in Figure 5-15, representing the indoor temperature profiles of a generic ADR event in a generic room, in this case the Bedroom 2.

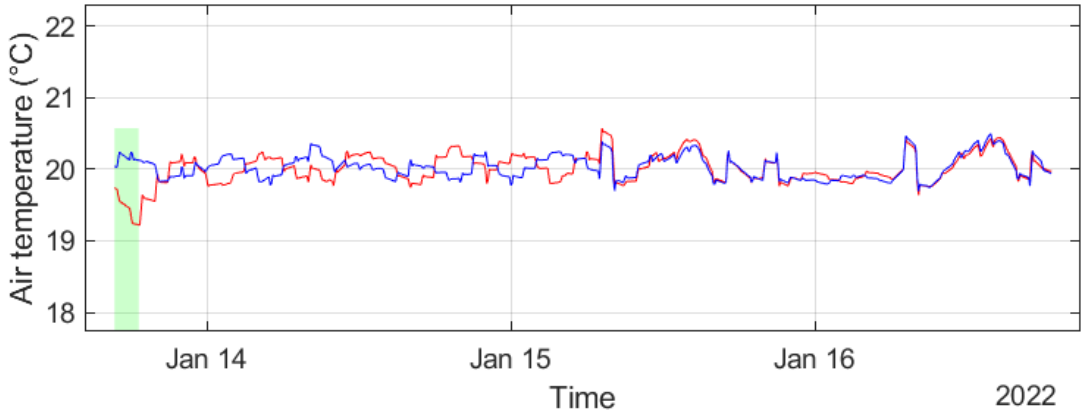

Figure 5-15: Indoor temperature profiles during a downward ADR event in Bedroom 2.

As expected, the indoor temperature decreases when the downward ADR event occurs, since the heating setpoint is decreased to 18°C and there is no more heating energy provided to the building, while in the reference simulation the temperature profile follows the heating setpoint of 20°C. There is a sort of oscillation generated from the fact that when the downward ADR event ends, the floor heating system, which is on/off system, provide an amount of energy needed to bring back the temperature above the heating setpoint, while in the reference simulation the amount of energy is provided in different time. This effect, that results in a not alignment of the two temperature profiles, decrease with the time until it stops in more or less two days and the two temperature profiles comes back aligned.

After the analysis of the simulation scenario A, the energy system of the building is changed and the heat pump coupled with the thermal storage tank is added to the system. The key performance indicators are calculated in the same way already presented and they are collected on monthly basis. Since one of the main objectives of the thesis is understand how the energy flexibility behavior vary changing with different energy systems, the results are presented comparing each one of the key performance indicators in the simulation scenario B, scenario C and scenario D.

The first simulation scenario analyzed is the Scenario B, in which the building is heated up through the radiant floor heating system and there is the thermal storage tank coupled with the heat pump. In this simulation scenario the ADR events are created changing the heating setpoint of the thermostats in the rooms of the building and the source of energy flexibility is the building structure.

To study the contribution of the thermal storage tank from the energy flexibility point of view, in Scenario C the upward ADR events are created forcing the state of operation of the heat pump that charge the thermal storage, which is always switched on for 2 hours.

In Scenario D the upward ADR events are created forcing the state of operation of the heat pump that charge the thermal storage, as done in Scenario C, but at the same time also the heating setpoint temperature of the thermostat of each room of the building is changed, as done in Scenario B.

This scenario allows to study the combination of the presence of both the types of upward ADR events, at building structure level and thermal storage level.

Since also the heat pump is present in the configuration of the system, the energy flexibility indicators are calculated starting from the thermal energy provided by the heat pump and the electrical energy used, resulting in indicators calculated based on the thermal and electrical energy demand.

The results quantifying the average available storage capacity on thermal basis $C_{ADR,th}$ of the upward ADR events in Scenario B, Scenario C and Scenario D are presented in Figure 5-16.

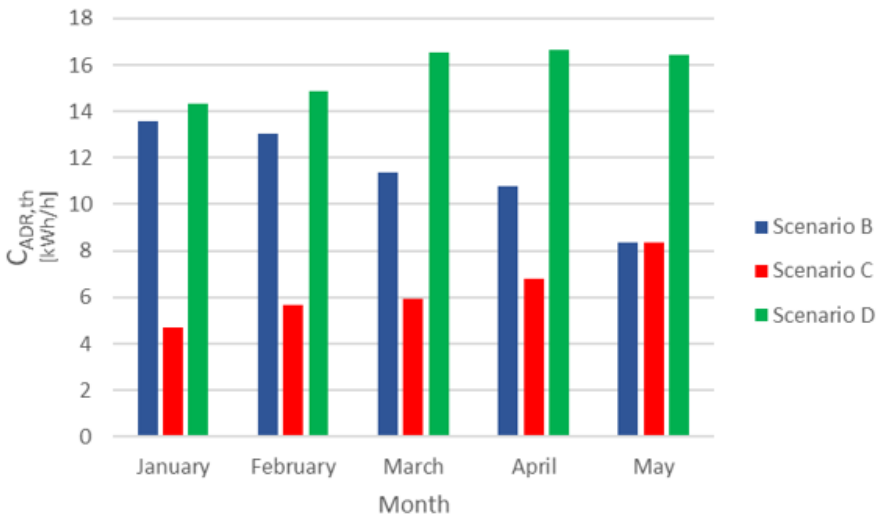

Figure 5-16: Available storage capacity $C_{ADR,th}$ of upward events on thermal basis in Scenario B, Scenario C and Scenario D.

Concerning Scenario B, as observed in Scenario A, the available storage capacity C_{ADR} decrease over time with the progression of the month. This trend is mainly caused by the external temperature which, on average, increases over time with the progression of the month. With higher external temperature indeed the energy consumptions needed to heat the building until the indoor temperature reaches the desired value is lower. This means that the energy consumption, on average, decreases over time with progression of the months, accordingly with the increase in external temperature. Since the heating consumption is lower, the energy provided to the building from the heating system is lower and lower is also the thermal energy stored in the building structure during the ADR events. This is the reason why in colder month the available storage capacity is higher and in warmer month is lower.

Moreover, it is noted that the value of the available storage capacity on thermal basis $C_{ADR,th}$ in Scenario B are substantially equal to the values of C_{ADR} in Scenario A. This aspect is due first to the fact that both the indicators are expressed on thermal basis, since in the Scenario A there is no heat pump, the C_{ADR} accounts for the thermal energy stored into the building structure and the $C_{ADR,th}$ in Scenario B is calculated in thermal terms. Then, the upward ADR events in Scenario B are created changing the heating setpoint temperature of the rooms as done in Scenario A, acting directly on the thermostat of the rooms. This means that the heat pump simply provides the amount of energy which is used to have the desired inlet temperature of the floor heating system, resulting in a similar situation of the Scenario A, in which the ADR events only act at the building structure level. In this case, thus, the source of flexibility is still only the building structure and the thermal storage tank is not actually exploited from the energy flexibility point of view, resulting in almost same values of C_{ADR} both in Scenario A and Scenario B.

Concerning Scenario C, as shown in Figure 5-16, the average available storage capacity on thermal basis $C_{ADR,th}$ increases with the progression of the months. This trend is explained through the following considerations. In Scenario C the heat pump is forced to remain switched on for 2 hours during the upward ADR events, while the heating setpoint temperature of the thermostat in the rooms of the building remains always constat and equal to 20°C. In this situation, forcing the heat pump to operate for 2 hours without a temperature-based control, the heat pump continuously charges the thermal storage tank until the high cut-out temperature of 70°C is reached in each upward ADR event.

The profile of the temperature at the thermostat level of the thermal storage tank during a generic upward ADR event is presented in Figure 5-17.

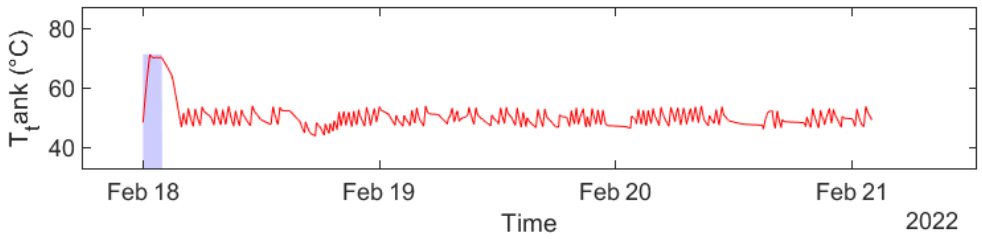

Figure 5-17: Thermal storage tank temperature profile during an upward ADR event in Scenario C.

Since for each event the temperature of 70°C in the thermal storage is reached, the tank has substantially the same flexibility potential for all the ADR events. What changes in the different months is the energy consumption of the building. As already explained, the energy consumption decreases with the increase in the external temperature and thus with the progression of the months. In the coldest months, when the energy consumption is higher, the energy that the thermal storage tank has to provide to the floor heating system is higher, resulting in higher use of the energy, and consequently hot water, stored in the thermal storage tank. Since the energy consumption in reference simulation in colder month is higher, the surplus of energy stored in the thermal storage is lower, resulting in lower average available storage capacity $C_{ADR,th}$. In the warmest months, instead, when the energy consumption is lower, the energy that the thermal storage tank has to provide to the floor heating system is lower, resulting in lower use of the energy, and consequently hot water, stored in the thermal storage tank. The energy consumption in the reference simulation is lower and thus the surplus of energy stored still available in the thermal storage is higher compared to coldest months, resulting in higher average available storage capacity $C_{ADR,th}$.

These considerations are confirmed by the fact that the amount of available storage capacity $C_{ADR,th}$ in the month of May, when the thermal storage tank is full exploited since the energy consumption is very low, is equal to approximately 8 kWh/h, which summed in two hours of event is exactly the energy that can be stored in the thermal storage tank.

In Scenario C the ADR events are created forcing the operation of the heat pump that charge the thermal storage and thus the source of energy flexibility is only the thermal storage tank.

Concerning Scenario D, as shown in Figure 5-16, the average available storage capacity on thermal basis $C_{ADR,th}$ increases with the progression of the first months and then remain almost constant. This trend is explained through the following considerations.

As said, in Scenario C the heat pump is forced to remains on for 2 hours during the upward ADR events while the heating setpoint temperature of the thermostat in the rooms of the building remains always constat and equal to 20°C. In this situation, forcing the heat pump to operate for 2 hours without a

temperature-based control, the heat pump continuously charges the thermal storage tank until the high cut-out temperature of 70°C is reached in each upward ADR event.

In Scenario D the operation of the heat pump is controlled in the same way, but the heating setpoint of the thermostat in the rooms of the building does not remain always constant, but is changed and set equal to 22°C during the upward ADR events. The fact that also the heating setpoint is changed results in an increase of the heating demand respect Scenario C, resulting in more thermal energy provided by the thermal storage to the floor heating system. This results in a higher use of the hot water in the tank which causes a lower increase in the temperature inside the tank respect the Scenario C. Because the higher energy consumption in Scenario D, in the colder month, indeed, the temperature inside the thermal storage tank does not reach the high cut-out temperature of 70°C as in Scenario C, resulting in lower average available storage capacity $C_{ADR,th}$ due to the thermal storage contribution.

The profile of the temperature at the thermostat level of the thermal storage tank during a generic upward ADR event of a colder month is presented in Figure 5-18.

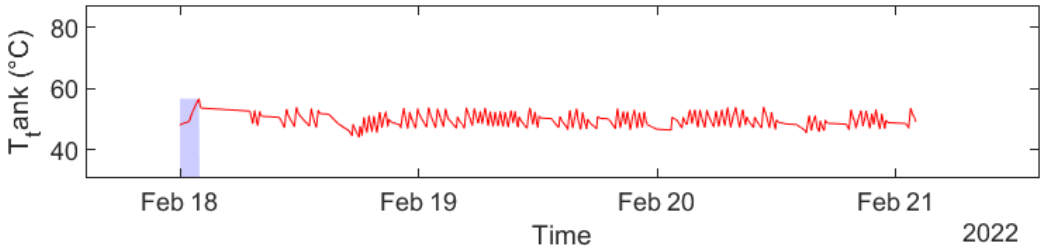

Figure 5-18: Thermal storage tank temperature profile during an upward ADR event in colder month in Scenario D.

When the energy consumption is lower, in warmer month, the thermal storage tank temperature, instead, reaches the 70°C and thus the surplus of energy stored in the thermal storage is higher, resulting in higher average available storage capacity $C_{ADR,th}$ due to the thermal storage contribution.

The profile of the temperature at the thermostat level of the thermal storage tank during a generic upward ADR event of a warmer month is presented in Figure 5-19.

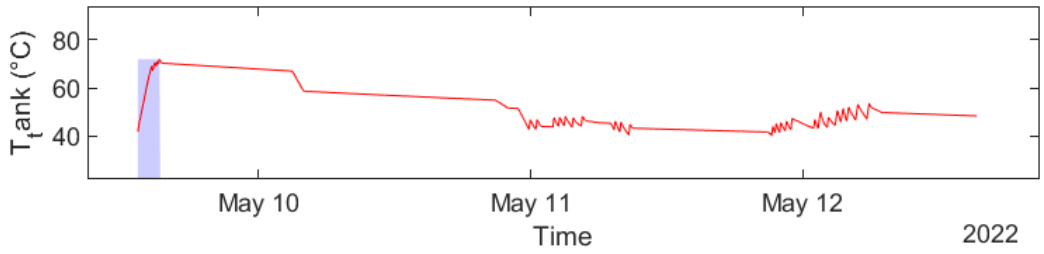

Figure 5-19: Thermal storage tank temperature profile during an upward ADR event in warmer month in Scenario D.

The contribution of the thermal storage to the overall energy flexibility potential increases as the energy consumption decreases because the more energy stored in the tank. The contribution to the available storage capacity $C_{ADR,th}$ due to the thermal storage is thus lower in the coldest months and increase in the warmest months. This effect is added to the energy flexibility contribution of the building structure, which present a decreasing trend as the energy consumption decreases with the progression of the months, as highlighted in Scenario B. The final results of the available storage capacity $C_{ADR,th}$
In Scenario D are thus a sort of sum of the contribution of both the thermal storage tank and the building structure, as highlighted form the higher values compared to the other scenarios. These considerations are confirmed by the fact that in the month of May, when the tank is exploited in the same way as in Scenario C, the available storage capacity is equal to approximately 16 kWh/h, which is the sum of the contribution of the thermal storage tank in Scenario C and the building structure in Scenario B.

The previous energy flexibility indicators are calculated on thermal basis, as done for the Scenario A.
Since in the simulation scenario B, C and D a heat pump coupled with the thermal storage tank is used, the energy flexibility indicators are also calculated on electrical basis, analyzing the electricity consumption of the heat pump in the ADR simulation and the reference simulation.
The results quantifying the average available storage capacity on electrical basis $C_{ADR,el}$ of the upward ADR events in Scenario B, Scenario C and Scenario D are presented in Figure 5-20.

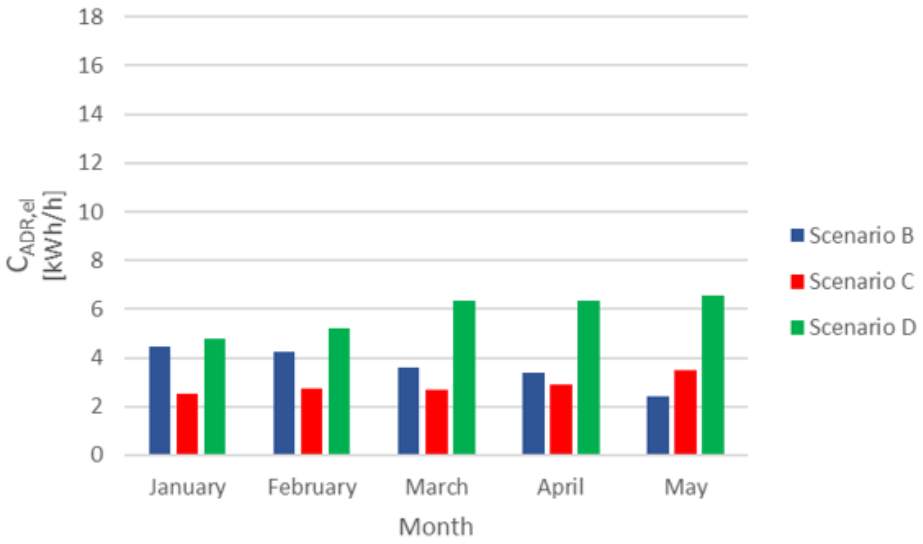

Figure 5-20: Available storage capacity $C_{ADR,el}$ of upward events on electrical basis in Scenario B, Scenario C and Scenario D.

The results of the available storage capacity $C_{ADR,el}$ on electrical basis follows the same trend highlighted for the same indicator calculated on thermal basis $C_{ADR,th}$ presented in Figure 5-16.

In order to understand the impact of the ADR events on the efficiency with which the system operates, the results quantifying the COP of the heat pump in the ADR simulation (COP_{ADR}) and the reference simulation (COP_{REF}) in all the simulation scenarios.

The results quantifying the COP_{ADR} and COP_{REF} in Scenario B are presented in Figure 5-21.

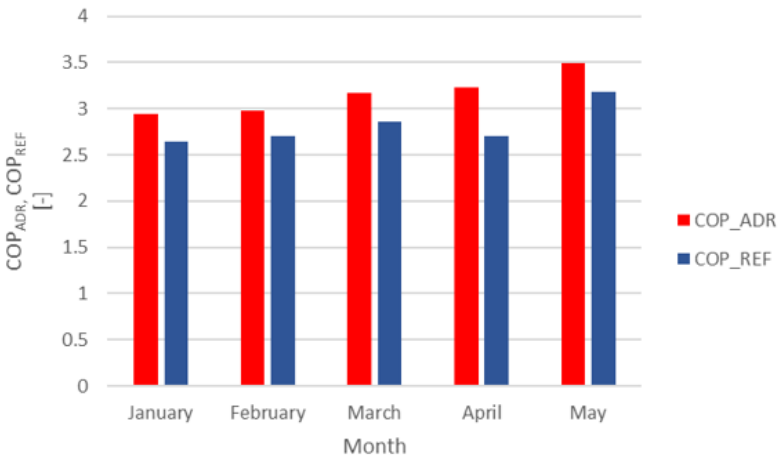

Figure 5-21: COP of the heat pump in the ADR simulation and reference simulation in Scenario B.

As expected, the COP of the ADR simulation, results to be the scaling factor between the values of the available storage capacity calculated in thermal basis $C_{ADR,th}$ and the one calculated on electrical basis $C_{ADR,el}$.

The COP_{ADR} presents values from 2.95 to 3.5 and from the graph an increasing trend of the COP with the progression of the months is observed.

This trend is due to the fact that the external temperature in general increases with the progression of the months affecting the COP of the heat pump. The temperature of the thermal storage tank, instead, remains almost constat and its small change during the ADR events does not affect significatively the behavior of the COP of the heat pump.

The COP_{ADR} shows the same trend of COP_{REF}, but COP_{ADR} presents higher values compared to the COP of the reference simulation COP_{REF}. This aspect is explained by the fact that the heating setpoint during the ADR events is increased until 22°C, resulting in higher energy consumptions. The higher consumption results in higher energy demand from the thermal storage tank compared to the reference simulation, resulting in lower temperature inside the thermal storage tank and thus higher values of the COP. The temperature of the thermal storage tank during the first event of February are shown in Figure 5-22.

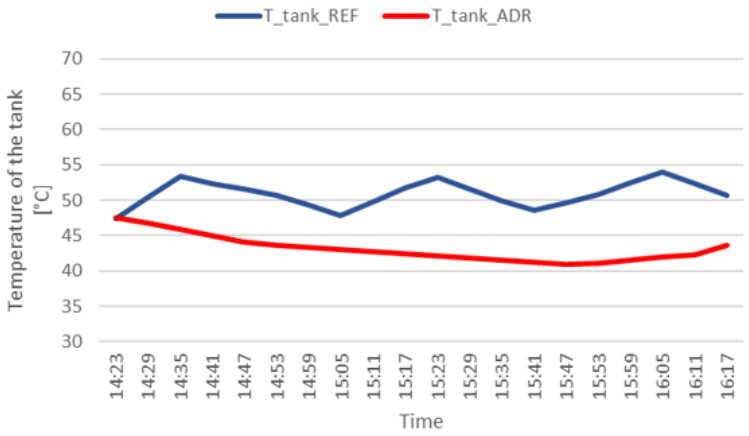

Figure 5-22: Thermal storage tank temperature in the ADR and reference simulation during the first event of February.

The results quantifying the COP_{ADR} and COP_{REF} in Scenario C are presented in Figure 5-23.

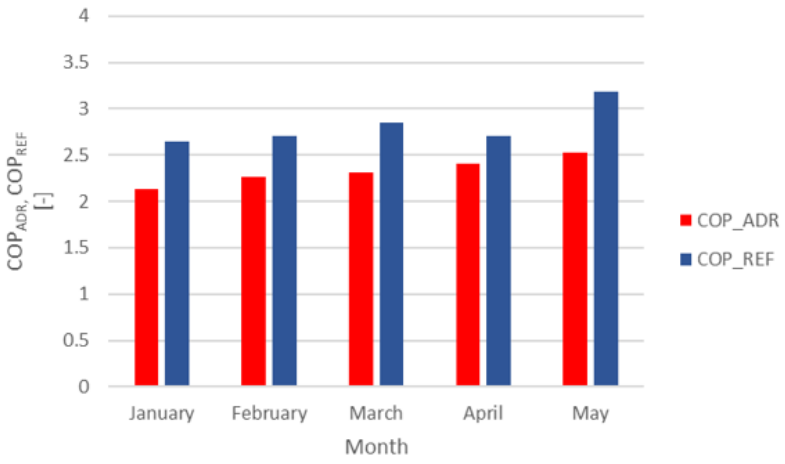

Figure 5-23: COP of the heat pump in the ADR simulation and reference simulation in Scenario C.

In this Scenario it is noted that the COP_{ADR} presents lower values compared to the values present in Scenario B.

The COP_{ADR} presents, indeed, values from 2.1 to 2.5, while in Scenario B the values are from 2.95 to 3.5. Also in this case, from the graph an increasing trend of the COP with the progression of the months is still observed, but with an increase slower respect the Scenario B.

The increasing trend observed also in Scenario B is due the fact that the external temperature in general increases with the progression of the months affecting the COP of the heat pump, while the temperature

of the thermal storage tank remains almost constat and this small change during the ADR events does not affect significatively the behavior of the COP of the heat pump. The difference in Scenario C is that the temperature of the thermal storage during the upward ADR events, as explained before, reaches values equal to 70°C, instead values around 50/55°C as in Scenario B. This higher temperature of the thermal storage tank during the ADR events results in lower values of the COP_{ADR} of the heat pump compared to Scenario B.

This situation results also in lower values of the COP_{ADR} compared to COP_{REF}, because the higher temperature reached in the thermal storage tank compared to the reference case, meaning that the heat pump in case of Scenario C operates with lower efficiency, but with acceptable values.

The results quantifying the COP_{ADR} and COP_{REF} in Scenario D are presented in Figure 5-24.

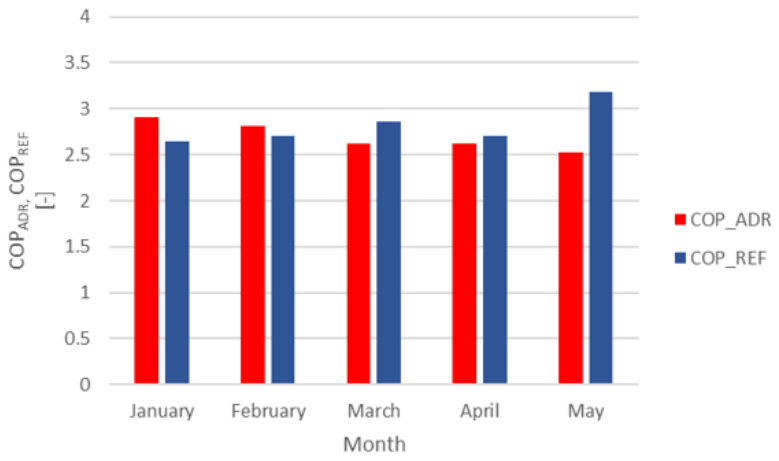

Figure 5-24: COP of the heat pump in the ADR simulation and reference simulation in Scenario D.

In this Scenario it is noted that the COP_{ADR} present a different behavior respect the previous cases.

From the graph a decreasing trend of the COP_{ADR} with the progression of the months is indeed observed. This trend is the result of two different contributions.

Since the external temperature in general increases with the progression of the months and affects the COP of the heat pump as in previous cases, the contribution of the external temperature result in an increasing trend, as in previous scenarios.

In Scenario C the heating setpoint temperature of the thermostats of the rooms of the building is set constant and equal to 20°C and the temperature of the thermal storage during the upward ADR events, as explained before, reaches values equal to 70°C.

In Scenario D, instead, during the ADR events, the heating setpoint temperature of the thermostats of the rooms of the building is changed and set equal to 22°C.

The fact that also the heating setpoint is changed results in an increase of the heating demand respect Scenario C, resulting in more thermal energy provided by the thermal storage to the floor heating system. This results in a higher use of the hot water in the tank which causes a lower increase in the temperature inside the tank compared to Scenario C. Because the higher energy consumption in Scenario D, in the colder month, indeed, the temperature inside the thermal storage tank does not reach the high cut-out temperature of 70°C as in Scenario C.

When the energy consumption is lower, in warmer month, the thermal storage tank temperature, instead, reaches the 70°C.

The fact that different temperatures are reached inside the tank, lower in colder month and higher in warmer month, causes a decreasing trend contribution of the COP of the heat pump.

The sum of both the contributions of the external temperature variation and the thermal storage tank temperature variation results in the decreasing trend of COP_{ADR} observed in Figure 5-24.

The previous considerations are confirmed by the fact that, when the boundary conditions of external temperature and thermal storage tank temperature are equal in Scenario C and Scenario D, in the month of May, the COP_{ADR} present equal values.

In this case COP_{ADR} results to be higher than COP_{REF} in the colder months when the temperature inside the thermal storage tank in the ADR simulation is lower compared to the reference case, while is lower in the warmer months, when the temperature inside the tank is higher.

During the ADR events, in general, the heat pump operates with higher efficiency in the colder month and with lower efficiency in the warmer month compared to the reference case.

Concerning the storage efficiency η_{ADR} of the upwards ADR events, the results of the indicator evaluated in Scenario B, Scenario C and Scenario D are presented in Figure 5-25.

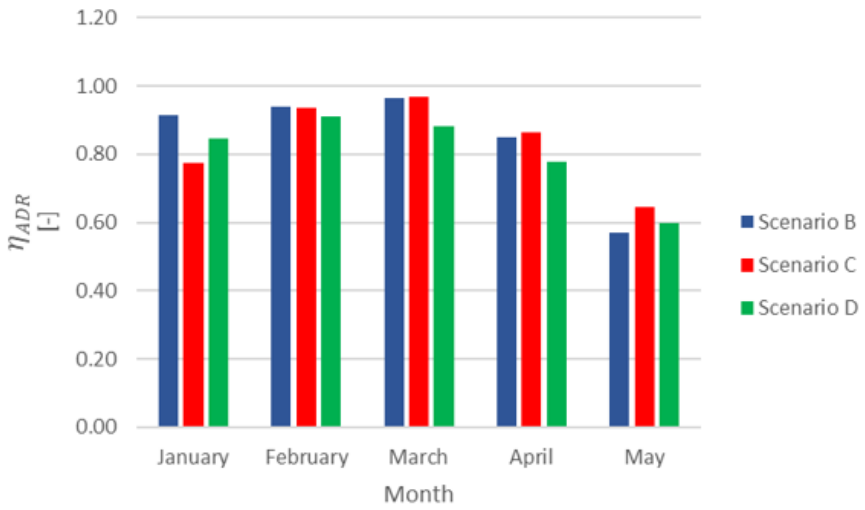

Figure 5-25: Storage efficiency η_{ADR} of the upward ADR events on monthly basis in Scenario B, Scenario C and Scenario D.

Similarly, as for Scenario A, these results come from the average of the storage efficiency of each one of the different events happened during each month. Generally, indeed, the efficiency of the different events can vary depending on the time of the day in which the ADR event is started, which is the amount of energy released from the heating system during normal operations in the hours before the event and the consequently amount of energy stored in the building structure. Also the external temperature, which varies not always gradually during the month, has an impact on the thermal behavior of the building and consequently on the storage efficiency, since this indicator is evaluated in the 72 hours after the ADR event. For these reasons the values of the storage efficiency can be affected by some oscillations. In general, it is noted that the storage efficiency η_{ADR} present values between 0.95 and 0.6 and decrease in the warmer month. This trend is explained by the increase in the external temperature, which results in a lower heating consumption of the building. This means that, when the heating setpoint is increased and some energy is stored in the building structure during the ADR event, the surplus of energy is not used properly to decrease the heating consumptions in the hours after the ADR event itself since the energy consumption is already low.

It is also noted that, in Scenario C, where the thermal storage tank is exploited for the energy flexibility point of view and the temperature inside the tank reaches 70°C, the efficiency is a bit lower in the coldest month respect the Scenario B. This is explained by the fact that adding the use of the thermal storage which reaches higher temperature, there is an increase in the thermal losses, in particular in colder month. This aspect affects in part also the efficiency of the ADR events.

Similarly, in Scenario D, since also in this case the thermal storage tank is exploited, the storage efficiency is lower in the coldest month respect Scenario B, but a bit higher respect Scenario C. This aspect is

explained by the fact that the temperature reached inside the thermal storage tank in Scenario D respect Scenario C is lower, as already explained before, and thus also the thermal losses are lower, resulting in higher efficiency.

Concerning the overheating index OHI_{ADR} it is remembered that in the case of the upward ADR events this index not properly define a real discomfort, but simply takes into account how much and for how long time the indoor temperature of the rooms composing the building rise above the heating setpoint of 22°C.

The results quantifying the overheating index OHI_{ADR} of the upward ADR events in Scenario B, Scenario C and Scenario D are presented in Figure 5-26.

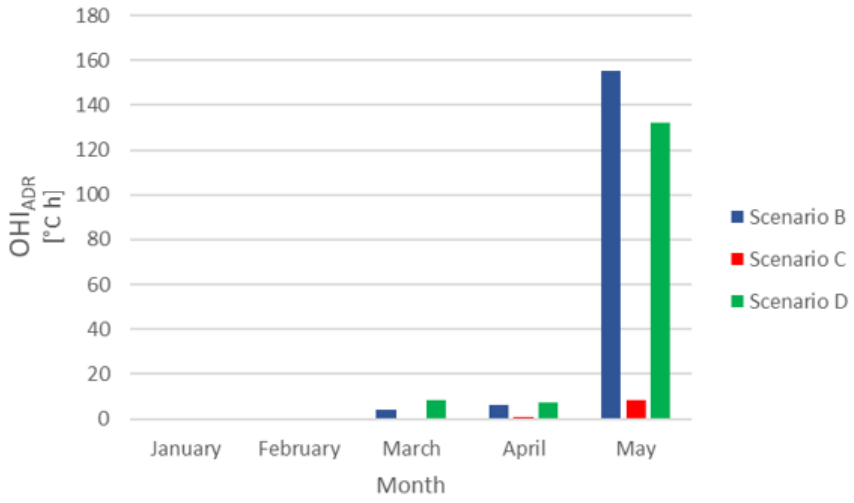

Figure 5-26: Overheating index of the upward ADR events in Scenario B, Scenario C and Scenario D.

The overheating index OHI_{ADR} increases from the colder month to the warmer month.

Concerning Scenario B, it presents null values for January and February, since the external temperature is very low and during the ADR events, when the setpoint temperature is increased at 22°C, in general, in 2 hours the heating system bring the indoor temperature near 22°C but never passing them. When the ADR events ends, indeed, the heating system switched off for a while since the heating setpoint is back to 20°C and there is no need of heat. In this situation the indoor temperature starts quickly to decrease naturally because the thermal losses.

In the case of warmer month, when the external temperature is higher, it is possible that the heating system brings the indoor temperature at 22°C or more, remembering the presence of a dead band of 0.5°C in the room's thermostats. After the ADR events, since the external temperature is higher, the thermal losses are low respect colder months and the indoor temperature remains naturally above 22°C for more time. In the month of May this behavior is extremized because during the last ADR event the

external temperature is relatively very high, above 20°C. This means that, when the heating system switched on because the increase in the heating setpoint during the ADR event, a part of the energy released increases the indoor temperature, while a part is stored in the building structure. When the ADR event ends, the temperature is above 22°C but also the external temperature presents similar values, resulting in a very slow decrease of the indoor temperature which remain above 22°C for a long period respect the other months, resulting in higher values of the index. Also, during the event is present also the contribution of the heat gains due to the solar radiation that normally increases the indoor temperature. This contribution facilitates the fact that the temperature profile in the ADR simulation reaches higher values, increasing the degree-hours of duration above the limit of 22°C used to calculate the overheating index OHI_{ADR}.

In Scenario B the heating setpoint temperature of the thermostats is maintained constant and equal to 20°C during normal operation and also during the ADR events, which are created only forcing the state of operation of the heat pump.

Concerning Scenario C, the results in Figure 5-26 suggest that the thermal storage tank does not contribute to the thermal discomfort of the building. This aspect is explained through the following considerations.

During the upward ADR events the heat pump remains switched on for 2 hours, resulting in an increase in the temperature inside the thermal storage tank, but the control of the inlet temperature of the radiant floor heating system which heat up the building adapts to the temperature inside the tank. The controller, indeed, decrease the amount of hot water coming from the thermal storage tank and increase the amount of cold water which bypass the tank in order to have the desired inlet temperature of the radiant floor heating system, without affecting the indoor temperature conditions inside the rooms. The small value of the month of May is due to the fact there is a little mismatch between the temperature profiles in ADR simulations and the reference simulation when the temperature inside the room is higher than 22°C and it is accounted in the indicator.

Concerning Scenario D, the overheating index OHI_{ADR} increases from the colder month to the warmer month, as in Scenario B. The same considerations made before are still valid. It is observed a little decrease in the value of the indicator in the month of May respect scenario B. This can be due in part by the fact that in this case, since the thermal storage tank reaches higher temperature, some thermal losses are introduced in the system and in part because part of the thermal energy remains charged in the thermal storage without affecting the temperature in the rooms.

A rough analysis from the economic point of view is performed in the different simulation scenarios to have a general idea of how the introduction of the ADR events can bring economic advantages also to the building owners, remembering that this is only a part of the scope of the Active Demand Response program.

The cost saving indicator is calculated weighting the difference in the energy consumption in the ADR simulation and the reference simulation in a specific time with the electricity price in that time.

The results quantifying the cost saving of the upward ADR events in Scenario B, Scenario C and Scenario D are presented in Figure 5-27.

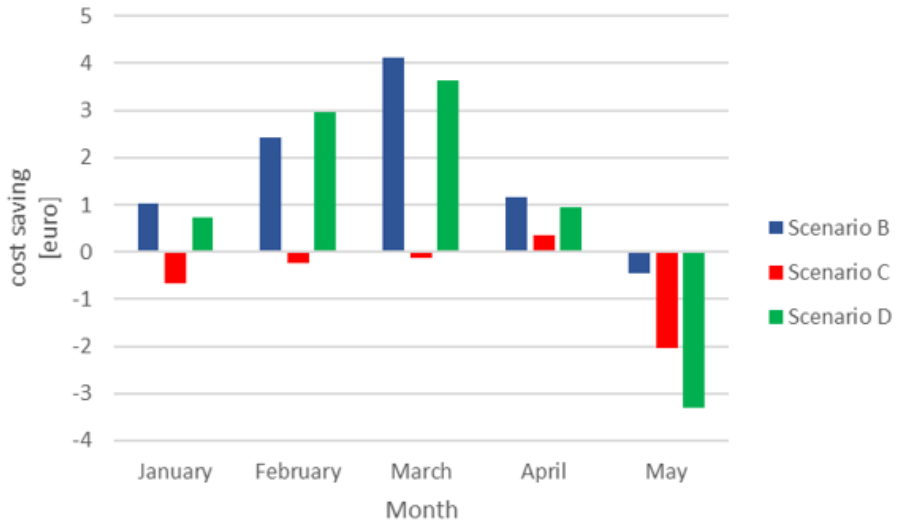

Figure 5-27: Cost saving results for the upward ADR events in Scenario B, Scenario C and Scenario D.

Concerning Scenario B, the first observation made is that in almost all the month the cost saving presents positive values, meaning that applying some upward ADR events to the system is convenient in economic terms for the building owners.

Since the cost saving is driven by the price of the electricity in the different time of the day and the months in which the ADR events occurs, the cost saving can be affected by some alterations which depend on external factors, making difficult to establish a general rule.

Anyway, in this case the trend cost saving appears to be a trade-off between three different aspects. In the colder months the energy consumption is in general higher, resulting in higher costs, even if the consumption is increased during low-price periods through the upward ADR events and decrease after the events. The cost saving is thus related to the fact that the energy consumption is decreased in a period in which cost more respect the price in which the energy consumption is increased. When the energy consumption decreases in warmer months, the fact that the consumption is increased increasing

the heating setpoint temperature during the upward ADR events results in higher costs. Since the energy demand in these months is lower, the surplus of energy charged into the building structure is not used properly to decrease the energy consumption after the ADR events, resulting in lower cost saving related to the cost of this energy. The result is a decrease in the cost saving in warmer months related to the fact that the energy is consumed more in low price-period, but after the events there is not enough saving to justify the increase in the consumption during the events.

Moreover, it is observed that the electricity price has, in general, a higher variation between the lowest and the highest price in the days of the middle month, like March, and lower variations during the first and last months of the simulation, as January and May. This aspect is shown in Figure 5-28, remembering that the different ADR events happen in different time of the day and the month, making difficult to establish a general rule based only on the monthly average difference in the electricity price.

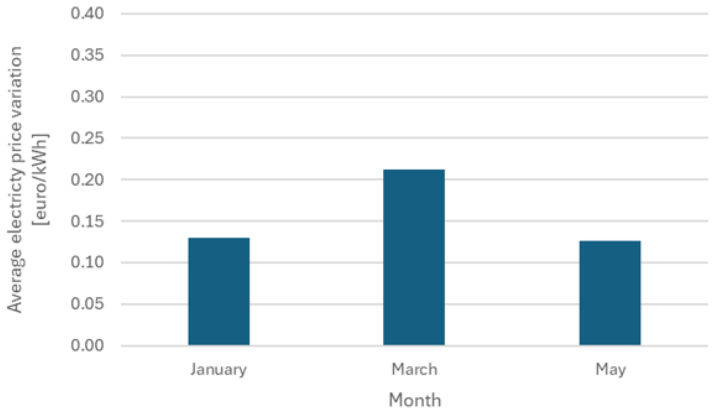

Figure 5-28: Average electricity price difference between the maximum and minimum daily price.

Anyway, a possible consideration is the following. The higher difference in price in the days of March increases the possibility that an upward ADR events increases the energy consumption during low-price period which present higher difference in price respect the time period in which the consumption is instead decreased, resulting in higher cost saving.

Similarly, if the electricity prices are more similar during and after the ADR events, the increase in the energy consumption, that in general increase the cost because the cost of energy, has a higher impact in the cost saving respect the lower consumption at higher price after the ADR events, resulting in lower cost saving.

Concerning Scenario C, in this case the ADR events are created only forcing the operation of the heat pump coupled with the thermal storage and the amount of energy shifted is in general lower respect Scenario B.

Since during the upward ADR events the heat pump is forced to stay switched on, the energy consumption in the ADR simulation is higher respect the reference simulation and consequently also the total costs, related to the cost of the electricity, are higher. Right after the ADR events the energy consumptions is lower respect the reference simulation, when the price of the electricity is higher respect the period of the ADR events and this result in a cost saving.
From the total results seems that the amount of energy shifted with only the thermal storage tank and the corresponding energy saved right after the ADR event does not create enough cost saving to balance the increase in the energy consumption and thus the related cost during the ADR events.

Concerning Scenario D, where the upward ADR events are created both changing the heating setpoint temperature of the thermostats in the rooms and forcing the operation of the heat pump, the results quantifying the cost saving seems to be the result of the contribution of both the situations describe in Scenario B and Scenario C.
The cost saving is indeed positive, meaning that the contribution of both the type of events results in a positive advantage also for the building owner.
The cost saving increase from January to March and then start to decrease, becoming negative in the month of May, where the increase in the energy consumption is not justified by the decrease in the electricity price when the energy is consumed.
In general, the cost saving in the different month results to be between the 2% and the 6% of the overall cost of the electricity consumed in the reference simulation during the period of evaluation of the effect of the upward ADR events.
This result, even if can appears as a small economic advantage, is motivated by the following considerations.
First of all, the Active Demand response program does not only bring advantages to the building owners but is intended to bring advantages mainly to the overall electrical system.
By shifting or reducing electricity demand during peak periods, indeed, ADR program can help alleviate strain on the grid, lower overall energy costs and mitigate environmental impacts associated with energy production, helps alleviate congestion problems, enhances grid security and efficiency.
In other hand, the number of ADR events created in this work is equal to 3 or 4 events per months, but this number can be increased, increasing also the economic advantages for the building owners.
Also the number of hours of duration of the ADR events, which in this work is of only 2 hours, can be increased, resulting in a higher amount of energy shifted and thus also higher cost saving.

As done for the upward ADR events, after the presentation of the results of the key performance indicators, a similar analysis and discussion of the results is provided for the downward ADR events.

Since the analysis of the simulation scenario A is already provided at the beginning of the chapter, the results are now presented comparing each one of the key performance indicators in the simulation scenario B, scenario C and scenario D. The key performance indicators are calculated in the same way already presented and they are collected on monthly basis.

Similarly to the upward ADR events, since also the heat pump is present in the configuration of the system, the energy flexibility indicators are calculated starting from the thermal energy provided by the heat pump and the electrical energy used, resulting in indicators calculated on thermal basis and electrical basis.

The results quantifying the average available storage capacity on thermal basis $C_{ADR,th}$ of the downward ADR events in Scenario B, Scenario C and Scenario D are presented in Figure 5-29.

Figure 5-29: Available storage capacity $C_{ADR,th}$ of downward events on thermal basis in Scenario B, Scenario C and Scenario D.

As already explained in Scenario A, in the case of downward events the available storage capacity presents negative values. This happen because when the heating setpoint is changed to 18°C, the energy consumption profile in the ADR simulation presents lower values respect the reference simulation during the ADR event, resulting in negative values. The meaning of negative values of available storage capacity is that this amount of energy is saved and not used respect the reference simulation.

The first simulation scenario analyzed is the Scenario B, in which the building is heated up through the radiant floor heating system and there is the thermal storage tank coupled with the heat pump. In this simulation scenario the ADR events are created changing the heating setpoint of the thermostats in the rooms composing the building and the source of energy flexibility is the building structure.

From the previous a graph a trend is observed: the available storage capacity C_{ADR} decrease in absolute value over time with the progression of the months, similarly to Scenario A.
This trend is mainly caused by the external temperature which, on average, increases over time with the progression of the months. With higher external temperature indeed the energy consumptions needed to heat up the building until the indoor temperature reaches the desired value is lower. This means that the energy consumption, on average, decreases over time with progression of the month, accordingly with the increase in external temperature. Since the heating consumption is lower, the energy saved during the ADR events respect the reference simulation from the heating system is lower. This is the reason why in colder month the available storage capacity is higher in absolute value and in warmer month is lower.
In Scenario B lower absolute values of the available storage capacity C_{ADR} are observed respect Scenario A. This aspect is motivated through the following consideration. In Scenario B the technological setup is also composed by the heat pump coupled with the thermal storage tank. In this case to heat up the building, the heat pump switched on when the control based on the temperature inside the thermal storage goes below the setpoint. In Scenario B, when the rooms temperature starts to decrease, the floor heating system switched on and the thermal storage tank provide the hot water already present in the tank, resulting in lower switching on of the heat pump respect Scenario A. Since the heat pump is switched on for less time, the energy consumption is lower and thus also the energy that can be saved during the downward ADR events is lower, resulting in lower absolute values of the available storage capacity C_{ADR}.

Concerning Scenario C, as in the previous case, the same trend is observed: the available storage capacity C_{ADR} decrease in absolute value over time with the progression of the months.
This trend is mainly caused by the external temperature which, on average, increases over time with the progression of the months, resulting in lower energy consumption and thus lower energy saved during the downward ADR event.
In Scenario C higher absolute values of the available storage capacity C_{ADR} are observed respect Scenario B. This aspect is motivated through the following consideration. In Scenario C the technological setup is composed by the heat pump coupled with the thermal storage tank as in Scenario B, but the difference is that in Scenario C the heat pump is forced to stay always off during the ADR events, while in Scenario B the operation is controlled through the temperature inside the thermal storage tank. This aspect results in less accension of the heat pump in the ADR simulation of the Scenario C respect Scenario B and thus higher difference with the reference simulation, resulting in higher amount of possible energy saved and thus higher absolute values of the available storage capacity C_{ADR}.

Concerning Scenario D, as in the previous cases, the same trend is observed: the available storage capacity C_{ADR} decrease in absolute value over time with the progression of the months. The motivations are the same explained before.

In Scenario D the same absolute values of the available storage capacity C_{ADR} present in Scenario B are observed. This aspect is motivated through the following considerations.

When the downward ADR events occur in Scenario C, the heat pump is switched off for 2 hours and the heating setpoint temperature of the thermostats in the rooms is set equal to 20°C, resulting in a decrease in the thermal storage tank temperature.

When the downward ADR events occur in Scenario D, the heat pump is switched off for 2 hours but at the same time the heating setpoint temperature of the thermostats in the rooms is set equal to 18°C, resulting in a lower decrease in the thermal storage tank temperature, since the energy consumption is lower.

What changes in the two scenarios is the temperature reached inside the thermal storage tank during the downward ADR events, but in both cases the heat pump is always switched off, resulting in the same amount of energy consumption difference between the reference simulation and the ADR simulation, in which the consumption is null. For these reasons the amount of energy saved during the downward ADR events is the same in both Scenario C and Scenario D, resulting in the same absolute values of the available storage capacity C_{ADR}.

This different behavior of the downward ADR events respect the upward ADR events is due to the fact that in the case of the upward events there is a high limit in the temperature which the thermal storage tank can reach, which in consequence affects the behavior of the heat pump, while in the case of downward events the temperature can decrease without limit and the heat pump remains always switched off.

The previous energy flexibility indicators are calculated on thermal basis, as done for the Scenario A.

Since in the simulation scenario B, C and D a heat pump coupled with the thermal storage tank is used, the energy flexibility indicators are also calculated on electrical basis, analyzing the electricity consumption of the heat pump in the ADR simulation and the reference simulation.

The results quantifying the average available storage capacity on electrical basis $C_{ADR,el}$ of the downward ADR events in Scenario B, Scenario C and Scenario D are presented in Figure 5-30.

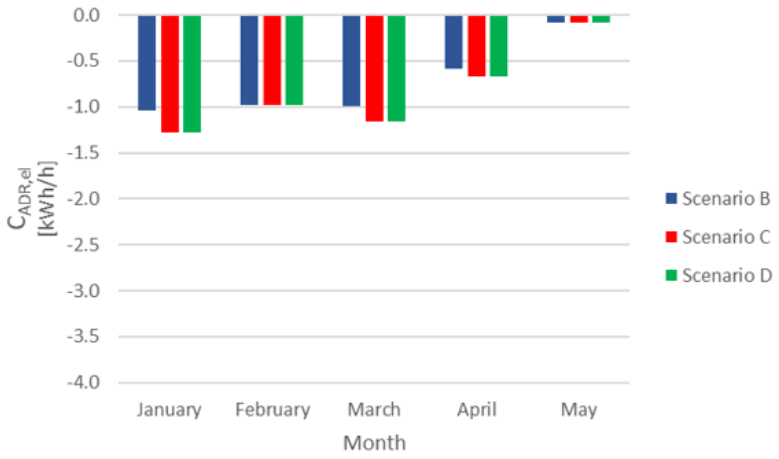

Figure 5-30: Available storage capacity $C_{ADR,el}$ of downward events on thermal basis in Scenario B, Scenario C and Scenario D.

The results of the available storage capacity $C_{ADR,el}$ on electrical basis follows the same trend highlighted for the same indicator calculated on thermal basis $C_{ADR,th}$.

Concerning the COP of the heat pump in case of downward ADR events, the heat pump is forced to stay always off in Scenario C and Scenario D and results almost always off also during most of the events of Scenario B. In these cases, it is not possible to calculate the COP during the ADR simulation COP_{ADR} since the heat pump does not operates. The consideration made is that in general the heat pump operates with the same efficiency in both the ADR simulation and the reference simulation, not real affecting the efficiency of the system. The COP with which the heat pump in general operates is presented in Figure 5-31

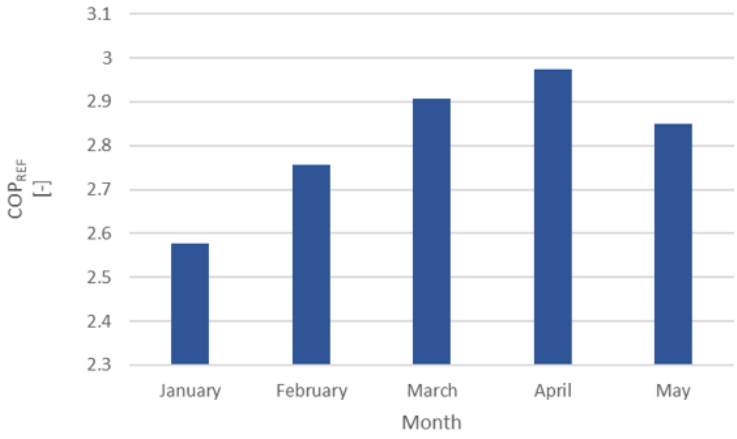

Figure 5-31: COP of the heat pump during the reference simulation.

The trend observed from the previous graphs is an increasing trend of the COP with the progressions of the months. This trend is due to the fact that, in general, the external temperature increases with the progression of the months, resulting in an increasing trend of the COP.
The result of the COP of the month of May, which appears to be lower than the previous months, is simply due to the fact that during this month only one event presents an available storage capacity different from 0. This is due to the fact that also in the reference simulation the energy consumptions is null and thus also the possible energy saved. This event occurs during the night, resulting in lower external temperature compared to the average of the previous months and thus lower COP.

Concerning the storage efficiency η_{ADR} of the upwards ADR events, the results of the indicator evaluated in Scenario B, Scenario C and Scenario D are presented in Figure 5-32

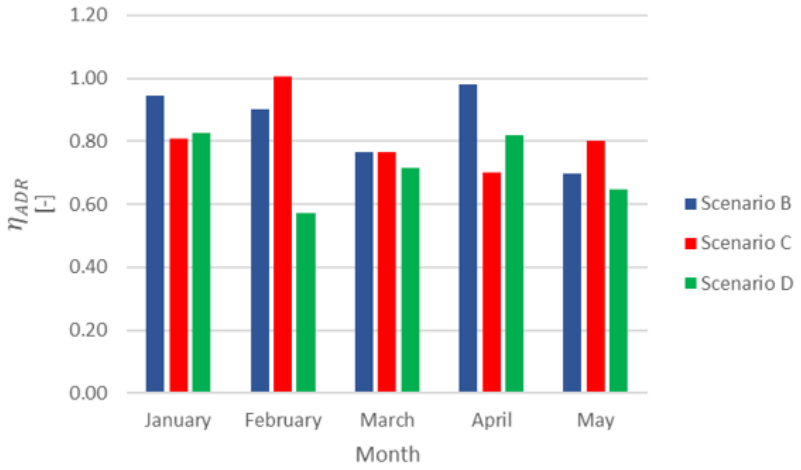

Figure 5-32: Storage efficiency η_{ADR} of the downward ADR events on monthly basis in Scenario B, Scenario C and Scenario D.

Similarly, as for Scenario A, these results come from the average of the storage efficiency of each one of the different events happened during each month. Generally, indeed, the efficiency of the different events can vary depending on the time of the day in which the ADR event is started, which is the amount of energy released from the heating system during normal operations in the hours before the event and the consequently amount of energy already stored in the system. Also the external temperature, which varies not always gradually during the day and the month, has an impact on the thermal behavior of the building and consequently on the storage efficiency, since this indicator is evaluated in the 72 hours after the ADR event.
Moreover, respect the case of the upward ADR events, in this case the absolute values of available storage capacity are lower and sometimes near to zero, resulting in higher impact of some possible misalignments between the ADR simulation and the reference simulation, which can affect more the

results of the storage efficiency. For these reasons the values of the storage efficiency can be affected by some alterations which depend on external factors, making difficult to establish a general rule.
In general, it is noted that the storage efficiency η_{ADR} present values between 0.99 and 0.57, varying in the different months, meaning that in case of downward ADR events the energy saved during the 2 hours of event is lower than the surplus of energy which can be used to restore the desired temperature after the ADR events.

Concerning the thermal discomfort index TDI_{ADR} it is remembered that in the case of the downward ADR events this index takes into account how much and for how long time the indoor temperature of the rooms composing the building felt below the lower comfort limit of 20°C.
The results quantifying the thermal discomfort index TDI_{ADR} of the downward ADR events in Scenario B, Scenario C and Scenario D are presented in Figure 5-33.

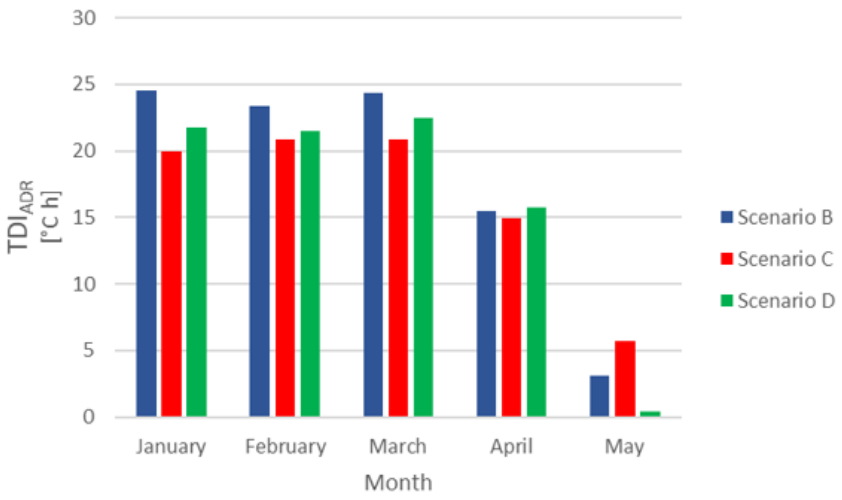

Figure 5-33: Thermal discomfort index of the downward ADR events in Scenario B, Scenario C and Scenario D.

Concerning Scenario B, from the results in the graph a general trend is observed: the thermal discomfort index TDI_{ADR} remains almost constant during the colder months and then starts to decrease in the warmer months.
In particular it presents higher values for January, February and March, since the external temperature when the ADR events occur is in general enough similar in these months.
During these months, when the downward ADR events occur, the heating setpoint is decrease to 18°C and the indoor temperature starts naturally decrease because thermal losses, since there is no more heating energy provided from the radiant floor system to the building. In the warmer months this

behavior is still similar, but since the external temperature is generally higher, the thermal losses are lower and the indoor temperature decrease slowly respect the colder months, resulting in lower degree-hours of thermal discomfort due to the forced shout-down of the heating system during the ADR events. The values of the thermal discomfort index TDI_{ADR} in Scenario B are very similar to the ones present in Scenario A, since the thermal storage is not exploited and the heating setpoint temperature of the thermostats of the rooms is changed in the same way.

Concerning Scenario C, the trend of the thermal discomfort index TDI_{ADR} is similar to the one observed in the previous scenarios but it is noted that the values of the TDI_{ADR} in Scenario C are lower respect the ones present in Scenario B. This aspect is explained through the following consideration.
In Scenario B the downward ADR events are created decreasing the heating setpoint temperature of the thermostats until 18°C.
In Scenario C, instead, the heating setpoint temperature of the thermostats of the rooms is maintained constant and equal to 20°C during normal operation and also during the ADR events, which are created only forcing the state of operation of the heat pump. In this way, even if the heat pump stop the operation, the energy consumption request by the building is higher respect the previous case and an higher part of the energy available in the thermal storage tank is used to try to maintain the desired temperature in the room, resulting in lower thermal discomfort respect the previous case.

Concerning Scenario D, the trend of the thermal discomfort index TDI_{ADR} is similar to the one observed in the previous scenarios but it is noted that the values of the TDI_{ADR} in Scenario D higher respect the ones present in Scenario C. This aspect is explained through the following consideration.
In Scenario C the ADR events are created forcing the operation of the heat pump to stay off while the heating setpoint temperature remains equal to 20°C.
In Scenario D the downward ADR events are created forcing the state of operation of the heat pump to stay off, but the heating setpoint temperature of the thermostats is decreased until 18°C. In this way the same time the energy consumption is lower respect Scenario C, resulting in lower use of the energy stored in the thermal storage, and thus higher TDI_{ADR} respect Scenario C.

Also in the case of downward ADR events a rough analysis from the economic point of view is performed in the different simulation scenarios to have a general idea of how the introduction of the ADR events can bring economic advantages also to the building owners, remembering that this is only a part of the scope of the Active Demand Response program.
The cost saving indicator is calculated weighting the difference in the energy consumption in the ADR simulation and the reference simulation in a specific time with the electricity price in that time.

The results quantifying the cost saving of the upward ADR events in Scenario B, Scenario C and Scenario D are presented in Figure 5-34.

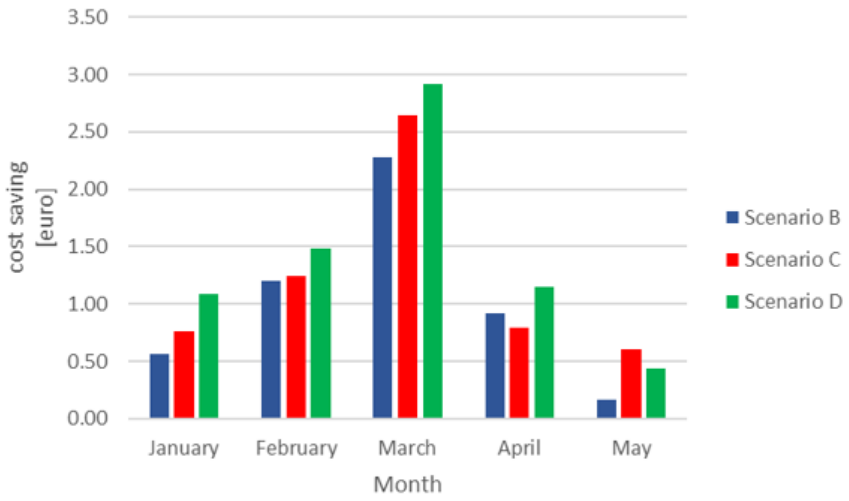

Figure 5-34: Cost saving results for the downward ADR events in Scenario B, Scenario C and Scenario D.

The first observation made is that in all the month the cost saving presents positive values, meaning that applying some downward ADR events to the system is convenient in economic terms for the building owners. The cost saving is due to the fact that during the downward ADR events, when the price is higher, the energy consumption is lower respect the reference simulation, resulting in a save also in economic terms. The increase in the energy consumption after the events occurs at lower price respect the one present during the ADR events, resulting in an increase in the cost respect the reference simulation, but lower than the save in economic terms during the ADR events.

Since the cost saving is driven by the price of the electricity in the different time of the day and the months in which the ADR events occurs, the cost saving can be affected by some alterations which depend on external factors, making difficult to establish a general rule.

Anyway, in all the simulation scenario the trend observed is the same, increasing from January to March and decreasing from March to May.

This trend is probably due to the combination of two considerations. The first is that, since the energy available storage capacity is higher in the colder month respect the warmer month, the cost saving related to the energy saving during the high price period is higher in colder months. This explains why in all scenarios January and February present higher cost saving respect April and May. The second observation is related to the fact that the price variation between the maximum and the minimum price in the month of March is higher respect the other months. The higher difference in price in the days of

March increases the possibility that a downward ADR events decreases the energy consumption during higher-price period which present higher difference in price compared to the time period in which the consumption is instead increased, resulting in higher cost saving.

Similarly, if the electricity prices are more similar during and after the ADR events, the decrease in the energy consumption, that in general decrease the cost because the cost of energy, has a lower impact in the cost saving compared to the higher consumption at higher price after the ADR events, resulting in lower cost saving.

The results of Scenario D present in general higher values of the cost saving because the contribution of both the situation present in Scenario B and Scenario C.

6 Conclusion

The energy flexibility potential of a building is the ability to manage its demand and generation according to user needs, local weather conditions and external factors such as signals from grid operators. The participation to Active Demand Response (ADR) programs are intended to change the electric usage of end-use customers from their normal consumption patterns in response to changes in the price of electricity over time. By leveraging their energy flexibility, buildings can contribute to alleviate problems at energy system level, such as reducing peak loads by shifting energy consumption towards off-peak hours, as well as improve operation for single users by increasing self-consumption from local renewable energy production plants, lowering overall energy costs etc., thus reducing the environmental impact and at the same time saving money for the building owners.

This thesis quantified the energy flexibility potential of a Danish single-family house and investigated to what extent the latter changes depending on the boundary conditions of the analysis. In particular, the energy flexibility potential is given by shifting the energy consumption required for the heating system of the considered building.

The energy flexibility potential is quantified through some energy flexibility indicators. for instance, the available storage capacity (C_{ADR}) represents the energy that can be shifted during an Active Demand Response event, and the storage efficiency (η_{ADR}) describes the relative amount of energy lost after the event due to the changed operation of the heating and cooling system.

Other key performance indicators are calculated to have a comprehensive analysis of the energy flexibility potential also from the thermal comfort and the economic point of view.

The analysis is carried out in different simulation scenarios to understand how the energy flexibility potential vary with different -heating energy systems and different type of ADR events. Two different configurations are analyzed, one in which the building is heated up only through a radiant floor heating system served by district heating and one in which also a heat pump coupled with a thermal storage tank is used.

The ADR events are driven by the electricity price and can be upward modulation or downward modulation depending on whether more or less energy is supplied to the building during a certain ADR event. The source of the energy flexibility can be the building structure or the thermal storage tank.

The simulations of the building and plant include five months of the heating season, from the beginning of January to the end of May. The key performance indicators are grouped on monthly basis to assess how the energy flexibility varies with the seasonality.

In general, results show that in all the simulation scenarios, varying the technological setup and the type of ADR events, the available storage capacity (C_{ADR}) provided by the upward ADR events is higher in

absolute values respect the same provided by the downward ADR events. This result is related to the size of the heating system, which, when is forced to operate more compared to normal operations, during the upward events, is able to charge the system with a surplus of energy higher compared the amount of energy saved during the downward events.

Concerning the upward ADR events, the available storage capacity shows a decreasing trend from the colder months to the warmer months in the scenarios in which only the building structure is exploited as source of energy flexibility. This is mainly due to the influence of the external temperature, which increase the energy consumption in colder months and decrease in warmer months, resulting in higher energy shifting potential in colder months compared to warmer months.

In the scenarios in which the also the thermal storage tank is exploited as a source of flexibility, the trend is inverted and the available storage capacity increases with increasing external temperature. This occurs mainly because the thermal energy that can be stored in the tank is more exploited during the colder months due to the higher energy consumption. In the scenario when only the storage tank is exploited as a source of flexibility, the energy potential of the thermal storage tank is similar for each event, since the temperature reached during the ADR events is similar.

In the scenario in which both the thermal storage tank and the building structure are exploited as source of flexibility, the contribution of the thermal storage increases towards warmer months, because when the energy consumption is higher (during January and February), the temperature reached from the storage is lower compared to the one reached during the warmer months, when the energy consumption is lower.

In general, the thermal storage tank alone provides less flexibility potential compared to the building structure.

In the simulation scenarios in which the heat pump is used, the thermal storage capacity is calculated based on both thermal and electrical energy use. The COP of the heat pump is calculated for both the ADR simulation and the reference simulation.

The COP_{ADR} presents an increasing trend towards warmer months in the scenarios in which only the building structure or only the thermal storage tank are exploited as sources of energy flexibility. In the first case the trend in explained with the increase in the external air temperature. In the second case the trend is similar, but the values of the COP_{ADR} are lower since the thermal storage temperature is higher compared to the previous case. In the scenario in which both flexibility sources are present, the COP_{ADR} presents a decreasing trend and this is manly due to the fact that when the heating demand is higher during the colder months, the temperature reached by the storage is lower compared to the one reached during the warmer months., Therefore, when both flexibility sources are exploited, events in the warmer months show a significant drop in the COP_{ADR}.

Concerning the efficiency of the system, in the scenario in which only the building structure is exploited the COP_{ADR} present higher values compared to COP_{REF} because the lower temperature reached in the tank, while in the case where only the thermal storage tank is exploited the COP_{ADR} present lower values compared to COP_{REF} because the higher temperature reached in the tank. In the scenario in which both are exploited, COP_{ADR} present higher values compared to COP_{REF} in the colder months and became lower in the warmer month.

In the scenario in which only the building structure is exploited as source of flexibility, the COP_{ADR} present higher values compared to COP_{REF} . This effect is explained by the higher energy consumptions during the ADR events and thus lower temperature reached in the tank, resulting in higher COP and higher efficiency of the system.

In the case in which only the thermal storage tank is exploited as source of flexibility, instead, the COP_{ADR} present lower values compared to COP_{REF}. This effect is explained by the fact that the heat pump is forced to stay on and thus higher temperature is reached in the tank, resulting in lower COP and lower efficiency of the system.

In the scenario in which both are exploited, COP_{ADR} present higher values compared to COP_{REF} in the colder months and became lower in the warmer month.

Concerning the storage efficiency (η_{ADR}) the trend is similar in all the simulation scenarios considered, in which the efficiency decreases in the warmer months. This trend is mainly due to the increase in the external temperature, which results in a lower heating demand of the building and thus the surplus of energy supplied during an upward modulation event is not used properly to decrease the heating consumption in the hours after the ADR event, as it does in colder periods with higher heating demand.

The overheating index depends on the indoor air temperature in the rooms of the building. In the case when only the thermal storage tank is used, since the control of the inlet temperature of the radiant floor heating system is the same of the normal operations, the thermal storage tank does not contribute actively in the overheating of the rooms. . The trend of the overheating index observed the other cases is similar. In particular, during the coldest month, there is no overheating according to the simulation results. and then starts to increase, until the month of May shows high values. The trend is mainly related to the fact that during the colder months the external temperature is lower and the thermal losses of which the indoor environment is subjected are higher, while in warmer months the thermal losses are lower because the higher temperature, resulting in higher degree-hours in which the temperature remains above the limit considered.

Shifting electric energy consumption from hours with higher electricity price towards hours with lower electricity price can lead to cost saving for the building owners.

The economic analysis performed shows different trends in the different scenarios. When only the building structure is exploited as source of flexibility the cost saving is almost always positive and

increases from January to March and decreases from March to May. The trend appears to be a trade-off between three different aspects. The cost saving is lower in colder month because the increase in the consumption results in higher cost which decrease the effect due to the shift part of the consumption from high price period to low price period, while in warmer month only a part of the energy stored during the events is used to decrease the consumption after the event, thus decreasing the effect of shifting energy in economic terms. During the month of March the cost saving is higher also because it is the period with the highest variability in the electricity price, evaluated as average difference between maximum and minimum daily electricity price. This condition makes the shift of energy consumption more effective in economic terms.

Concerning the downward ADR events, the available storage capacity presents negative values, this because during the events the energy consumption is decreased respect normal operations and the energy is saved. The indicator shows a decreasing trend in absolute values from the coldest months to the warmest months. In particular, the values in the first months, from January to March, remain enough constant and then, in April and May, starts to decrease. This trend is mainly due to the contribution of the external temperature, which remains enough similar in the coldest months, resulting in similar amount of energy saved during the ADR events compared to normal operation. In the warmest months, instead, the temperature increases and the energy consumption decreases. In this way the amount of energy which can be shifted and thus saved during the ADR events is lower, resulting in a decrease in the available storage capacity.

In the scenarios in which only the building structure is exploited as source of energy flexibility the results shows lower values compared to the cases in which there is also the contribution of the thermal storage tank. This aspect is mainly related to the fact that in the cases in which also the thermal storage tank is exploited, the heat pump is forced to stay off because the ADR events, while in the cases in which only the building structure is exploited, the heat pump normally operates, resulting in higher consumption during ADR events and thus lower amount of energy saved respect when the heat pump is always off.

In the simulation scenarios in which the heat pump is used, the thermal storage capacity is calculated both in thermal basis and in electrical basis.

The cases in which the heat pump is forced to stay off present the same values of available storage capacity. This fact is explained because the heat pump in both cases is forced to stay off and the amount of energy saved during the event is the same, since the reference simulation behave in the same way in both cases.

Also in case of downward events, in the simulation scenarios in which the heat pump is used, the thermal storage capacity is calculated based on both thermal and electrical energy use. In this case, when the heat pump is off because the ADR events, the calculation of the COP in the ADR simulation is not possible

since the energy consumption is null. To have an idea of the behavior of the efficiency of the heat pump only the COP in the reference simulation is observed.

The COP presents an increasing trend with the progression of the months in all the scenarios since it depends on the external temperature which increases from the coldest months to the warmest months. The efficiency of the operation of the heat pump during the downward events is not affected by the events itself.

The storage efficiency (η_{ADR}) of the different events can vary depending on the time of the day in which the ADR event is started, which is the amount of energy released from the heating system during normal operations in the hours before the event and the consequently amount of energy already stored in the system. Also the external temperature, which varies not always gradually during the day and the month, has an impact on the thermal behavior of the building and consequently on the storage efficiency, since this indicator is evaluated in the 72 hours after the ADR event.

Moreover, compared to the case of the upward ADR events, in this case the absolute values of available storage capacity are lower and sometimes near to zero, resulting in higher impact of some possible misalignments between the ADR simulation and the reference simulation, which can affect more the results of the storage efficiency. For these reasons the values of the storage efficiency can be affected by some alterations which depend on external factors, making difficult to establish a general rule.

The thermal discomfort index in case of downward ADR events takes into account the degree-hours in which the indoor temperature goes below the limit of 20°C.

The thermal discomfort index presents similar trend in all the scenarios analyzed. It remains almost constant during the coldest months and then starts to decrease in the warmest months. The trend is mainly related to the fact that during the coldest months the external temperature is lower and the thermal losses at which the indoor environment is subjected are higher, resulting in higher decrease in the indoor temperature during the events. In warmest months, as April and May, the external temperature is generally higher, resulting in lower thermal losses and lower decrease in the indoor temperature, resulting in lower thermal discomfort.

Also in case of downward events shifting electric energy consumption from hours with higher electricity price towards hours with lower electricity price can lead to cost saving for the building owners.

The rough economic analysis performed show positive values in each month and for all the scenarios, meaning the application of downward events gives back economic advantages for the building owners.

The results shows a similar trend in all the scenarios. The cost saving increase from January to March and then decrease from March to May. The cost saving in the coldest months, as January and February, are higher compared to the warmest months, as April and May. This is explained by the fact that in the coldest months the amount of energy shifted from high price period to low price period is higher compared to warmest months, resulting in higher cost saving. The high values observed in March are due also by the

contribution of the higher variability in the maximum and minimum price of the electricity compared to the other months observed also in case of upward events.

In conclusion, the Active Demand Response program applied to the building of the case study considered shows that the building structure and the use of a heat pump coupled with the thermal storage tank can provide a significative energy flexibility potential. The fact that it is possible to shift some amount of energy from the peak hours helps the electricity grid to alleviate congestion problems and at the same time brings also economic advantages for the building owners.

The flexibility potential variation is mainly related to the boundary conditions of the weather conditions and the electricity price. Moreover, it is observed that the use of both the building structure and the thermal storage tank as source of energy flexibility results in higher flexibility potential respect the separate use of the sources for both the upward and downward events.

The results show that shifting the energy consumption through the ADR events in case of the upward events result in a decrease of the COP of the heat pump respect normal operation when the thermal storage tank is exploited as source of flexibility, even if this decrease is low. The results show also that the creation of the upward ADR events results in very low increase in the overheating inside the rooms, except for the month of May, in which the impact is significative higher. The downward ADR events impact of the thermal discomfort is higher, but not significative, in the coldest months and almost null in the warmest months.

The results of the economic analysis show that in case of downward events the use of both the sources of energy flexibility brings more cost saving compared the single use, even if also in case of separate use the cost saving is positive. In case of the upward events, instead, the contribution of the thermal storage result in lower cost saving, which remains positive, but bring higher flexibility potential, resulting in a good trade-off.

For future studies it is suggested to increase the number of Active Demand Response events for each month. In this way is expected to have higher energy flexibility potential and higher cost saving for the building owners, without affecting too much the efficiency of the system or the thermal comfort since the duration of the events remains the same.

This study assumes that the building of the considered case-study is heated up only through a radiant floor heating system, it will be interesting to perform the same study accounting also for the radiators.

In this work the analysis is performed modelling on/off energy systems to heat up the building considered, it will be interesting to repeat the analysis using continuous operation energy systems, as a variable speed heat pump.

7 Bibliography

[1] I. - International Energy Agency, “World Energy Outlook 2023,” 2023. [Online]. Available: www.iea.org/terms

[2] S. Ø. Jensen *et al.*, “IEA EBC Annex 67 Energy Flexible Buildings,” *Energy Build*, vol. 155, pp. 25–34, Nov. 2017, doi: 10.1016/j.enbuild.2017.08.044.

[3] R. D’hulst, W. Labeeuw, B. Beusen, S. Claessens, G. Deconinck, and K. Vanthournout, “Demand response flexibility and flexibility potential of residential smart appliances: Experiences from large pilot test in Belgium,” *Appl Energy*, vol. 155, pp. 79–90, Oct. 2015, doi: 10.1016/j.apenergy.2015.05.101.

[4] O. /. OCDE and International Energy Agency, *World Energy Outlook 2014.*

[5] Gellings W. Clark, “The Concept of Demand-Side Management for Electric Utilities,” 1985.

[6] P. Baggio, E. Bee, and A. Prada, “Demand-side management of air-source heat pump and photovoltaic systems for heating applications in the italian context,” *Environments - MDPI*, vol. 5, no. 12, pp. 1–12, Dec. 2018, doi: 10.3390/environments5120132.

[7] J. Vivian, U. Chiodarelli, G. Emmi, and A. Zarrella, “A sensitivity analysis on the heating and cooling energy flexibility of residential buildings,” *Sustain Cities Soc*, vol. 52, Jan. 2020, doi: 10.1016/j.scs.2019.101815.

[8] A. Bampoulas, M. Saffari, F. Pallonetto, E. Mangina, and D. P. Finn, “A fundamental unified framework to quantify and characterise energy flexibility of residential buildings with multiple electrical and thermal energy systems,” *Appl Energy*, vol. 282, Jan. 2021, doi: 10.1016/j.apenergy.2020.116096.

[9] R. E. Hedegaard, M. H. Kristensen, T. H. Pedersen, A. Brun, and S. Petersen, “Bottom-up modelling methodology for urban-scale analysis of residential space heating demand response,” *Appl Energy*, vol. 242, pp. 181–204, May 2019, doi: 10.1016/j.apenergy.2019.03.063.

[10] V. Amato, “PRACTICAL REALIZATION OF SPACE HEATING DEMAND RESPONSE IN RESIDENTIAL BUILDINGS,” 2022. [Online]. Available: https://phd.tech.au.dk/

[11] V. Amato, “PRACTICAL REALIZATION OF SPACE HEATING DEMAND RESPONSE IN RESIDENTIAL BUILDINGS,” 2022. [Online]. Available: https://phd.tech.au.dk/

[12] “https://climate.onebuilding.org/.”

[13] Team European Energy Efficiency Platfrom (E3P), “European Commission - DG JRC, Directorate C - Energy, Transport and Climate.”

[14] “Google SketchUp 8”.

[15] “TRNSYS.”

[16] “Trnsys 18,” 2019. [Online]. Available: http://sel.me.wisc.edu/trnsyshttp://software.cstb.frhttp://www.tess-inc.com

[17] “Trnsys3d Tutorial,” 2012. [Online]. Available: http://www.trnsys.de

[18] “T R N F L O W A module of an air flow network for coupled simulation with TYPE 56 (multi-zone building of TRNSYS),” 2009.

[19] H. ; Johra, P. K. Heiselberg, and J. L. Dreau, “Numerical Analysis of the Influence of Thermal Mass, Phase Change Materials and Furniture / Indoor Content on Building Energy Flexibility,” 2017. [Online]. Available: http://www.ibpsa.org/proceedings/BS2017/BS2017_012.pdf

[20] H. ; Johra and Heiselberg, “Aalborg Universitet Description and Validation of a MATLAB Simulink Single Family House Energy Model with Furniture and Phase Change Materials.”

[21] “TRNSYS 18,” 2017. [Online]. Available: http://sel.me.wisc.edu/trnsyshttp://software.cstb.frhttp://www.tess-inc.com

[22] S. Bordignon, G. Emmi, A. Zarrella, and M. De Carli, “Energy analysis of different configurations for a reversible ground source heat pump using a new flexible TRNSYS Type,” *Appl Therm Eng*, vol. 197, Oct. 2021, doi: 10.1016/j.applthermaleng.2021.117413.

[23] © 2024 - STIEBEL ELTRON GmbH & Co. KG (DE), “https://www.stiebel-eltron.com/en/home/products-solutions/information-engineering/refrigerant-r454c.html.”

[24] Eurostat, “https://ec.europa.eu/eurostat/statistics-explained/index.php?title=Glossary:Global-warming_potential_(GWP)#:~:text=Global%2Dwarming%20potential%2C%20abbreviated%20as,remains%20active%20in%20the%20atmosphere.”

[25] “TYPE 68: SHADING OF OPENINGS BY EXTERNAL OBJECTS.”

[26] B. Bundesverband Wärmepumpe, “https://www.gridx.ai/knowledge/sg-ready.”

[27] A. Kathirgamanathan *et al.*, “Towards standardising market-independent indicators for quantifying energy flexibility in buildings,” *Energy Build*, vol. 220, Aug. 2020, doi: 10.1016/j.enbuild.2020.110027.

[28] M. E. SIMULAZIONE DINAMICA DELLE PRESTAZIONI RELATORE Ing Adriana Angelotti, “POLITECNICO DI MILANO SCUOLA DI INGEGNERIA INDUSTRIALE E DELL’INFORMAZIONE TESI DI LAUREA MAGISTRALE IN INGEGNERIA ENERGETICA RECUPERO TERMICO SULLA VENTILAZIONE TRAMITE POMPA DI CALORE”.

[29] G. Reynders, J. Diriken, and D. Saelens, “Generic characterization method for energy flexibility: Applied to structural thermal storage in residential buildings,” *Appl Energy*, vol. 198, pp. 192–202, 2017, doi: 10.1016/j.apenergy.2017.04.061.

[30] G. Reynders, R. Amaral Lopes, A. Marszal-Pomianowska, D. Aelenei, J. Martins, and D. Saelens, “Energy flexible buildings: An evaluation of definitions and quantification methodologies applied

to thermal storage," *Energy and Buildings*, vol. 166. Elsevier Ltd, pp. 372–390, May 01, 2018. doi: 10.1016/j.enbuild.2018.02.040.